

**Application of Mellin-Barnes
representations to the evaluation
of radiative loop diagrams
in Bhabha Scattering**

Diplomarbeit
zur Erlangung des wissenschaftlichen Grades
Diplom-Physiker

vorgelegt von

Felix Simon Haas^a
geboren am 07.05.1982 in Berlin

Betreuer: Dr. Tord Riemann^b

^a *Universität Potsdam, Institut für Physik
Am Neuen Palais 10, D-14469 Potsdam*

^b *Deutsches Elektronen-Synchrotron, DESY
Platanenallee 6, D-15738 Zeuthen*

eingereicht am 15. Januar 2008

Gutachter:

Dr. Tord Riemann, DESY, Zeuthen

Prof. Dr. Martin Wilkens, Universität Potsdam

Contents

1	Introduction	5
1.1	The making of the standard model	5
1.2	Bhabha scattering	6
1.3	Structure of the thesis	7
2	Perturbative calculations in QFT	8
2.1	The S-matrix	8
2.2	Cross section and decay rate	10
3	Electroweak part of the standard model	11
3.1	Classical GWS Lagrangian	11
3.2	Quantum part of the GWS Lagrangian	12
4	Infrared divergences and Bloch-Nordsieck cancellation	14
4.1	IR loop divergences	14
4.2	Bloch-Nordsieck cancellation	15
4.3	Factorization of real soft-photon contributions	15
4.4	Real soft-photon contribution	16
4.5	Virtual soft-photon contribution	17
4.6	Cancellation of the IR-divergences	18
5	Soft photon correction to Bhabha scattering	19
5.1	Factorization of the IR-divergence	19
5.2	The Born cross section	19
5.3	The IR-divergent factor δ^{IR}	20
5.4	Initial state radiation	22
5.5	Interference of initial- and final state radiation	23
6	Mellin-Barnes representation	25
6.1	Mellin-Barnes representation	25
6.2	Mellin-Barnes representation for multiple propagators	25
6.3	AMBRE.m and the scalar 1-loop box B412m	26
6.4	Regularization of MB-integrals	28
6.5	MB.m and analytic continuation in ϵ	29
6.6	Barnes' first and second lemma	31
7	The five-point function in Bhabha scattering	32
7.1	Bhabha scattering	32
7.2	Kinematic invariants	33
7.3	Five point topologies	34
7.4	M-matrix and divergence structure of $\mathcal{M}_{(uc,s,r)}$	35
7.5	The five-point MB-integral	37
7.6	The divergent integrals	38
8	The cross section	41
8.1	Kinematic conventions	41
8.2	The M-matrix	41
8.3	The loop integral contributions	42
8.4	The cross section	43
8.5	Bloch-Nordsieck cancellation	45

9	The photon phase space integrals	46
9.1	The P_1 integral	46
9.2	The P_2 integral	49
9.3	The divergent part	51
10	Summary and Results	52
11	Appendix	54
A	Conventions	55
B	Feynman Rules of QED	57
B.1	General rules	57
B.2	Free particles	57
B.3	Propagators and vertex	57
C	Functions and sums	58
C.1	Gamma function	58
C.2	Feynman parameter representations	58
C.3	Pochhammer symbol	58
C.4	Beta function	59
C.5	Polygamma function	59
C.6	Polylogarithms	59
C.7	Nielsen integrals	60
C.8	Harmonic sums	60
C.9	σ -values	60
C.10	Riemann zeta function	61
C.11	Hypergeometric series	61
C.12	Mellin transform	61
C.13	Harmonic polylogarithms	61
C.14	Inverse binomial sums	62
D	Integration of L-loop, N-point functions	64
D.1	General setup	64
D.2	Concrete evaluation	66
E	Phase space	70
E.1	Two particle phase space	70
E.2	Three particle phase space	71
F	Bhabha phase space integrals	72
F.1	Further x-integrals for section 9	72
F.2	Feynman parameter integrals for section 9	72
G	Muon decay	74
G.1	Feynman rules	74
G.2	M-matrix	75
G.3	The kinematic approach	76
G.4	M-matrix with tensor integrals	78
G.5	Phase space tensor integrals	79
G.6	Energy spectrum	80
G.7	Total decay rate	82

G.8	Integrals	83
G.9	Numerical input	84
H	W^+W^- production	85
H.1	M-matrix	85
H.2	Squaring \mathcal{M}	86
H.3	Rewriting $ \mathcal{M} ^2$	87
H.4	Cross section	88
H.5	Breit-Wigner factors	88
H.6	Results	89
H.7	The CC3 cross section	90
H.8	Four body kinematics	92

1 Introduction

1.1 The making of the standard model

During the last century, both the development of quantum theory and the investigation of the substructure of matter have seen immense progress and have changed our view of the world profoundly. The beginning of quantum theory is usually set in 1900, when M. Planck assumed that energy is quantized in order to derive a formula predicting the observed frequency dependence of the energy emitted by a black body [7]. In 1905, A. Einstein explained the photoelectric effect [8] by postulating that light energy comes in quanta later called photons. In 1913, N. Bohr invoked quantization in his proposed explanation of the spectral lines of the hydrogen atom [9], introducing the theory of electrons traveling in orbits around the atom's nucleus, the chemical properties of the element being largely determined by the number of electrons in the outer orbits. Bohr also introduced the idea that an electron could relax from a higher-energy orbit to a lower one, emitting a photon of discrete energy.

In his PhD thesis 1924, L. de Broglie proposed the wave-like nature of subatomic particles [10]. Building on the work by A. Einstein and M. Planck, L. de Broglie postulated the wave-particle duality of matter, further stating that any moving particle or object had an associated wave.

Modern quantum mechanics was born in 1925 with W. Heisenberg's matrix mechanics [11] and E. Schrödinger's wave mechanics and the Schrödinger equation [12], which was a non-relativistic generalization of de Broglie's relativistic approach. Schrödinger subsequently showed that these two approaches were equivalent. In 1927, Heisenberg formulated his uncertainty principle [13], and the Copenhagen interpretation of quantum mechanics began to take shape. Around this time, P.M. Dirac, in work culminating in his 1930 monograph [14] finally joined quantum mechanics and special relativity, pioneered the use of operator theory, and devised the bra-ket notation. In 1932, J. von Neumann formulated the rigorous mathematical basis for quantum mechanics as the theory of linear operators on Hilbert spaces [15].

Soon physicists began to try to apply the principles of quantum mechanics to classical field theories, most noticeably Maxwell theory. This research program culminated in the 1940s in Quantum Electrodynamics (QED) developed by Richard Feynman, Sin-Itiro Tomonaga, Julian Schwinger (shared Nobel Prize in Physics 1965) and Freeman Dyson. QED holds almost all of the conceptual novelties that were to make up the coming theories of elementary particles. It is a special relativistic, renormalizable quantum field theory with one abelian, massless gauge field. QED makes extremely accurate predictions of quantities like the anomalous magnetic moment of the electron, and the Lamb shift of the energy levels of hydrogen.

A generalization of quantum field theories to non-abelian symmetry groups was studied by C.N. Yang and R.L. Mills in 1954 [16]. However their results were given only little attention until the work of S. Glashow [17], A. Salam [18] and most importantly S. Weinberg in 1967 [19] who proposed a unified electroweak model based on the non-abelian gauge group $U(1)_Y \times SU(2)_L$. Further, the Glashow-Weinberg-Salam (GWS) model applies the Brout-Englert-Higgs mechanism (also Higgs-Kibble mechanism) [20], [21], [22] to the electroweak symmetry breaking. A scalar $SU(2)_L$ -doublet -the Higgs-field- is introduced, which – by acquiring a non-zero vacuum expectation value (vev) – spontaneously breaks the electroweak- down to the electromagnetic gauge symmetry, thereby giving masses to the W^\pm and the Z^0 boson. The GWS theory was proved to be renormalizable by G. t'Hooft and M. Veltman in 1972 [23].

In 1970 S.L. Glashow, J. Iliopoulos and L. Maiani [24] hypothesized the charm-quark in order to explain the small branching ratio of the $K^0 \rightarrow \mu^+ \mu^-$ decay. Including the charm quark it was possible to construct the CKM quark mixing matrix (N. Cabibbo [25] and M. Kobayashi, T. Maskawa [26])

which describes the mixing of mass- and flavor-eigenstates in the standard model. The unitarity of the CKM-matrix lets the neutral current be flavor-diagonal. This in turn implies that neutral weak processes obey certain flavor selection rules, that forbid flavor changing neutral currents (FCNC) on tree level and thus explain the small measured branching ratio of the above decay which has the order of magnitude of higher-order electroweak effects $\Gamma(K^0 \rightarrow \mu^+ \mu^-)/\Gamma_{tot}(K^0) \approx 10^{-7}$. This explanation for the absence of FCNC is now referred to as the GIM-mechanism.

In 1973, M. Gell-Mann, H. Fritzsch and H. Leutwyler [27], put forward an addition to the GWS model which became to be known as Quantum Chromodynamics (QCD), the massless Yang-Mills theory of the strong force coupling to a new charge called color. This theory combined with the GWS model has the gauge group $U(1)_Y \times SU(2)_L \times SU(3)_c$ ¹ and became to be known as the standard model of elementary particles. $SU(3)_c$ was chosen as the gauge group of QCD since it is the only compact simple Lie group that admits a complex triplet representation accounting for the three colors and admitting antiquark states. The existence of the color quantum number was proposed already before, to explain the apparent violation of the Pauli-principle in the description of baryons containing the same flavor and spin, as e.g. in the Δ^{++} state. The experimental lack of observed colored particles led to the believe that all physical asymptotic states must be $SU(3)_c$ singlets (color neutral). This assumption was proved in 1973 by D. Gross and F. Wilczek, [28], and by H. Politzer, [29], who showed in a 1-loop calculation, that QCD is asymptotically free, which means that the strong force between two quarks grows as the distance between them increases, thus making it impossible to isolate and observe a colored particle (infrared slavery). Or, from a dual stand point: only at high energies does the running strong coupling constant become sufficiently small to do perturbative calculations.

The nonperturbative character of low energy QCD was one of the main motivations for the development of lattice QFT [30], where space-time is discretized and acts as a natural UV-regulator. Today, other than low energy QCD, lattice QFT also investigates other nonperturbative aspects of QFTs such as topologically non-trivial field configurations (solitons, instantons, monopoles).

1.2 Bhabha scattering

The main objective of this thesis is the calculation of higher order Bremsstrahlung corrections to Bhabha scattering

$$e^+e^- \rightarrow e^+e^- \tag{1}$$

Even though the leading order contribution of Bhabha scattering was first calculated by Homi J. Bhabha already in 1936 [32], today it remains an important process for luminosity monitoring at e^+e^- colliders such as the Large Electron Positron Collider (LEP) and the International Linear Collider (ILC). Luminosity monitoring is important because it directly influences the accuracy of the measurement outcome and therewith the predictability of the experiment.

Bhabha scattering is divided into two classes depending on the kinematic region: the small-angle Bhabha scattering (SABH) for a scattering angle $1^\circ \lesssim \theta_e \lesssim 6^\circ$ and the large angle Bhabha scattering (LABH) for $\theta_e \gtrsim 10^\circ$.

In general Bhabha scattering is mediated by both the γ and Z^0 bosons exchanged both in s- and t-channels.

Bhabha scattering has a long history. Following the Born level calculation [32], the complete electroweak one-loop correction was first calculated in [33]. The analytic expression for photonic

¹It has been stressed [31] that by modding out the kernel of the fermionic-, gauge- and Higgs-representation of the standard model gauge group, one does not lose any physically relevant symmetry, since any representation $\rho : G \rightarrow \text{End}(V)$ of the group G sends elements of the kernel to the identity transformation on the vector space V , so they only act as symmetries in a trivial sort of way. Hence, as the "true" -i.e. smallest possible - internal symmetry group of the standard model one should consider $(U(1)_Y \times SU(2)_L \times SU(3)_c)/(\mathbb{Z}_2 \times \mathbb{Z}_3)$.

two-loop massless Bhabha scattering was derived in [34]. Subsequently the massive expression was given in [35], [36] and [37]. NNLO contributions with electron loop insertions were calculated in [38], [39], [40] and [41]. The full $n_f = 1$ two-loop Bhabha cross section evaluation was completed with [42], [43] and [44].

1.3 Structure of the thesis

We calculate the cross section of the interference of the one-loop QED 5-point Bremsstrahlung corrections to Bhabha scattering (listed in chapter 7 figures 6 and 7) with the QED-Bremsstrahlung topologies.

In the calculation of any cross section one has to include Bremsstrahlung corrections, since photons are massless and can thus be produced with arbitrarily small energy. Any physical detector has a minimal energy detection threshold ω . Emitted photons with an energy below ω are not being detected and thus Bremsstrahlung diagrams must be included since one cannot distinguish between the process under consideration and the corresponding Bremsstrahlung process with real photons of energy smaller than ω . As stated, Bremsstrahlung can be of arbitrarily small energy and the photon phase space integration includes an energy integration from 0 to ω . The lower limit gives rise to an infinite expression known as infrared (IR)-divergence since it arises from the low energy region.

The 5-point Bhabha functions have IR-divergences coming both from the virtual loop integral and the real phase space integration. The general treatment of IR-divergences in the standard model will be discussed in section 4. However since the real divergences coming from the 5-point function cancel virtual divergences from other topologies (including higher order graphs), we will not be able to show the cancellation in this thesis.

First we will start by briefly giving an introduction to the generation of perturbation series in Quantum Field Theory (QFT) and the structure of the electroweak part of the standard model. Following the above mentioned discussion of IR-divergences we will calculate both the Born cross section for QED-Bhabha scattering and the Born contribution to QED-Bhabha-Bremsstrahlung diagrams.

After introducing Mellin-Barnes (MB) representations and briefly discussing the `Mathematica` [54] packages `AMBRE.m` [55] and `MB.m` [56], we will deduce all the MB-integrals for the scalar, vector and tensor Feynman integrals. We will discuss and use the crossing symmetry between the different graphs, in order to reduce the calculation to the evaluation of merely two of the eight 5-point diagrams. The cross section will be given in terms of the phase space integrals (at the end of section 8) which are solved to $\mathcal{O}(\epsilon^{-1})$ in section 9. Further the $\mathcal{O}(\epsilon^0)$ phase space integrals are reduced to the Feynman parameter integrals.

In addition to the calculation of the Bhabha cross section we calculated the leading order muon decay rate in appendix G using two different techniques. At last the σ_{cc3} cross section of W^+W^- -production is deduced in appendix H using Breit-Wigner factors.

2 Perturbative calculations in QFT

In the first part of this section we give a brief introduction to the S-matrix formalism in QFT and the generation of the perturbation series in the path integral formalism. In the second part the general expressions for both cross section and decay rate are listed.

The Scattering matrix (S-matrix) is of central importance in scattering theory, as it relates the initial state and the final state for an interaction of particles. To know the S-matrix elements is to know the probability for the given process.

2.1 The S-matrix

In QFT the probability P of finding a system in a state $|\text{Final}\rangle$ at t_f when it was prepared in a state $|\text{Initial}\rangle$ at t_i is

$$P = |\langle \text{Final} | e^{-iH(t_f-t_i)} | \text{Initial} \rangle|^2 = |\langle \text{Final}, t_f | \text{Initial}, t_i \rangle|^2, \quad (2)$$

where H is the second quantized Hamiltonian of the theory and the second scalar product is written in the Heisenberg picture. Since interacting fields cannot be expanded in terms of creation- and annihilation operators, we are interested in the limit $t \rightarrow \pm\infty$ where we expect the theory to reduce to a free theory.² For this purpose we define the S-matrix:

$$\mathcal{S} = \lim_{(t_f-t_i)\rightarrow\infty} \left[e^{-iH(t_f-t_i)} \right]. \quad (3)$$

The unitarity $\mathcal{S}^\dagger \mathcal{S} = 1$ expresses the probability conservation. One normally proceeds in defining a T-matrix, that contains the interaction part of the S-matrix:

$$\mathcal{S} = \mathbf{1} + i\mathcal{T}. \quad (4)$$

In the following we will discuss the build-up of a QFT for a scalar field ϕ . The above assumption that the theory reduces to a free theory as $t \rightarrow \pm\infty$ is formalized in the hypothesis³

$$\lim_{t\rightarrow-\infty} \phi(x) = Z^{1/2} \phi_{\text{in}}(x), \quad \lim_{t\rightarrow+\infty} \phi(x) = Z^{1/2} \phi_{\text{out}}(x), \quad (5)$$

where Z is a c-number, known as wave function renormalization. With the introduction of in- and out-fields the theory now has two distinct Hilbert-spaces \mathcal{H}_{in} and \mathcal{H}_{out} on which the free field operators $\phi_{\text{in}}(x)$ and $\phi_{\text{out}}(x)$ act. \mathcal{S} is then a mapping between these two spaces.

Due to Lehmann, Symanzik and Zimmermann (LSZ-reduction formula) [57], one can rewrite the matrix element for a scattering of m particles of momentum k_i into n particles of momentum p_j in terms of the vev of a time-ordered product of the field operators:

$$\begin{aligned} & \prod_{i=1}^m \int d^4x_i e^{-ik_i x_i} \prod_{j=1}^n \int d^4y_j e^{-ip_j y_j} \langle 0 | T [\phi(x_1) \dots \phi(x_m) \phi(y_1) \dots \phi(y_n)] | 0 \rangle \\ &= \left[\prod_{i=1}^m \frac{iZ^{1/2}}{k_i^2 - m^2} \right] \left[\prod_{j=1}^n \frac{iZ^{1/2}}{p_j^2 - m^2} \right] \langle p_1 \dots p_n | i\mathcal{T} | k_1 \dots k_m \rangle, \end{aligned} \quad (6)$$

where $T[\phi(x)\phi(y)]$ is the time-ordered product. Note that the LSZ-factors on the right hand side of (6) account for the poles that the Green's function on the left hand side develops on mass shell,

²An important example of a QFT that is not a free theory at $t \rightarrow \pm\infty$ is QCD. However QCD is asymptotically free, i.e. it can be considered a free field theory for $x \rightarrow 0$.

³These limits are to be understood in the weak sense, i.e. they are assumed to hold only when we take matrix elements.

i.e. $p_j^2 = m^2$ and $k_i^2 = m^2$. In the realm of canonical quantization the next step would be to switch to the interaction picture which introduces an exponential of the interaction Hamiltonian, which when expanded, gives rise to the well known perturbative series of QFT. Finally one makes use of Wick's theorem which reduces the vev of a product of n fields to a sum of products of Feynman propagators.

Instead, in particle physics, one frequently chooses to work in the path integral quantization, which is related to the operator formalism via

$$\langle 0 | T [\phi(x_1) \dots \phi(x_n)] | 0 \rangle = \frac{\int \mathcal{D}[\phi] \phi(x_1) \dots \phi(x_n) e^{iS} e^{-\epsilon \int d^4x \phi^2/2}}{\int \mathcal{D}[\phi] e^{iS} e^{-\epsilon \int d^4x \phi^2/2}}, \quad (7)$$

where $S = \int d^4x \mathcal{L}$ is the action of the theory and the damping term $e^{-\epsilon \int d^4x \phi^2/2}$ was introduced to insure the convergence of the integration. A remarkable fact is that the damping factor $\epsilon > 0$ will later be responsible for our theory to have the correct causal structure (it will appear as a $+i\epsilon$ in the denominator of the Feynman propagator). Introducing a source J and using the functional identity

$$\frac{\delta}{\delta J(y)} \int d^4x J(x) \phi(x) = \phi(y), \quad (8)$$

one can rewrite the n -point function $G(x_1, \dots, x_n)$ in terms of functional derivatives of the generating functional $Z[\phi, J]$:

$$\begin{aligned} G(x_1, \dots, x_n) &= \int \mathcal{D}[\phi] \phi(x_1) \dots \phi(x_n) e^{iS} = \left[\frac{\delta}{i\delta J(x_1)} \dots \frac{\delta}{i\delta J(x_n)} Z[\phi, J] \right]_{J=0}, \\ Z[\phi, J] &= \int \mathcal{D}[\phi] \exp \left[iS[\phi] + i \int d^4x J(x) \phi(x) \right]. \end{aligned} \quad (9)$$

We generalize the above formalism to include interacting gauge fields A^μ and Grassmann valued matter fields ψ . The simplest such physical QFT is QED:

$$\mathcal{L}_{\text{QED}} = \underbrace{\bar{\psi}[i\cancel{\partial} - m]\psi}_{\mathcal{L}_0^F} - \underbrace{\frac{1}{4} F_{\mu\nu} F^{\mu\nu}}_{\mathcal{L}_0^G} - \underbrace{\frac{1}{2\xi} (\partial_\mu A^\mu)^2}_{\mathcal{L}_{\text{int}}} - \underbrace{e\bar{\psi}\cancel{A}\psi}_{\mathcal{L}_{\text{int}}}. \quad (10)$$

With the Grassmann source functions η and $\bar{\eta}$, we can write the generating functional of QED as

$$\begin{aligned} Z_{\text{QED}} &= \int \mathcal{D}[A^\mu, \psi, \bar{\psi}] \exp [iS_{\text{Int}}[A^\mu, \psi, \bar{\psi}]] \exp \left[iS_0^F + iS_0^G + i \int d^4x (\bar{\eta}\psi + \bar{\psi}\eta + J_\mu A^\mu) \right] \\ &= \exp \left[iS_{\text{Int}} \left[\frac{\delta}{i\delta J_\mu}, \frac{\delta}{i\delta \bar{\eta}}, \frac{\delta}{i\delta (-\eta)} \right] \right] \int \mathcal{D}[A^\mu, \psi, \bar{\psi}] \exp \left[iS_0^F + iS_0^G + i \int d^4x (\bar{\eta}\psi + \bar{\psi}\eta + J_\mu A^\mu) \right] \\ &= \exp \left[iS_{\text{Int}} \left[\frac{\delta}{i\delta J_\mu}, \frac{\delta}{i\delta \bar{\eta}}, \frac{\delta}{i\delta (-\eta)} \right] \right] \\ &\quad \times \exp \left[i \int d^4x d^4y \left(\bar{\eta}(x) S_F(x-y) \eta(y) + J^\mu(x) \frac{D_{\mu\nu}(x-y)}{2} J^\nu(y) \right) \right], \end{aligned} \quad (11)$$

where $S_F(x-y)$ and $D_{\mu\nu}(x-y)$ are the Feynman propagators of the electron and photon. In the first step we made use of a generalization of (8) and in the second the functional integration over the physical fields was performed, which amounts to solving infinite dimensional Gaussian integrals. The Feynman perturbation series is now generated by power expanding the first exponential and, order by order, letting the functional derivatives act on the second. In principle we could now set out to calculate 4-point, 5-point functions and so on (following (9)), but we would find the

reappearance of the same expressions, only differently arranged. Further there is an overall Dirac delta, which inspires the definition of the M-Matrix \mathcal{M}_{fi}

$$\langle p_1 \dots p_n | i\mathcal{T} | k_1 \dots k_m \rangle = (2\pi)^4 \delta^4 [\sum_i p_i - \sum_j k_j] i\mathcal{M}_{fi}. \quad (12)$$

In practice one identifies the Feynman graphs of appendix B to the different propagators etc., so that the evaluation of an n-point function to $\mathcal{O}(k)$ in e is equivalent to drawing all the topologically different possible Feynman diagrams to $\mathcal{O}(k)$ in e and writing down their corresponding Feynman rules.

The Feynman rule e.g. for the electron-electron-photon vertex can be deduced by considering the QED 3-point function (analogue to (9)) to order e and truncating the two point Green functions of the photon and the ingoing- and outgoing electron.

2.2 Cross section and decay rate

The differential scattering cross section is defined as:

$$\frac{d\sigma}{d\Omega} = \frac{\text{Scattered flux / Unit of solid angle}}{\text{Incident flux / Unit of surface}}. \quad (13)$$

The differential cross section for the scattering of two particles with momenta p_1 and p_2 and masses m_1 and m_2 into n particles with momenta k_1, \dots, k_n is:

$$d\sigma = \frac{1}{4\sqrt{(p_1 \cdot p_2)^2 - m_1^2 m_2^2}} |\mathcal{M}_{fi}|^2 \left[(2\pi)^4 \delta^4 \left(p_1 + p_2 - \sum k_i \right) \frac{d^3 k_1}{(2\pi)^3 2E_1} \cdots \frac{d^3 k_n}{(2\pi)^3 2E_n} \right], \quad (14)$$

where the first factor is the so called flux factor, the second the squared invariant matrix element \mathcal{M} and the last the Lorentz invariant phase space $d\mathcal{PS}(n)$ which –depending on the kinematics of the process– can be substantially simplified. This is carried out in detail for 2,3 and 4 particle phase spaces in appendix E. An especially simple case arises in e.g. Bhabha scattering, where all particles have the same mass. Using the simplifications of appendix E, we can rewrite the $2 \rightarrow 2$ differential cross section of Bhabha scattering in the center of mass (cm) frame as

$$\frac{d\sigma}{d\Omega} = \frac{|\mathcal{M}_{fi}|^2}{64\pi^2 s} \quad (15)$$

with the solid angle $d\Omega = d\phi d\cos\theta$ and the Mandelstam invariant $s = (p_1 + p_2)^2$.

The decay width Γ is a measure for the number of decayed particles per unit time. The decay width of a particle with 4-momentum $p^\mu = (E, p)$ into a final state with n particles with momenta k_1, \dots, k_n is:

$$d\Gamma = \frac{1}{2E} |\mathcal{M}_{fi}|^2 \left[(2\pi)^4 \delta^4 \left(p - \sum k_i \right) \frac{d^3 k_1}{(2\pi)^3 2E_1} \cdots \frac{d^3 k_n}{(2\pi)^3 2E_n} \right]. \quad (16)$$

3 Electroweak part of the standard model

In this section we give a brief introduction to the structure of the GWS theory [17], [18] and [19]. Each term of the Lagrangian is given explicitly and their individual roles are explained. The whole GWS Lagrangian consists out of the following summands:

$$\mathcal{L}_{\text{GWS}} = \underbrace{\mathcal{L}_{\text{gauge}} + \mathcal{L}_{\text{fermionic}} + \mathcal{L}_{\text{Higgs}} + \mathcal{L}_{\text{Yukawa}}}_{\text{classical}} + \underbrace{\mathcal{L}_{\text{fix}} + \mathcal{L}_{\text{ghost}}}_{\text{quantum}}, \quad (17)$$

where a consistent quantization of the classical part demands the introduction of a gauge fixing \mathcal{L}_{fix} and a ghost term $\mathcal{L}_{\text{ghost}}$.

3.1 Classical GWS Lagrangian

The Lagrangians of pure gauge theory and the fermionic part are

$$\mathcal{L}_{\text{gauge}} = -\frac{1}{4}F_{\mu\nu}^a F^{a\mu\nu} - \frac{1}{4}G_{\mu\nu} G^{\mu\nu}, \quad (18)$$

$$\mathcal{L}_{\text{fermionic}} = \sum_i [\bar{L}_i^L(i\not{D})L_i^L + \bar{Q}_i^L(i\not{D})Q_i^L + \bar{l}_i^R(i\not{D})l_i^R + \bar{u}_i^R(i\not{D})u_i^R + \bar{d}_i^R(i\not{D})d_i^R], \quad (19)$$

where $F_{\mu\nu}^a$ is the field strength tensor of $SU(2)_L$ Yang-Mills theory (where L indicates the action only on left handed doublets) and $G_{\mu\nu}$ the field strength tensor of $U(1)_Y$ abelian gauge theory:

$$\begin{aligned} F_{\mu\nu}^a &= \partial_\mu W_\nu^a - \partial_\nu W_\mu^a - g_2 \epsilon^{abc} W_\mu^b W_\nu^c, \\ G_{\mu\nu} &= \partial_\mu B_\nu - \partial_\nu B_\mu. \end{aligned} \quad (20)$$

Right-handed fermions are $SU(2)_L$ -singlets, left-handed fermions are $SU(2)_L$ -doublets, with the particle in the upper entry having weak isospin $I_W^3 = +1$ and the particle in the lower entry $I_W^3 = -1$. The left handed leptonic- L_i^L and left handed quark-doublets Q_i^L (i labels the three generations and for quarks color), as well as the covariant derivative D_μ are defined as follows:

$$\begin{aligned} \Psi_L &= \frac{1 - \gamma_5}{2} \Psi, \quad L_i^L = \begin{pmatrix} \nu_i^L \\ l_i^L \end{pmatrix}, \quad Q_i^L = \begin{pmatrix} u_i^L \\ d_i^L \end{pmatrix}, \quad i = 1, 2, 3 \\ D_\mu &= \left[\mathbb{1}_{SU(2)} \left(\partial_\mu + ig_1 \frac{Y_W}{2} B_\mu \right) - ig_2 I_W^a W_\mu^a \right]. \end{aligned} \quad (21)$$

Since explicit mass terms for the gauge bosons break gauge invariance (which in turn is essential for both current conservation and the proof of renormalizability [23]) and the naive introduction of fermionic mass terms in a chiral theory is not possible, one introduces the Higgs- and Yukawa-Lagrangian $\mathcal{L}_{\text{Higgs}}$ and $\mathcal{L}_{\text{Yukawa}}$ (in which the fermionic mass terms mix the left- and right-handed fermions, since mass terms with purely left- or purely right-handed fermions vanish identically: $\bar{\psi}^R \psi^R = \bar{\psi}^L \psi^L = 0$). Due to the value of the Higgs coupling constant and mass $\mu^2, \lambda > 0$, the new Lagrangian (that is labeled as classical above) is said to inhibit *spontaneous symmetry breaking* which is really a somewhat misleading term, since the whole reason for introducing the Higgs mechanism into the GWS theory is to not break the gauge symmetry. What is broken by the Higgs' acquisition of a non-zero vev is the rotational invariance of the Higgs potential, but not the gauge symmetry. The necessity to choose one of the physically equivalent ground states as basis for the perturbation theory merely hides the gauge invariance. Further the symmetry breaking in the standard model is not a dynamical process like e.g. in ferromagnets. In ferromagnets above the Curie temperature T_c the dipoles are randomly orientated and the system is invariant under spacial rotations. Below T_c , however, the magnetization (measuring the magnetic dipole density) acquires a constant nonzero value which points in a certain direction. The rotational symmetry is broken by

the transition of the system below T_c . In the electroweak model however a similar transition from a phase of unbroken- to broken $U(1)_Y \times SU(2)_L$ would amount to varying the constants μ^2 and λ . Such a variation is possible on a cosmic scale, however symmetry breaking in the electroweak model should not be viewed as a process that happens "spontaneously" in the sense that it might be observed at a particular point in time in a laboratory. So –if one wants to exaggerate the point– one has to assess that *spontaneous symmetry breaking* in the standard model is neither spontaneous nor does it break a gauge symmetry.

As a last remark the appearance of new massless scalar particles due to the Goldstone theorem should be mentioned, their number equals the number of broken generators of the group. However in gauge theories, these scalars are unphysical degrees of freedom, since they can be gauged away in a so called unitary gauge. In a general gauge choice they appear as virtual particles in Feynman diagrams and are referred to as would-be Goldstone bosons.

Explicitly the Higgs and Yukawa terms read:

$$\begin{aligned}\mathcal{L}_{\text{Higgs}} &= (D_\mu \Phi)^\dagger (D^\mu \Phi) - V(\Phi), \quad V(\Phi) = \frac{\lambda}{4} (\Phi^\dagger \Phi)^2 - \mu^2 \Phi^\dagger \Phi, \\ \mathcal{L}_{\text{Yukawa}} &= \sum_{ij} \left[\bar{L}_i^L (G_{ij}^l) l_j^R \Phi + \bar{Q}_i^L (G_{ij}^u) u_j^R \Phi^c + \bar{Q}_i^L (G_{ij}^d) d_j^R \Phi + h.c. \right].\end{aligned}\quad (22)$$

In order to quantize the Higgs doublet, one expands it around an energy minimum v :

$$\begin{aligned}\Phi(x) &= \begin{pmatrix} \phi^+(x) \\ \frac{1}{\sqrt{2}}[v + \eta(x) + i\chi(x)] \end{pmatrix}, \quad \phi^- \equiv [\phi^+]^\dagger, \quad \Phi_0 \equiv \begin{pmatrix} 0 \\ v/\sqrt{2} \end{pmatrix}, \\ \Phi^c &= i\tau_2 \Phi^* = (\phi^{0*}, -\phi^-), \quad M_{ij}^f = \frac{v}{\sqrt{2}} G_{ij}^f,\end{aligned}\quad (23)$$

with the would-be Goldstone bosons ϕ^\pm, χ . The Higgs mechanism breaks the $U(1)_Y \times SU(2)_L$ symmetry in such a way that the electromagnetic symmetry $U(1)_{em}$ is the remaining symmetry. The resulting physical fields are related to the ones in $U(1)_Y \times SU(2)_L$ by:

$$W_\mu^\pm = \frac{1}{\sqrt{2}} [W_\mu^1 \mp iW_\mu^2], \quad \begin{pmatrix} A_\mu \\ Z_\mu \end{pmatrix} = \begin{pmatrix} \cos \theta_W & -\sin \theta_W \\ \sin \theta_W & \cos \theta_W \end{pmatrix} \begin{pmatrix} B_\mu \\ W_\mu^3 \end{pmatrix},\quad (24)$$

with the Weinberg angle θ_W defined through

$$\cos \theta_W = \frac{g_2}{\sqrt{g_1^2 + g_2^2}} = \frac{M_W}{M_Z}, \quad \sin \theta_W = \frac{g_1}{\sqrt{g_1^2 + g_2^2}}.\quad (25)$$

The masses of the weak gauge fields and the Higgs particle are

$$M_W = \frac{v}{2} g_2, \quad M_Z = \frac{v}{2} \sqrt{g_1^2 + g_2^2}, \quad M_H = \sqrt{2} \mu,\quad (26)$$

and the electric charge e is

$$e = g_1 \cos \theta_W = g_2 \sin \theta_W.\quad (27)$$

Further the third generator of weak isospin I_W^3 and the generator of weak hypercharge Y_W are combined in the Gell-Mann-Nishijima relation and give the generator of the electric charge:

$$Q = I_W^3 + \frac{Y_W}{2}.\quad (28)$$

3.2 Quantum part of the GWS Lagrangian

When quantizing gauge theories, one faces multiple subtleties. The most obvious might be that –using canonical quantization– the conjugate momentum to the time component of the field is zero and we do not know how to implement the canonical commutation relations. Formally fixing a gauge is equivalent to imposing a set of constraints⁴ on the fields. These constraints (e.g. $X^\mu B_\mu = 0$ for

⁴For a general and mathematically rigorous discussion of Dirac quantization of constraint systems see [61].

an appropriate X^μ) are imposed by introducing a Lagrange multiplier $\lambda = -1/2\xi$. For the classical part of the GWS Lagrangian this means that we need to add the following term:

$$\mathcal{L}_{\text{fix}} = -\frac{1}{2\xi_A}(C^A)^2 - \frac{1}{2\xi_Z}(C^Z)^2 - \frac{1}{2\xi_W}C^+C^-, \quad (29)$$

with

$$C^A := \partial^\mu A_\mu, \quad C^Z := \partial^\mu Z_\mu - M_Z \xi'_Z \chi, \quad C^\pm := \partial^\mu W_\mu^\pm \mp iM_W \xi'_W \phi^\pm. \quad (30)$$

Where we implemented a Lorentz (covariant) gauge, i.e. $X^\mu = \partial^\mu$.

In the path integral formalism the necessity for introducing a gauge fixing term arises from the fact that otherwise the propagator for the gauge fields cannot be defined. This is the case because the propagator is defined as the Greens function (functional inverse) of the operator that is being sandwiched by the fields (pure gauge theory can easily be brought into this form by adding a total derivative to the above Lagrangian), but without the fixing term the operator has zero eigenvalue and thus no inverse.

The introduction of the ghost term

$$\mathcal{L}_{\text{ghost}} = - \int d^4z d^4y \left[\bar{u}^a(x) \left[\frac{\delta C^a(x)}{\delta V_\mu^c(z)} \frac{\delta V_\mu^c(z)}{\delta \theta^b(y)} + \frac{\delta C^a(x)}{\delta \phi^c(z)} \frac{\delta \phi^c(z)}{\delta \theta^b(y)} \right] u^b(y) \right], \quad (31)$$

with the ghost fields u^a , $\phi^Z := \chi$, $a, b, c \in \{A, Z, \pm\}$ and $V_\mu^c \in \{A_\mu, Z_\mu, W_\mu^\pm\}$, is also necessitated by the redundancies in our theory connected with the gauge freedom of the vector bosons. In solving the path integral over the gauge field in (11), we neglected discussing these subtleties. It turns out however, that this was no blunder, since the theory we were discussing was QED which is abelian. In abelian theories the ghost term gives only an irrelevant normalization factor and can be omitted. In non-abelian theories – such as GSW or QCD – the introduction is necessary to assure (BRS-)gauge invariance and thus unitarity, conservation laws, renormalizability.

Loosely speaking, the ghost term repairs what the fixing term broke: gauge invariance. However – in the standard model – it is not the classical non-abelian $SU(2) \times SU(3)$ symmetry that is being restored, but the so called Becchi-Rouet-Stora (BRS) symmetry⁵ [58] which leaves the classical and the quantum part of the Lagrangian separately invariant.

In the path integral picture the integration over the physically equivalent configurations results for each space-time point in the volume of the gauge group and thus in an infinite overall factor of the generating functional $Z[J^\mu]$. This factor drops out since one only deals with the ratio $Z[J^\mu]/Z[0]$. L.D. Faddeev and V.N. Popov [59] developed a method to separate this factor, introducing Grassmann valued scalar ghost fields. These fields violate the spin-statistic theorem, which however is not problematic, since they are purely virtual, unphysical particles.

⁵In canonical quantization BRS symmetry is often discussed using auxiliary Nakanishi-Lautrup fields.

4 Infrared divergences and Bloch-Nordsieck cancellation

As stressed in the introduction, Bremsstrahlung diagrams with soft photons of energy E_γ below the detection threshold ω must be added to any process since they are indistinguishable from the diagrams without radiation.

In this section we discuss the Bloch-Nordsieck cancellation [62], which is the statement, that QED is IR-finite. IR-divergences are divergences that are due to the vanishing of the denominator in the low energy $E_\gamma \rightarrow 0$ region. They arise both from virtual (loop)- and real (phase space)-integrations. Ultra violet (UV)-divergences on the other hand are purely virtual and are due to the divergence of the numerator structure in the high energy $E_\gamma \rightarrow \infty$ region.

IR- and UV-divergences are treated very differently in the standard model. The Kinoshita-Lee-Nauenberg (KLN) theorem [63] and [64] (a generalization of the Bloch-Nordsieck cancellation) assures that the standard model is IR-finite, i.e. we need to evaluate real IR-divergent diagrams and add them to the virtually IR-divergent diagrams they cancel. Where UV-divergences on the other hand must be treated in the context of renormalization. The KLN theorem is crucial to the renormalizability of the standard model.

4.1 IR loop divergences

A massless line in a loop between two outer on shell lines always gives a IR-divergence.

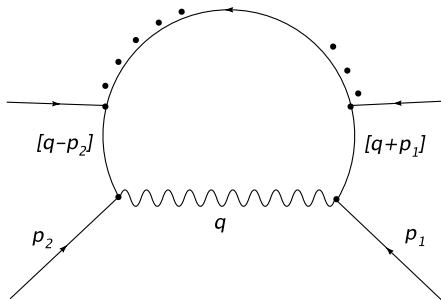


Figure 1: One loop diagram with N legs, at least two of them on shell, with a massless line between them

As in Figure 1, let the two outer particles have the incoming momenta p_1 and p_2 . The momentum of the massless line can be chosen to be the loop momentum q . This gives the massless propagator $d_0 = q^2$ and the propagators left (d_2) and right (d_1) of the massless line:

$$d_1 = [(q + p_1)^2 - m^2] = [2p_1 \cdot q], \quad d_2 = [(q - p_2)^2 - m^2] = [-2p_2 \cdot q]. \quad (32)$$

All other propagators have a more complicated momentum structure which gives extra summands that contain constant terms in q . The loop integral then reads

$$\int \frac{d^4 q X}{q^2 [2p_1 \cdot q] [-2p_2 \cdot q] d_3 d_4 \cdots d_N} \quad (33)$$

With some numerator structure $X(q^\mu, q^\mu q^\nu, \dots)$.

In the IR $q \rightarrow 0$ all propagators d_3, d_4, \dots, d_N are proportional to a constant, due to their constant

summands. The integral is then proportional to the expression

$$\int_0^\infty \frac{dq q^3 X}{q^4} = \int_0^\infty \frac{dq X}{q} \stackrel{X \equiv 1}{=} \ln[q]_0^\infty \quad (34)$$

Which is IR divergent at $q = 0$. The behavior of the whole integral (33) for $X \neq 1$ depends on the structure of the other propagators and cannot be generalized, they might however very well also be IR divergent.

We note, that when we are dealing with a diagram that has a massless line between two on shell lines, we always get a IR divergent integral.

4.2 Bloch-Nordsieck cancellation

The Standard Model as a whole is IR - finite. This result is known as the KLN theorem [63] and [64]. Summing up all real and virtual contributions of massless gauge bosons (photons and gluons), the IR divergences of the loop corrections are canceled by the real IR divergent contributions, yielding as a whole an IR finite theory.

This mechanism at one loop order in QED was first understood by Bloch and Nordsieck [62] in 1937. It was generalized to arbitrary loop order by Yennie et al in [65]. Their proof was presented in a much simplified analysis by Weinberg [66] in 1965.

Since we consider only QED contributions to Bhabha scattering we will follow Weinbergs discussion, limiting ourselves to QED.

4.3 Factorization of real soft-photon contributions

If we for example consider the initial particle 1 to radiate a IR photon with momentum k , according to the Feynman rules out of appendix B we will get the following expression for the leg including radiation:

$$\frac{i(\not{p}_1 - \not{k} + m)}{[(p_1 - k)^2 - m^2 + i\epsilon]} (i e \not{\epsilon}^*) u_1 = \frac{e}{[2(p_1 \cdot k) + i\epsilon]} (\not{p}_1 - \not{k} + m) \not{\epsilon}^* u_1. \quad (35)$$

If we now take the limit of zero photon momentum in the numerator, the gamma matrices turn

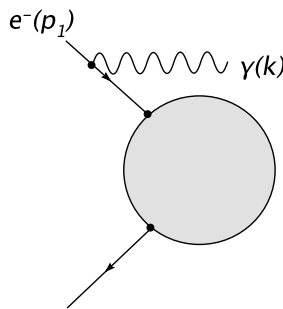


Figure 2: Soft emission in an arbitrary process from an initial particle

into a simple factor and the whole soft divergence factorizes out of the M-Matrix. The limit gives

$$(\not{p}_1 + m) \not{\epsilon}^* u_1 = m \not{\epsilon}^* u_1 + (2 p_1 \cdot \epsilon^* - \not{\epsilon}^* \not{p}_1) u_1 = 2 p_1 \cdot \epsilon^* u_1 - \underbrace{\not{\epsilon}^* (\not{p}_1 - m) u_1}_{=0}. \quad (36)$$

For a photon emission by the incoming particle 1 this limit yields

$$\mathcal{M}_{\text{particle},in}^{\text{IR}} = \frac{e p_1^\mu}{(p_1 \cdot k + i\epsilon)} \mathcal{M}^{\text{Born}} \epsilon_\mu^* \quad (37)$$

For an emission by an antiparticle 2, the momentum sign of the propagator changes, since the momentum flow and the fermion arrow are anti-parallel. For initial state radiation, omitting constants and the denominator, we get

$$\bar{v}_2 \not{\epsilon}^* (-\not{p}_2 + \not{k} + m) \xrightarrow{k \rightarrow 0} \bar{v}_2 \not{\epsilon}^* (-\not{p}_2 + m) = -2p_2 \cdot \epsilon^* \bar{v}_2 + \underbrace{\bar{v}_2 (\not{p}_2 + m)}_{=0} \not{\epsilon}^*, \quad (38)$$

yielding the factorization

$$\mathcal{M}_{\text{antiparticle},in}^{\text{IR}} = \frac{-e p_2^\mu}{(p_2 \cdot k + i\epsilon)} \mathcal{M}^{\text{Born}} \epsilon_\mu^* \quad (39)$$

We find that the M-Matrix factorizes as follow:

$$\mathcal{M}_{f,\eta}^{\text{IR}} = \frac{e Q_f p_i^\mu}{(\eta_f p_i \cdot k + i\epsilon)} \mathcal{M}^{\text{Born}} \epsilon_\mu^* \quad (40)$$

Where Q_f is the charge of the radiative fermion and η_f accounts for whether the fermion is in- or outgoing ($\eta_{in} = -1, \eta_{out} = +1$). η_f is needed because for an incoming fermion we have to subtract the photon momentum from the external fermion momentum to get the one of the propagator, while we add it for an outgoing one.

4.4 Real soft-photon contribution

As shown in the previous section, in the soft limit the contribution from the radiation of a soft photon factorizes out of the Born matrix element. Since all outer fermionic legs can be radiative we sum over all contributions:

$$\mathcal{M}^{i \rightarrow f \gamma} \xrightarrow{k \rightarrow 0} \mathcal{M}^{i \rightarrow f} \left[\sum_l \frac{e Q_l p_l \cdot \epsilon^*}{(\eta_l p_l \cdot k + i\epsilon)} \right]. \quad (41)$$

Further, this can be generalized to the emission of n soft photons. For the emission of two photons we have two contributions, one where photon 1 is emitted first and one where photon 2 is emitted first. The infrared factor for one leg, then reads (omitting the $(i\epsilon)$'s)

$$\begin{aligned} & \left(\frac{e Q p \cdot \epsilon_1^*}{p \cdot k_1} \right) \left(\frac{e Q p \cdot \epsilon_2^*}{p \cdot (k_1 + k_2)} \right) + \left(\frac{e Q p \cdot \epsilon_2^*}{p \cdot k_2} \right) \left(\frac{e Q p \cdot \epsilon_1^*}{p \cdot (k_1 + k_2)} \right) \\ &= \frac{e^2 Q^2 (p \cdot \epsilon_1^*) (p \cdot \epsilon_2^*)}{p_\mu p_\nu} \left[\frac{1}{(k_1 + k_2)^\mu} \left(\frac{1}{k_1^\nu} + \frac{1}{k_2^\nu} \right) \right] = \left(\frac{e Q p \cdot \epsilon_1^*}{p \cdot k_1} \right) \left(\frac{e Q p \cdot \epsilon_2^*}{p \cdot k_2} \right). \end{aligned} \quad (42)$$

This is the product of two factors for single photon emission. By induction it can be proved that the general formula for the amplitude for the emission of n soft photons with momenta k_1, \dots, k_n is given by:

$$\mathcal{M}^{i \rightarrow f(n\gamma)} = \mathcal{M}^{i \rightarrow f} \times \prod_{i=1}^n \left[\sum_l \frac{e Q_l p_l \cdot \epsilon_i^*}{(\eta_l p_l \cdot k_i + i\epsilon)} \right]. \quad (43)$$

There is no limitation on the number of emitted soft photons. We are thus interested in the limit $n \rightarrow \infty$, which we take after squaring the above matrix element. Using the polarization sum

$\sum \epsilon_\mu^* \epsilon_\nu = -g_{\mu\nu}$ and introducing a factor $1/n!$ accounting for the n identical photons in the final state, we get the cross section

$$\begin{aligned} d\sigma_{\text{real, soft}} &= \lim_{n \rightarrow \infty} d\sigma^{i \rightarrow f(n\gamma)} = \lim_{n \rightarrow \infty} d\sigma^{i \rightarrow f} \frac{1}{n!} \left[\prod_{i=1}^n \int \frac{d^3 k_i}{(2\pi)^3 2E_i} \sum_{l,m} \frac{-e^2 Q_l Q_m (p_l \cdot p_m)}{(\eta_l p_l \cdot k_i + i\epsilon)(\eta_m p_m \cdot k_i + i\epsilon)} \right] \\ &= \lim_{n \rightarrow \infty} d\sigma^{i \rightarrow f} \frac{1}{n!} \left[\sum_{l,m} e^2 Q_l Q_m I_{lm} \right]^n = d\sigma^{i \rightarrow f} \exp \left[\underbrace{\sum_{l,m} e^2 Q_l Q_m I_{lm}}_{\delta_{\text{real, soft}}} \right], \end{aligned} \quad (44)$$

where E_i is the energy of the photon i , and

$$I_{lm} = - \int \frac{d^3 k}{(2\pi)^3 2E} \frac{(p_l \cdot p_m)}{(\eta_l p_l \cdot k_i + i\epsilon)(\eta_m p_m \cdot k_i + i\epsilon)} = - \frac{\eta_l \eta_m}{8\pi^2 \beta_{lm}} \log \frac{1 + \beta_{lm}}{1 - \beta_{lm}} \log \frac{\Delta E}{k_{\min}}. \quad (45)$$

Where ΔE is the maximal photon energy and k_{\min} is the minimal photon energy, which was introduced as a regulator of the IR divergence. β_{lm} is given by

$$\beta_{lm} = \sqrt{1 - \frac{m_l^2 m_m^2}{(p_l \cdot p_m)^2}}. \quad (46)$$

4.5 Virtual soft-photon contribution

We know that virtual IR-divergences can only arise if we have a massless inner line between two on shell legs. I.e. we can safely limit ourselves to the contribution of loops involving photon propagators.

The key idea of the proof is to realize that all virtual corrections to any process involving inner photon lines can be generated out of diagrams with an even number of real soft emissions by joining pairs to form virtual photons. Some examples are given in Figure 3. We are still interested in an

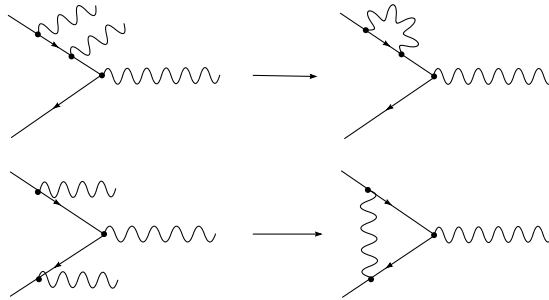


Figure 3: We can obtain all loop corrections involving massless inner lines, by considering an even number of soft emissions and joining pairs to form massless propagators.

analysis that includes virtual soft photons of all orders of perturbation theory (the limit $n \rightarrow \infty$). Omitting the photon polarization tensors in (43) and introducing a propagator term $-ig^{\mu\nu}/(k^2 + i\epsilon)$ for each generated inner photon line, we get the virtual corrections due to n photons

$$\mathcal{M}_{\text{virtual, soft}}^{i \rightarrow f} = \lim_{n \rightarrow \infty} \mathcal{M}^{i \rightarrow f} \times \frac{1}{n!} \left[\frac{1}{2} \sum_{l,m} e^2 Q_l Q_m J_{lm} \right]^n = \mathcal{M}^{i \rightarrow f} \exp \left[\frac{1}{2} \sum_{l,m} e^2 Q_l Q_m J_{lm} \right] \quad (47)$$

with

$$J_{lm} = \int \frac{d^4k}{(2\pi)^4} \frac{-ig^{\mu\nu}}{(k^2 + i\epsilon)} \frac{p_l^\mu p_m^\mu}{(\eta_l p_l \cdot k + i\epsilon)(-\eta_m p_m \cdot k + i\epsilon)}. \quad (48)$$

The factor $1/n!$ cancels the $n!$ equivalent permutations of the ends of the photon lines that we join together to form photon propagators. The $1/2$ takes the 2 equivalent contributions into account that result from exchanging the two photon lines that are joined to form one inner line. And finally we have changed the sign of $(p_m \cdot k)$ in one of the denominators, because after joining, the photon momentum at one of the vertices must be ingoing.

One might be sceptical whether (48) also holds for $l = m$. E.g. (48) has three propagator terms, where as for a simple fermionic self energy (which is the graph we get in the $l = m$ case) we only have two. However, it has been shown by [65] that (47) is also valid for $l = m$. Introducing the UV- and IR-regulators k_{max} and k_{min} , the evaluation of (48) yields

$$J_{lm} = \frac{\eta_l \eta_m}{8\pi^2 \beta_{lm}} \left[\log \frac{1 + \beta_{lm}}{1 - \beta_{lm}} - 2\pi i \theta(\eta_l \eta_m) \right] \log \frac{k_{max}}{k_{min}}. \quad (49)$$

Since the number of outer particles for the virtual corrections is the same as for the Born contribution, we can write the cross section as

$$\begin{aligned} d\sigma_{\text{virtual,soft}} &= \exp \left[\frac{1}{2} \sum_{l,m} e^2 Q_l Q_m (J_{lm} + J_{lm}^*) \right] d\sigma^{i \rightarrow f} \\ &= \exp \left[\sum_{l,m} e^2 Q_l Q_m \text{Re}[J_{lm}] \right] d\sigma^{i \rightarrow f}. \end{aligned} \quad (50)$$

4.6 Cancellation of the IR-divergences

The general factorization (43) holds no matter if we consider the photon emission from a Born diagram or a diagram with an arbitrary number of loops. That is (43) yields the independence of the virtual and real factors. The whole contribution is:

$$\begin{aligned} d\sigma_{\text{soft}} &= \delta^{\text{real,soft}} \times d\sigma_{\text{virtual,soft}} = \exp \left[\sum_{l,m} e^2 Q_l Q_m (\text{Re}[J_{lm}] + I_{lm}) \right] d\sigma^{i \rightarrow f} \\ &= \exp \left[\sum_{l,m} e^2 Q_l Q_m \frac{\eta_l \eta_m}{8\pi^2 \beta_{lm}} \log \frac{1 + \beta_{lm}}{1 - \beta_{lm}} \left(\log \frac{k_{max}}{k_{min}} - \log \frac{\Delta E}{k_{min}} \right) \right] d\sigma^{i \rightarrow f} \\ &= \exp \left[\sum_{l,m} e^2 Q_l Q_m \frac{\eta_l \eta_m}{8\pi^2 \beta_{lm}} \log \frac{1 + \beta_{lm}}{1 - \beta_{lm}} \log \frac{k_{max}}{\Delta E} \right] d\sigma^{i \rightarrow f} \end{aligned} \quad (51)$$

We see that the IR cut-off k_{min} drops out and yields $d\sigma_{\text{soft}}$ IR-finite. The UV-divergence which is still present through the regulator k_{max} would now need to be treated through renormalization.

5 Soft photon correction to Bhabha scattering

Photons are massless gauge bosons, which allows them to be produced at arbitrarily small energies. Any physical calorimeter has a finite resolution. We therefore have to take soft photon emission below the resolution ω into account, by evaluating diagrams like the ones in Figure 4.

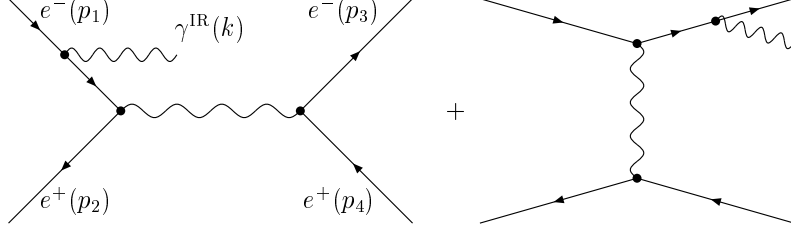


Figure 4: s-channel and t-channel Bhabha Scattering with a soft photon emission

We have a total of eight radiative Born diagrams, the s- and t-channel contributions with soft emission from any of the four legs.

5.1 Factorization of the IR-divergence

Applying the IR-factorization deduced in the last section, to single soft photon emission from all four legs in Born level Bhabha Scattering, we find

$$\mathcal{M}^{\text{IR}} = \left[\frac{e p_1^\mu}{(p_1 \cdot k)} - \frac{e p_2^\mu}{(p_2 \cdot k)} - \frac{e p_3^\mu}{(p_3 \cdot k)} + \frac{e p_4^\mu}{(p_4 \cdot k)} \right] \mathcal{M}^{\text{Born}} \epsilon_\mu^*. \quad (52)$$

The whole cross section then reads

$$\frac{d\sigma^{\text{IR}}}{d \cos \theta} = \left[\frac{\alpha}{\pi} \delta^{\text{IR}} \right] \times \frac{d\sigma^{\text{Born}}}{d \cos \theta}, \quad (53)$$

with the infrared factor

$$\delta^{\text{IR}} = 4\pi^2 \int \left[\frac{d^3k}{(2\pi)^3 2E_\gamma} \Theta[\omega - E_\gamma] \right] \left[\frac{p_1}{(p_1 \cdot k)} - \frac{p_2}{(p_2 \cdot k)} - \frac{p_3}{(p_3 \cdot k)} + \frac{p_4}{(p_4 \cdot k)} \right]_{\mu\nu}^2 \underbrace{\left[\sum_{\lambda=1}^2 \epsilon_\lambda^{*\mu} \epsilon_\lambda^\nu \right]}_{=-g^{\mu\nu}}, \quad (54)$$

and the photon energy E_γ .

5.2 The Born cross section

For the evaluation of the Born cross section we choose the center-of-mass (cm) system of the incoming particles, which is given by

$$p_{1,2} = \sqrt{s}/2(1, 0, 0, \pm\beta), \quad p_{3,4} = \sqrt{s}/2(1, \pm\beta \sin \theta, 0, \pm\beta \cos \theta). \quad (55)$$

The masses and energies of all particles are equal, which yields that the absolute values of all 3-vectors are also equal:

$$p := |\vec{p}_i| = \sqrt{E_i^2 - m^2} = \frac{\sqrt{s}}{2}\beta, \quad (56)$$

with the velocity $\beta := \frac{p}{E} = \sqrt{1 - \frac{4m^2}{s}}$.

We use the Mandelstam invariants

$$\begin{aligned} s &= (p_1 + p_2)^2 = (p_3 + p_4)^2, \\ t &= (p_1 + p_3)^2 = (p_2 - p_4)^2 = 2m^2 - s/2(1 - \beta \cos \theta), \\ u &= (p_1 + p_4)^2 = (p_2 - p_3)^2 = 2m^2 - s/2(1 + \beta \cos \theta), \end{aligned} \quad (57)$$

to express the Born QED cross section, which is

$$\frac{d\sigma^{\text{QED,Born}}}{d\cos\theta} = \frac{e^4}{\pi} [\sigma_s + \sigma_{st} + \sigma_t], \quad (58)$$

with

$$\begin{aligned} \sigma_s &= \frac{1}{8s^3} \left[\frac{s^2}{2} + st + (2m^2 - t)^2 \right], \\ \sigma_{st} &= \frac{1}{8s^2t} [(s+t)^2 - 4m^4], \\ \sigma_t &= \frac{1}{8st^2} \left[\frac{t^2}{2} + st + (2m^2 - s)^2 \right]. \end{aligned} \quad (59)$$

5.3 The IR-divergent factor δ^{IR}

The emitted Bremsstrahlung is soft, i.e. the photon energy E_γ is below the detection threshold ω :

$$E_\gamma < \omega < \sqrt{s}, m. \quad (60)$$

The infrared factor takes the form

$$\delta^{\text{IR}} = 4\pi^2 \int \left[\frac{d^3k}{(2\pi)^3 2E_\gamma} \Theta[\omega - E_\gamma] \right] I^{\text{IR}}, \quad (61)$$

with

$$\begin{aligned} I^{\text{IR}} &:= \underbrace{\left[\frac{2p_1 \cdot p_2}{(p_1 \cdot k)(p_2 \cdot k)} - \frac{p_1^2}{(p_1 \cdot k)^2} - \frac{p_2^2}{(p_2 \cdot k)^2} \right]}_{:=I_{(12)}^{\text{IR}}} + \underbrace{\left[\frac{2p_3 \cdot p_4}{(p_3 \cdot k)(p_4 \cdot k)} - \frac{p_3^2}{(p_3 \cdot k)^2} - \frac{p_4^2}{(p_4 \cdot k)^2} \right]}_{:=I_{(34)}^{\text{IR}}} \\ &+ 2 \left[\underbrace{\left[\frac{p_1 \cdot p_3}{(p_1 \cdot k)(p_3 \cdot k)} - \frac{p_1 \cdot p_4}{(p_1 \cdot k)(p_4 \cdot k)} \right]}_{:=I_{(13)}^{\text{IR}}} + \underbrace{\left[\frac{p_2 \cdot p_4}{(p_2 \cdot k)(p_4 \cdot k)} - \frac{p_2 \cdot p_3}{(p_2 \cdot k)(p_3 \cdot k)} \right]}_{:=I_{(24)}^{\text{IR}}} \right]. \end{aligned} \quad (62)$$

We will use the on-shell condition $p_i^2 = m^2$ as well as the Mandelstam relations

$$\begin{aligned} 2p_1 \cdot p_2 &= 2p_3 \cdot p_4 = (s - 2m^2) \\ T &:= 2p_1 \cdot p_3 = 2p_2 \cdot p_4 = (2m^2 - t) \\ U &:= 2p_1 \cdot p_4 = 2p_2 \cdot p_3 = (2m^2 - u). \end{aligned} \quad (63)$$

For two arbitrary 4-vectors q_1, q_2 , one can write their scalar product as

$$q_1 \cdot q_2 = q_1^0 q_2^0 (1 - \beta_1 \beta_2 \cos \theta). \quad (64)$$

Since for massless particles their energy and the absolute value of their momentum are equal, we have $\beta_\gamma = \frac{|\vec{k}|}{E_\gamma} = 1$, which yields

$$p_i \cdot k = p_i^0 E_\gamma (1 - \beta_i \cos \theta_i), \quad \beta_i = \frac{|\vec{p}_i|}{p_i^0}. \quad (65)$$

Each non-interference term now only depends on one variable, namely $\cos \theta_i$. To apply the same formalism for the interference terms with $i \neq j$, we introduce a Feynman parameter α

$$\frac{p_i \cdot p_j}{(p_i \cdot k)(p_j \cdot k)} = \int_0^1 d\alpha \frac{p_i \cdot p_j}{(p_\alpha^{(ij)} \cdot k)^2}, \quad p_\alpha^{(ij)} = p_i \alpha + p_j (1 - \alpha). \quad (66)$$

The fact that all energies are equal, gives

$$p_\alpha^0 = p_i^0 = \sqrt{s}/2 \quad (67)$$

for all $p_\alpha^{(ij)}$. The momenta and therefore the velocities $\beta_\alpha^{(ij)}$ differ however. For initial- $\beta_\alpha^{(12)}$ and final state $\beta_\alpha^{(34)}$ radiation, these relations are still fairly simple

$$(p_\alpha^{(12)})^2 = (p_\alpha^{(34)})^2 = m^2 + (s - 4m^2)\alpha(1 - \alpha), \quad (68)$$

which gives us the velocities

$$\beta_\alpha^{(12)} = \beta_\alpha^{(34)} = \beta \sqrt{(1 - 2\alpha)^2}. \quad (69)$$

The equality of not only the individual velocities and energies, but also the ones of the initial interference terms and final interference terms, give the equality of $I_{(12)}^{\text{IR}}$ and $I_{(34)}^{\text{IR}}$.

Using kinematic relations we further find

$$\begin{aligned} (p_\alpha^{(13)})^2 = (p_\alpha^{(24)})^2 &= m^2 + (T - 2m^2)\alpha(1 - \alpha) \\ (p_\alpha^{(14)})^2 = (p_\alpha^{(23)})^2 &= m^2 + (U - 2m^2)\alpha(1 - \alpha), \end{aligned} \quad (70)$$

which yields the equality of $I_{(13)}^{\text{IR}}$ and $I_{(24)}^{\text{IR}}$. In conclusion we rewrite

$$\delta^{\text{IR}} = 4\pi^2 \int_0^1 d\alpha \int \left[\frac{d^3 k}{(2\pi)^3 2E_\gamma} \Theta[\omega - E_\gamma] \right] \left[2\mathcal{I}_{(12)}^{\text{IR}} + 2\mathcal{I}_{(13)}^{\text{IR}} \right], \quad (71)$$

with

$$\begin{aligned} \mathcal{I}_{(12)}^{\text{IR}} &= \frac{(s - 2m^2)}{(p_\alpha^{(12)} \cdot k)^2} - \frac{2m^2}{(p_1 \cdot k)^2} = \frac{1}{E_\gamma^2} \left[\frac{(s - 2m^2)}{(p_\alpha^0)^2 (1 - \beta_\alpha^{(12)} \cos \theta)} - \frac{2m^2}{(p_1^0)^2 (1 - \beta \cos \theta)} \right], \\ \mathcal{I}_{(13)}^{\text{IR}} &= \frac{T}{(p_\alpha^{(13)} \cdot k)^2} - \frac{U}{(p_\alpha^{(23)} \cdot k)^2} = \frac{1}{E_\gamma^2} \left[\frac{T}{(p_\alpha^0)^2 (1 - \beta_\alpha^{(13)} \cos \theta)} - \frac{U}{(p_\alpha^0)^2 (1 - \beta_\alpha^{(23)} \cos \theta)} \right]. \end{aligned} \quad (72)$$

The angles are in fact all different to one another. Normally we would have to distinguish them, but since in each summand there is only one angle, we can always choose that angle to be the angular integration variable.

The E_γ^{-2} in $\mathcal{I}_{(ij)}^{\text{IR}}$ combined with the E_γ^{-1} in the measure give the IR divergence

$$\int \frac{d^3 k}{E_\gamma^3} \Theta[\omega - E_\gamma] = \int d\Omega_\gamma \int_0^\omega \frac{dE_\gamma E_\gamma^2}{E_\gamma^3} = \int d\Omega_\gamma [\ln(E_\gamma)]_0^\omega, \quad (73)$$

which we will treat with dimensional regularization.

5.4 Initial state radiation

The pure initial state radiation, which - as we noted in the last section - is equal to pure final state radiation, gives the contribution

$$\delta^{\text{IR},\text{in}} = 4\pi^2 \int_0^1 d\alpha \int \left[\frac{d^3k}{(2\pi)^3 2E_\gamma} \Theta[\omega - E_\gamma] \right] \mathcal{I}_{(12)}^{\text{IR}}, \quad (74)$$

to the whole IR-factor. As already mentioned, this integral is IR-divergent and we therefore dimensionally regularize it by the standard way of going from $d = 4$ to $d = 4 - 2\epsilon$ dimensions. Note however, that the regularization parameter ϵ has to be negative for the case of pure IR-divergences.

$$d^3k \longrightarrow d^{(d-1)}k = dE_\gamma E_\gamma^{d-2} d\Omega_{(d-1)} \quad (75)$$

with

$$d\Omega_{(d-1)} = \prod_{l=1}^{d-2} \sin^{d-2-l} \theta_l d\theta_l = \left[\sin^{d-3} \theta_1 d\theta_1 \right] d\Omega_{(d-2)} = \frac{2\pi^{d/2-1}}{\Gamma[d/2-1]} \left[\sin^{d-3} \theta_1 d\theta_1 \right]. \quad (76)$$

where we have integrated over $d\Omega_{(d-2)}$ in the last step.

$$\delta^{\text{IR},\text{in}} \longrightarrow \frac{2\pi^{d/2-1}}{\Gamma[d/2-1]} \frac{(2\pi\mu)^{(4-d)}}{4\pi} \int_0^1 d\alpha \int_0^\omega \frac{dE_\gamma}{E_\gamma^{(3-d)}} \int_0^\pi d\theta \sin^{d-3} \theta \mathcal{I}_{(12)}^{\text{IR}} \quad (77)$$

The conventional factor $(2\pi\mu)^{(4-d)}$ is multiplied onto the expression, to account for dimensional transmutation. We use the integrals

$$\begin{aligned} \int_0^\omega \frac{dE_\gamma}{\mu^{(d-4)}} E_\gamma^{(d-5)} &= \frac{(\omega/\mu)^{(d-4)}}{d-4} = \frac{1}{d-4} [1 + (d-4) \ln[\omega/\mu] + \mathcal{O}(\epsilon)], \\ \int_0^\pi \frac{d\theta \sin^{d-3} \theta}{(1 - \beta_i \cos \theta)^2} &= \int_{-1}^{+1} \frac{dx (1-x^2)^{(d/2-2)}}{(1 - \beta_i x)^2} \\ &= \int_{-1}^{+1} \frac{dx}{(1 - \beta_i x)^2} \left[1 + \frac{d-4}{2} \ln[1-x^2] + \mathcal{O}(\epsilon^2) \right], \end{aligned} \quad (78)$$

and neglect terms of $\mathcal{O}(\epsilon)$ in the first and of $\mathcal{O}(\epsilon^2)$ in the second integral. Using the expansion

$$\frac{2\pi^{d/2-1}}{\Gamma[d/2-1]} \frac{(2\pi)^{(4-d)}}{4\pi} = \frac{1}{2} + \mathcal{O}(\epsilon), \quad (79)$$

we get

$$\begin{aligned} \delta^{\text{IR},\text{in}} &= [\text{P}^{\text{IR}} + \ln[\omega/\mu]] \frac{1}{2} \int_0^1 d\alpha \int_{-1}^{+1} dx \mathcal{F}(\alpha, x) \\ &+ \frac{1}{4} \int_0^1 d\alpha \int_{-1}^{+1} dx \ln[1-x^2] \mathcal{F}(\alpha, x), \end{aligned} \quad (80)$$

with

$$\mathcal{F}(\alpha, x) = \frac{s - 2m^2}{(p_\alpha^0)^2 (1 - \beta_\alpha^{(12)} x)^2} - \frac{8m^2}{s(1 - \beta x)^2}, \quad \text{P}^{\text{IR}} = \frac{-1}{2\epsilon}. \quad (81)$$

The IR-divergence appears as the ϵ -pol P^{IR} . We further proceed by evaluating the x-integrals

$$\begin{aligned} \int_{-1}^{+1} \frac{1}{(1 - \beta_i x)^2} &= \frac{2}{1 - \beta_i^2} \\ \int_{-1}^{+1} \frac{\ln[1-x^2]}{(1 - \beta_i x)^2} &= \frac{2}{1 - \beta_i^2} \left[2 \ln 2 - \frac{1}{\beta_i} \ln \frac{1 + \beta_i}{1 - \beta_i} \right]. \end{aligned} \quad (82)$$

Using $(p_i^0)^2(1 - \beta_i^2) = (p_i)^2$ we get

$$\begin{aligned} \frac{1}{2} \int_0^1 d\alpha \int_{-1}^{+1} dx \mathcal{F}(\alpha, x) &= (s - 2m^2) \int_0^1 \frac{d\alpha}{(p_\alpha^{(12)})^2} - 2 \\ \frac{1}{4} \int_0^1 d\alpha \int_{-1}^{+1} dx \ln[1 - x^2] \mathcal{F}(\alpha, x) &= \ln 2 \left[(s - 2m^2) \int_0^1 \frac{d\alpha}{(p_\alpha^{(12)})^2} - 2 \right] - \frac{1}{\beta} \ln \frac{1 - \beta}{1 + \beta} \\ &+ \frac{s - 2m^2}{2} \left[\int_0^1 \frac{d\alpha}{\beta_\alpha (p_\alpha^{(12)})^2} \ln \frac{1 - \beta_\alpha}{1 + \beta_\alpha} \right], \end{aligned} \quad (83)$$

with the Feynman parameter integrals

$$\int_0^1 \frac{d\alpha}{(p_\alpha^{(12)})^2} = \int_0^1 \frac{d\alpha}{(s - 4m^2)\alpha(1 - \alpha) + m^2} = \frac{2}{s\beta} \ln \frac{1 + \beta}{1 - \beta} \quad (84)$$

and

$$\begin{aligned} \int_0^1 \frac{d\alpha}{\beta_\alpha (p_\alpha^{(12)})^2} \ln \frac{1 - \beta_\alpha}{1 + \beta_\alpha} &= \int_0^1 \frac{d\alpha}{(s - 4m^2)\alpha(1 - \alpha) + m^2} \frac{1}{\beta\sqrt{(1 - 2\alpha)^2}} \ln \frac{1 - \beta\sqrt{(1 - 2\alpha)^2}}{1 + \beta\sqrt{(1 - 2\alpha)^2}} \\ &= \frac{4}{s\beta} \int_0^1 \frac{dy}{y(1 - \beta y)(1 + \beta y)} \ln \frac{1 - \beta y}{1 + \beta y} \\ &= \frac{-2}{s\beta} \left[2\text{Li}_2[-\beta] - \text{Li}_2\left[\frac{1 - \beta}{2}\right] - 2\text{Li}_2[\beta] + \text{Li}_2\left[\frac{\beta + 1}{2}\right] \right. \\ &\quad \left. - \frac{1}{2} \ln^2 \frac{1 - \beta}{2} + \frac{1}{2} \ln^2 \frac{\beta + 1}{2} \right]. \end{aligned} \quad (85)$$

Inserting these integrals, we find the final result

$$\begin{aligned} \delta^{\text{IR, in}} &= 2 [\text{P}^{\text{IR}} + \ln[2\omega/\mu]] \left[\frac{(s - 2m^2)}{s\beta} \ln \frac{1 + \beta}{1 - \beta} \right] - \frac{1}{\beta} \ln \frac{1 - \beta}{1 + \beta} \\ &- \frac{s - 2m^2}{s\beta} \left[2\text{Li}_2[-\beta] - \text{Li}_2\left[\frac{1 - \beta}{2}\right] - 2\text{Li}_2[\beta] + \text{Li}_2\left[\frac{1 + \beta}{2}\right] \right. \\ &\quad \left. - \frac{1}{2} \ln^2 \frac{1 - \beta}{2} + \frac{1}{2} \ln^2 \frac{\beta + 1}{2} \right]. \end{aligned} \quad (86)$$

5.5 Interference of initial- and final state radiation

Note that in the previous section we could have also calculated the interference term without having to introduce Feynman parameters. This is possible by making use of the simple relation

$$\frac{1}{(p_1 \cdot k)(p_2 \cdot k)} = \frac{1}{(p_1 + p_2) \cdot k} \left[\frac{1}{(p_1 \cdot k)} + \frac{1}{(p_2 \cdot k)} \right] = \frac{1}{\sqrt{s} E_\gamma} \left[\frac{1}{(p_1 \cdot k)} + \frac{1}{(p_2 \cdot k)} \right]. \quad (87)$$

We did however choose the seemingly harder path via Feynman parameters, because in the interference term of initial- and final state radiation, we have no such identity that would allow us to choose a more direct approach. The following calculation is now analogous to the one presented in the previous section. We evaluate the following integral

$$\delta^{\text{IR, in, out}} = 4\pi^2 \int_0^1 d\alpha \int \left[\frac{d^3 k}{(2\pi)^3 2E_\gamma} \Theta[\omega - E_\gamma] \right] 2\mathcal{I}_{(13)}^{\text{IR}}. \quad (88)$$

Note that in (72) the only difference between $\mathcal{I}_{(12)}^{\text{IR}}$ and $\mathcal{I}_{(13)}^{\text{IR}}$, except for factors, are the $\beta_\alpha^{(ij)}$. The regularization will be the same as in (77) and the E_γ -, θ - and \mathbf{x} -integrals arising will be of the

exact same form as the ones in (78) and (82). However after having performed those integrals, the parameter integrals will differ, due to the difference of the $\beta_\alpha^{(ij)}$. After having done the above mentioned integrations, we are left with the following expression

$$\begin{aligned} \delta^{\text{IR},\text{in},\text{out}} &= 2 [\text{P}^{\text{IR}} + \ln[\omega/\mu]] \int_0^1 d\alpha \left[\frac{T}{(p_\alpha^{(13)})^2} - \frac{U}{(p_\alpha^{(14)})^2} \right] \\ &+ \underbrace{\int_0^1 d\alpha \left[\frac{2T \ln 2}{(p_\alpha^{(13)})^2} - \frac{2U \ln 2}{(p_\alpha^{(14)})^2} - \frac{T \ln \left[\frac{1+\beta_\alpha^{(13)}}{1-\beta_\alpha^{(13)}} \right]}{\beta_\alpha^{(13)} (p_\alpha^{(13)})^2} + \frac{U \ln \left[\frac{1+\beta_\alpha^{(14)}}{1-\beta_\alpha^{(14)}} \right]}{\beta_\alpha^{(14)} (p_\alpha^{(14)})^2} \right]}_{:=F}. \end{aligned} \quad (89)$$

We use (70) and the equivalent relations for $\beta_\alpha^{(13)}$ and $\beta_\alpha^{(14)}$:

$$\begin{aligned} \beta_\alpha^{(13)} &= \frac{2}{\sqrt{s}} [m^2 + (T - 2m^2)\alpha(1 - \alpha)]^{1/2} \\ \beta_\alpha^{(14)} &= \frac{2}{\sqrt{s}} [m^2 + (U - 2m^2)\alpha(1 - \alpha)]^{1/2} \end{aligned} \quad (90)$$

as well as the integrals

$$\begin{aligned} \int_0^1 \frac{d\alpha}{m^2 + (T - 2m^2)\alpha(1 - \alpha)} &= \frac{\ln \left[\frac{T + \sqrt{T^2 - 4m^4}}{T - \sqrt{T^2 - 4m^4}} \right]}{\sqrt{T^2 - 4m^4}} \\ \int_0^1 d\alpha F &= -2 \left[\text{Li}_2 \left[1 - \frac{1 - \beta}{1 - \beta \cos \theta} \right] + \text{Li}_2 \left[1 - \frac{1 + \beta}{1 - \beta \cos \theta} \right] \right. \\ &\quad \left. - \text{Li}_2 \left[1 - \frac{1 - \beta}{1 + \beta \cos \theta} \right] + \text{Li}_2 \left[1 - \frac{1 + \beta}{1 + \beta \cos \theta} \right] \right], \end{aligned} \quad (91)$$

to get the final result

$$\begin{aligned} \delta^{\text{IR},\text{in},\text{out}} &= 2 [\text{P}^{\text{IR}} + \ln[2\omega/\mu]] \left[T \frac{\ln \left[\frac{T + \sqrt{T^2 - 4m^4}}{T - \sqrt{T^2 - 4m^4}} \right]}{\sqrt{T^2 - 4m^4}} - U \frac{\ln \left[\frac{U + \sqrt{U^2 - 4m^4}}{U - \sqrt{U^2 - 4m^4}} \right]}{\sqrt{U^2 - 4m^4}} \right] \\ &- 2 \left[\text{Li}_2 \left[1 - \frac{1 - \beta}{1 - \beta \cos \theta} \right] + \text{Li}_2 \left[1 - \frac{1 + \beta}{1 - \beta \cos \theta} \right] \right. \\ &\quad \left. - \text{Li}_2 \left[1 - \frac{1 - \beta}{1 + \beta \cos \theta} \right] + \text{Li}_2 \left[1 - \frac{1 + \beta}{1 + \beta \cos \theta} \right] \right]. \end{aligned} \quad (92)$$

The whole correction term (71) is a sum out of (86) and (92):

$$\delta^{\text{IR}} = 2\delta^{\text{IR},\text{in}} + \delta^{\text{IR},\text{in},\text{out}}. \quad (93)$$

The factor 2 in front of $\delta^{\text{IR},\text{in}}$ appears since $\delta^{\text{IR},\text{in}} = \delta^{\text{IR},\text{out}}$ because of the identical masses of the in- and out-states.

6 Mellin-Barnes representation

6.1 Mellin-Barnes representation

The history of perturbative QFT has seen the development of a number of different techniques for the evaluation of Feynman diagrams. A comprehensive account of the different approaches is given in [5]. Likely the most important technique is the introduction of Feynman parameters [2] (see appendix C). As will be explained below, they also are an integral part of the application of Mellin-Barnes (MB) representations to Feynman integrals.

Today further important techniques are integration by parts and the reduction to master integrals [67], the use of difference equations as well as the application of MB representations. For the evaluation of the 5-Point function in Bhabha scattering, we will resort to the latter.

Even though the theory of Mellin-Barnes integrals is much older (see e.g. [68]), the first notable application to the evaluation of Feynman integrals was made in [69] and was further developed in [70]. The application to higher orders was carried out by [71] and [72] using different regularization techniques. Recently the application of MB-representation has seen an important automatization in [55] and [56].

The key identity is the so called Mellin-Barnes representation, which is in some sense an inverse Feynman parametrization, as it turns a sum in the denominator into a product:

$$(A + B)^{-a} = \frac{1}{2\pi i} \int_{-i\infty}^{+i\infty} dz [A^z B^{-a-z}] \frac{\Gamma[a+z]\Gamma[-z]}{\Gamma[a]}. \quad (94)$$

This identity may be proved, by Taylor expanding $(1-x)^{-a}$ around zero. The k -th derivative of $(1-x)^{-a}$ reads

$$\left. \frac{d^k}{dx^k} \right|_{x=0} (1-x)^{-a} = a(a+1)(a+2)\cdots(a+k-1)(1-x)^{-a-k}|_{x=0} = \frac{\Gamma[a+k]}{\Gamma[a]} = (a)_k, \quad (95)$$

Where $(a)_k$ is the Pochhammer symbol. For $|x| < 1$ this yields the identity

$$\frac{1}{(1-x)^a} = \sum_{k=0}^{\infty} \frac{d^k}{dx^k} \frac{1}{(1-x)^a} \Big|_{x=0} \frac{x^k}{k!} = \sum_{k=0}^{\infty} \frac{\Gamma[a+k]}{\Gamma[a]} \frac{x^k}{k!} = {}_2F_1[a, b; b; x], \quad (96)$$

where ${}_2F_1[a, b; c; x]$ is the Gauss hypergeometric function (see appendix C). Now the ${}_qF_p$ can be represented as the Mellin-Barnes Integral [68]:

$${}_2F_1[a, b; b; x] = \frac{1}{2\pi i} \frac{1}{\Gamma[a]} \int_{-i\infty}^{+i\infty} dz (-x)^z \Gamma[a+z]\Gamma[-z]. \quad (97)$$

Rewriting

$$(A + B)^{-a} = B^{-a} (1 - (-A/B))^{-a}, \quad (98)$$

we obtain the Mellin-Barnes representation (94). It is important to note, that the Mellin-Barnes representation of the hypergeometric function (97) is only valid, if the integration contour separates the left poles (i.e. poles of $\Gamma[\cdots + z]$) from the right poles (poles of $\Gamma[\cdots - z]$). Only if this is the case, does the sum of the residues of the left (or right) poles add up to give the hypergeometric series above.

6.2 Mellin-Barnes representation for multiple propagators

The application of Mellin-Barnes representations to multiple propagators might seem somewhat strange, since the idea is to -as usual- introduce Feynman parameters in order to turn the product

of propagators into a sum in the denominator and later apply MB-representations to turn this sum back into a product of the summands. How can this be helpful in the evaluation of loop integrals? Consider the general L-loop integral with measure $Dk_i \equiv (-i\pi^{-d/2})d^d k_i$, the scalar propagators $D_i \equiv [q_i^2 - m_i^2]$ and a numerator structure $X = X(k_1^{\mu_1}, \dots, k_L^{\mu_L})$:

$$G(X) = \int \frac{[Dk_1 \cdots Dk_L] \cdot X}{D_1^{n_1} \cdots D_N^{n_N}}. \quad (99)$$

With the introduction of Feynman parameters (see appendix C) this can be written as

$$G(X) = \Gamma[N_n] \int \frac{[Dk_1 \cdots Dk_L] \cdot X}{\Gamma[n_1] \cdots \Gamma[n_N]} \int_0^1 \prod_{j=1}^N [dx_j x_j^{n_j-1}] \frac{\delta(1 - x_1 \cdots - x_N)}{(x_1 D_1 + \cdots + x_N D_N)^{N_n}}. \quad (100)$$

Following this simplification, the loop momenta integrations reduce to a mere replacement. This is due to the fact that we can deduce the momentum integrals of this general structure for $X = 1, k_1^\mu, k_1^\mu k_2^\nu$ (see appendix D), however more general numerator structures can be evaluated and are implemented in the `Mathematica` package `AMBRE.m` [55]. As an example we give the scalar L-Loop result:

$$G(1) = (-1)^{N_n} \frac{\Gamma[N_n - Ld/2]}{\Gamma[n_1] \cdots \Gamma[n_N]} \int_0^1 \prod_{j=1}^N [dx_j x_j^{n_j-1}] \delta(1 - x_1 \cdots - x_N) \frac{U(x)^{N_n - d/2(L+1)}}{F(x)^{N_n - d/2L}}. \quad (101)$$

Where the U- and F-forms are sums of products of the Feynman parameters and Mandelstam invariants or masses (see appendix D for details). We are left with the Feynman parameter integrals. The key idea of Mellin-Barnes representation is to successively apply the MB-representation (94) to the U- and F-form till all the summands factorize, i.e. till all the sums involving Feynman parameters have vanished and one can apply e.g.:

$$\int_0^1 \prod_{j=1}^N [dx_j x_j^{\sigma_j-1}] \delta(1 - x_1 \cdots - x_N) = \frac{\Gamma[\sigma_1] \cdots \Gamma[\sigma_N]}{\Gamma[\sigma_1 + \cdots + \sigma_N]}, \quad (102)$$

which itself follows directly from the general Feynman parameter formula by setting all propagators equal to 1 (see appendix C).

6.3 `AMBRE.m` and the scalar 1-loop box B412m

As an example, we look at the scalar 1-loop Box B412m:

$$G_{\text{B412m}} = \int \frac{Dq}{[(q + p_1)^2 - m^2][(q + p_1 + p_2)^2][(q + p_3)^2 - m^2][q^2]}. \quad (103)$$

Following the steps explained in appendix D, we find the F-form

$$F_{\text{B412m}} = m^2(x_2 + x_4)^2 + (-s)x_1x_3 + (-t)x_2x_4. \quad (104)$$

Generally, for 1-loop integrals it holds that $U(x) = 1$. Whereas we first introduced Feynman parameters to make a sum out of the product of propagators, we now introduce MB-integrals in

order to reobtain a product out of the F-form. The successive application of (94) gives

$$\begin{aligned}
\frac{1}{(F_{\text{B412m}})^\nu} &= \frac{1}{2\pi i} \int_{-i\infty+a_1}^{+i\infty+a_1} dz_1 \frac{[m^2(x_2+x_4)^2]^{z_1}}{[(-s)x_1x_3+(-t)x_2x_4]^{\nu+z_1}} \frac{\Gamma[\nu+z_1]\Gamma[-z_1]}{\Gamma[\nu]} \\
&= \frac{1}{(2\pi i)^2} \prod_{i=1}^2 \int_{-i\infty+a_i}^{+i\infty+a_i} dz_i \frac{[m(x_2+x_4)]^{2z_1} [(-s)x_1x_3]^{z_2}}{[(-t)x_2x_4]^{\nu+z_1+z_2}} \\
&\quad \times \frac{\Gamma[\nu+z_1+z_2]\Gamma[-z_2]}{\Gamma[\nu+z_1]} \frac{\Gamma[\nu+z_1]\Gamma[-z_1]}{\Gamma[\nu]} \\
&= \frac{1}{(2\pi i)^3} \prod_{i=1}^3 \int_{-i\infty+a_i}^{+i\infty+a_i} dz_i (m)^{2z_1} (-s)^{z_2} (-t)^{-\nu-z_1-z_2} [x_1^{z_2} x_2^{-\nu-z_1-z_2+z_3} x_3^{z_2} x_4^{-\nu+z_1-z_2-z_3}] \\
&\quad \times \frac{\Gamma[-2z_1+z_3]\Gamma[-z_3]}{\Gamma[-2z_1]} \frac{\Gamma[\nu+z_1+z_2]\Gamma[-z_2]}{\Gamma[\nu+z_1]} \frac{\Gamma[\nu+z_1]\Gamma[-z_1]}{\Gamma[\nu]} \tag{105}
\end{aligned}$$

where $\nu = N_n - d/2L = 2 + \epsilon$. Now applying (102) gives

$$\begin{aligned}
\int_0^1 \prod_{j=1}^4 [dx_j] & [x_1^{z_2} x_2^{-\nu-z_1-z_2+z_3} x_3^{z_2} x_4^{-\nu+z_1-z_2-z_3}] \delta(1-x_1-x_2-x_3-x_4) \\
&= \frac{\Gamma[1+z_2]^2 \Gamma[-1-\epsilon-z_1-z_2+z_3] \Gamma[-1-\epsilon+z_1-z_2-z_3]}{\Gamma[-2\epsilon]}, \tag{106}
\end{aligned}$$

yielding the massive scalar 4-point function

$$\begin{aligned}
G_{\text{B412m}} &= \frac{1}{(2\pi i)^3} \prod_{i=1}^3 \int_{-i\infty+a_i}^{+i\infty+a_i} dz_i (m^2)^{z_1} (-s)^{z_2} (-t)^{-2-\epsilon-z_1-z_2} \Gamma[1+z_2]^2 \Gamma[2+\epsilon+z_1+z_2] \\
&\quad \times \Gamma[-z_1]\Gamma[-z_2] \frac{\Gamma[-2z_1+z_3]\Gamma[-1-\epsilon-z_1-z_2+z_3]\Gamma[-1-\epsilon+z_1-z_2-z_3]\Gamma[-z_3]}{\Gamma[-2\epsilon]\Gamma[-2z_1]}. \tag{107}
\end{aligned}$$

This can be significantly simplified by applying Barnes first lemma with respect to z_3 , which is given at the end of this section. The expression then reads

$$\begin{aligned}
G_{\text{B412m}} &= \frac{1}{(2\pi i)^2} \prod_{i=1}^2 \int_{-i\infty+a_i}^{+i\infty+a_i} dz_i (m^2)^{z_1} (-s)^{z_2} (-t)^{-2-\epsilon-z_1-z_2} \Gamma[-z_1]\Gamma[-z_2]\Gamma[1+z_2]^2 \\
&\quad \times \frac{\Gamma[2+\epsilon+z_1+z_2]\Gamma[-2-2\epsilon-2z_2]\Gamma[-1-\epsilon-z_1-z_2]^2}{\Gamma[-2\epsilon]\Gamma[-2\epsilon-2z_1-2z_2-2]}. \tag{108}
\end{aligned}$$

The deduction of the above MB-representation was automatized in the `Mathematica` package `AMBRE.m` [55]. The starting point of `AMBRE` is the definition of the loop integral. E.g. the integral (103) is

```

FullIntegral[{1}, {PR[q + p1, 0, n1] * PR[q + p1 + p2, m, n2] * PR[q + p3, m, n3] * PR[q, 0, n4]}, {q}]
invariants = {p1^2 -> m^2, ...}
IntPart[1],
\tag{109}

```

where the command `FullIntegral` was followed by a specification of a replacement list for the momentum contractions by invariants that need to be chosen carefully to get an F-form that is as compact as possible, in order to arrive at a representation with a minimal number of MB-integrals. Further `IntPart[n]` prepares the subloop `n` in multiple-loop integrals.

The central function in `AMBRE` is

$$\text{SubLoop}[\text{integral}], \tag{110}$$

this performs all the steps leading to (107), including the explicit calculation of both the U- and F-polynomial.

Finally there is an implemented command that tries to apply the Barnes lemmas:

$$\text{BarnesLemma}[\text{representation}, i], \quad (111)$$

where for i one can insert either 1 or 2 depending on which lemma one wants to apply.

6.4 Regularization of MB-integrals

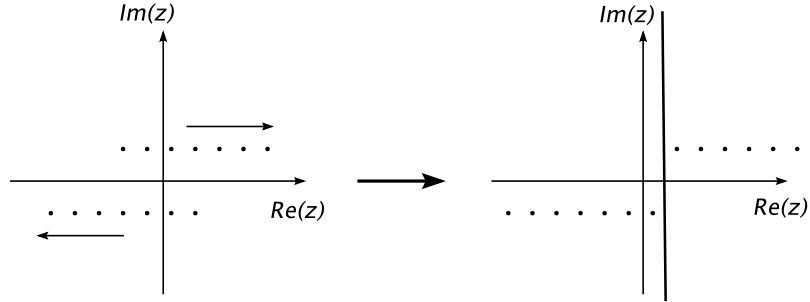


Figure 5: Regularization of the MB-integrals according to the Tausk method. Poles are being shifted (by choosing $\epsilon \neq 0$) in such a way, that the integration contour parallel to the imaginary axis separates the left- from the right poles.

As already stated, the Mellin-Barnes representation is only defined, if the integration contour is chosen in such a way, that it separates the left from the right poles. For a given combination of Γ -functions this will not be the case if UV- or IR-divergences are present and the contour is chosen to be a straight line parallel to the imaginary axis.

There are two known schemes of regularization and analytic continuation. The "Smirnov method" [71] which is based on deforming the contour and the "Tausk method" [72] which fixes the contours parallel to the imaginary axis and accounts for poles crossing in analytic continuation.

In our following discussion, we will use the latter, which was also used to automatize the analytic continuation in `MB.m` [56].

To regularize a MB-Integral means to choose an integration contour that separates the integrands left- from its right poles. In order to illustrate the "Tausk method", we focus on the general MB-integral

$$\int_{-i\infty}^{+i\infty} dz f(z) \Gamma_l[a_1 + z] \cdots \Gamma_l[a_n + z] \Gamma_r[b_1 - z] \cdots \Gamma_r[b_m - z], \quad a_i, b_j \in \mathbb{R} \quad (112)$$

where the indices l, r label the Gamma functions with left and right poles respectively and the function $f(z)$ is everywhere nonsingular and decreases sufficiently fast at infinity. As already mentioned, we will keep the contour parallel to the imaginary axis. Our goal is now to find a contour that stays right of all the left poles, i.e.:

$$\text{Re}[z] = -a_i + \delta_i, \quad \forall a_i, \text{ and } \delta_i > 0, \quad (113)$$

and left of all the right poles, i.e.:

$$\operatorname{Re}[z] = b_j - \delta_j, \quad \forall b_j, \text{ and } \delta_j > 0. \quad (114)$$

These conditions are equivalent to requiring the real parts of the arguments of all the Gamma functions in the numerator to be positive. This argument holds also for multidimensional MB-integrals. The regularization condition for the contour to separate the left from the right poles of

$$\int_{-i\infty}^{+i\infty} dz_1 \cdots \int_{-i\infty}^{+i\infty} dz_m \Gamma_1[A_1] \Gamma_2[A_2] \cdots \Gamma_n[A_n], \quad A_i = A_i(z_1, \dots, z_m; \epsilon) \quad (115)$$

is then equivalent to the condition

$$\operatorname{Re}[A_1] > 0, \operatorname{Re}[A_2] > 0, \dots, \operatorname{Re}[A_n] > 0. \quad (116)$$

In the application of MB-representations to Feynman integrals as described above, the only dependence of the arguments, other than on the integration variables, will be on the parameter ϵ that arises in dimensional regularization.

6.5 MB.m and analytic continuation in ϵ

In general, in order to fulfill the regularization condition (116), we will need to choose $\epsilon \neq 0$. Since we are interested in expressions (amplitudes, etc.) as Laurent series around $\epsilon = 0$, we must perform an analytic continuation towards $\epsilon = 0$. Note that, once we have found suitable regularization conditions, i.e. a set $\{\operatorname{Re}[\epsilon]; \operatorname{Re}[z_1], \operatorname{Re}[z_2], \dots, \operatorname{Re}[z_n]\} = \{c_0; c_1, c_2, \dots, c_n | c_i \in \mathbb{R}\}$ that fulfills (116), we keep the integration strips fixed (we do not change $\operatorname{Re}[z_i]$). The analytic continuation is a continuation only in ϵ . As ϵ approaches zero we will cross one or several poles of the Gamma functions. Each pole crossing is accounted for by adding or subtracting (depending on which side the contour is being closed) the residue in the relevant variable. For an n-fold MB-integral the residue is an (n-1)-fold MB-integral which might still contain poles in the remaining variables that are being crossed as $\epsilon \rightarrow 0$. These poles are of course to be treated the same way.

To illustrate analytical continuation we will go back to the scalar box integral (108) and introduce the coordinates $r_1 = z_2$ and $r_2 = -2 - \epsilon - z_1 - z_2$:

$$\begin{aligned} G_{\text{B412m}} &= \frac{1}{(2\pi i)^2} \prod_{i=1}^2 \int_{-i\infty+a_i}^{+i\infty+a_i} dr_i (m^2)^{-2-\epsilon} \left(-\frac{s}{m^2}\right)^{r_1} \left(-\frac{t}{m^2}\right)^{r_2} \frac{\Gamma[-r_1] \Gamma[1+r_1]^2 \Gamma[-r_2] \Gamma[1+r_2]^2}{\Gamma[-2\epsilon] \Gamma[2+2r_2]} \\ &\quad \times \Gamma[-2(1+\epsilon+r_1)] \Gamma[2+\epsilon+r_1+r_2]. \end{aligned} \quad (117)$$

This integral is regularized by the following choice:

$$a_1 = -3/4, \quad a_2 = -1/4, \quad \epsilon = -3/4. \quad (118)$$

A set that fulfills (116) can be easily found using the MB command

$$\text{MBOptimizedRules}[\text{MBintegral}, \text{eps} \rightarrow 0, \{\}, \{\text{eps}\}], \quad (119)$$

where, in the third argument, one can demand e.g. the real part of one of the MB-integration strips to be greater or smaller than a given real value (e.g. $\text{r2} < -1/4$).

If we now keep a_1 and a_2 fixed and let ϵ approach zero, all the gamma functions in the numerator stay finite except for $\Gamma[-2(1+\epsilon+r_1)]$, which has a right pole at $\epsilon = -1/4$. Closing the r_1 contour

to the left, we have to subtract the residue at $r_1 = -1 - \epsilon$, since the corresponding pole runs into the area of integration when $\epsilon \rightarrow 0$. We therefore have

$$\begin{aligned}
G_{\text{B412m}} &= \frac{\lim_{\epsilon \rightarrow 0}}{(2\pi i)^2} \prod_{i=1}^2 \int_{-i\infty+a_i}^{+i\infty+a_i} dr_i (m^2)^{-2-\epsilon} \left(-\frac{s}{m^2}\right)^{r_1} \left(-\frac{t}{m^2}\right)^{r_2} \frac{\Gamma[-r_1]\Gamma[1+r_1]^2\Gamma[-r_2]\Gamma[1+r_2]^2}{\Gamma[-2\epsilon]\Gamma[2+2r_2]} \\
&\quad \times \Gamma[-2(1+\epsilon+r_1)]\Gamma[2+\epsilon+r_1+r_2] \\
&\quad - \frac{\lim_{\epsilon \rightarrow 0}}{(2\pi i)} \int_{-i\infty+a_2}^{+i\infty+a_2} dr_2 (m^2)^{-1-\epsilon} \left(-\frac{s}{m^2}\right)^{-\epsilon} \left(-\frac{t}{m^2}\right)^{r_2} \frac{\Gamma[-\epsilon]^2\Gamma[1+\epsilon]\Gamma[-r_2]\Gamma[1+r_2]^3}{2s\Gamma[-2\epsilon]\Gamma[2+2r_2]},
\end{aligned} \tag{120}$$

where the second summand is the subtracted residue in $r_1 = -1 - \epsilon$. Now, after the analytic continuation, we can expand G_{B412m} in a Laurent series around $\epsilon = 0$. The first summand turns out to give a contribution only in $\mathcal{O}(\epsilon)$ which we will neglect here. We thus only have to solve the second, one dimensional MB-integral:

$$\begin{aligned}
G_{\text{B412m}} &= \frac{\lim_{\epsilon \rightarrow 0}}{(2\pi i)} \int_{-i\infty-1/4}^{+i\infty-1/4} \frac{dr_2}{m^2 s} \left(-\frac{t}{m^2}\right)^{r_2} \frac{\Gamma[-r_2]\Gamma[1+r_2]^3}{\Gamma[2+2r_2]} \left(\frac{1}{\epsilon} - \ln(-s)\right) + \mathcal{O}(\epsilon) \\
&= \frac{\lim_{\epsilon \rightarrow 0}}{(2\pi i)} \int_{-i\infty-3/4}^{+i\infty-3/4} \frac{dr}{m^2 s} \left(-\frac{t}{m^2}\right)^{-1-r} \frac{\Gamma[-r]^3\Gamma[1+r]}{\Gamma[-2r]} \left(\frac{1}{\epsilon} - \ln(-s)\right) + \mathcal{O}(\epsilon).
\end{aligned} \tag{121}$$

Closing the contour to the left, this integral can be written as an infinite sum over the residues at $r = -1, -2, \dots$ by making use of the residue theorem:

$$\oint_{\gamma} dz f(z) = 2\pi i \sum_{\text{Res}} \text{Res}[f(z)], \tag{122}$$

which relates the contour integral of $f(z)$ along the curve γ to the sum over the residues $\text{Res}[f(z)]$ enclosed by γ . Applying this to the above expression gives

$$\begin{aligned}
G_{\text{B412m}} &= \frac{1}{m^2 s} \left(\frac{1}{\epsilon} - \ln(-s)\right) \sum_{n=0}^{\infty} \frac{\left(\frac{t}{m^2}\right)^n}{\binom{2n}{n} (2n+1)} + \mathcal{O}(\epsilon) \\
&= \frac{1}{m^2 s} \left(\frac{1}{\epsilon} - \ln(-s)\right) \frac{2y}{y^2-1} \ln(y) + \mathcal{O}(\epsilon).
\end{aligned} \tag{123}$$

where $y = y(t/m^2)$ and the conformal variable is

$$y(t) = \frac{\sqrt{1-4/t}-1}{\sqrt{1-4/t}+1}, \quad t = -\frac{(1-y(t))^2}{y(t)}. \tag{124}$$

It has further to be mentioned, that in order to rewrite the integration over the imaginary axis as a closed contour integral, so that we can apply the residue theorem, we need to ensure that the integration on the half-circle at infinity does not contribute (i.e. that the Jordan lemma is applicable). This is assumed in `MB.m`, however one needs to perform numerical checks to ensure that the Jordan lemma indeed holds.

It might very well be the case that the integrand converges to zero at infinity on one side of integration strip, but not on the other, thereby forcing us to close the contour to the side where the half-circle does not contribute.

The steps that led to (121) are implemented in `MB.m`, where the key function is

$$\text{MBcontinue}[\text{integrand}, \text{eps} \rightarrow 0, \text{rules}, \text{Verbose} \rightarrow \text{False}] \tag{125}$$

which performs the analytic continuation. The Laurent series expansion is performed by

$$\text{MBmerge}[\text{MBexpand}[\text{integral}, \text{Exp}[\text{eps} * \text{EulerGamma}], \{\text{eps}, 0, 0\}], \quad (126)$$

where we have called an additional `MBmerge` command that merges integrals with the same contour, which arise, when one has to add or subtract multiple residues.

We might face the situation that the set of necessary regularization conditions (116) cannot be satisfied. Using the package `MB.m` [56] this manifests itself in the command `MBopitmizedRules` giving no result. In this situation we are free to add further parameters to the arguments of the Gamma functions, making our integrals well defined in the above sense. To retrieve the original integrals we will have to proceed in complete analogy to the ϵ -continuation. We let the parameters approach zero and add the residua of every pole they cross on their way.

The introduction of new parameters can also be used to change the integration strips, which normally remain fixed. Usually one can find an infinite continua of solutions to (116). However these solutions vary only very little. E.g. we might be able to satisfy (116) with any $z_2 \in (-1, -1/2)$ but not be able to choose a $z_2 < -1$, which might be physically desirable. The introduction of a new parameter makes this choice possible. In practice this means, that if we choose $z_2 < -1$, we need to add the residue which the new parameter crosses as it approaches zero: the residue at $z_2 = -1$.

6.6 Barnes' first and second lemma

Barnes' first and second lemma assume the integration contour to separate the left- and right-poles of the integrand. The first lemma reads:

$$\int_{-i\infty}^{+i\infty} \frac{dz}{2\pi i} \Gamma[a_1 + z] \Gamma[a_2 + z] \Gamma[b_1 - z] \Gamma[b_2 - z] = \frac{\Gamma[a_1 + b_1] \Gamma[a_1 + b_2] \Gamma[a_2 + b_1] \Gamma[a_2 + b_2]}{\Gamma[a_1 + a_2 + b_1 + b_2]}, \quad (127)$$

and the second lemma:

$$\int_{-i\infty}^{+i\infty} \frac{dz}{2\pi i} \frac{\Gamma[a_1 + z] \Gamma[a_2 + z] \Gamma[a_3 + z] \Gamma[b_1 - z] \Gamma[b_2 - z]}{\Gamma[a_1 + a_2 + a_3 + b_1 + b_2 + z]} = \frac{\Gamma[a_1 + b_1] \Gamma[a_1 + b_2] \Gamma[a_2 + b_1] \Gamma[a_2 + b_2] \Gamma[a_3 + b_1] \Gamma[a_3 + b_2]}{\Gamma[a_1 + a_2 + b_1 + b_2] \Gamma[a_1 + a_3 + b_1 + b_2] \Gamma[a_2 + a_3 + b_1 + b_2]}. \quad (128)$$

When applying one of the lemmas, we need to be aware of the fact that, not only do we need a contour to separate the poles, but we might also encounter a singular expression if e.g. $a_1 = -b_1 - n$ with $n \in \mathbb{N}$. For this case there are the build in `MB.m` functions

$$\begin{aligned} &\text{Barnes1}[\text{MBint}[\text{integrand}, \{\{\text{eps} \rightarrow 0\}, \{z_1 \rightarrow a_1, \dots, z_n \rightarrow a_n\}\}], z_i], \\ &\text{Barnes2}[\text{MBint}[\text{integrand}, \{\{\text{eps} \rightarrow 0\}, \{z_1 \rightarrow a_1, \dots, z_n \rightarrow a_n\}\}], z_i], \end{aligned} \quad (129)$$

which introduce an infinitesimal shift in the arguments and then applies analytic continuation.

7 The five-point function in Bhabha scattering

After giving a more detailed introduction to Bhabha scattering in this section, we calculate the divergent part of the 5-point topologies shown in Figure 5 and 6. We will motivate and show, that all vector- and tensor-integrals have the same divergence structure as the scalar 5-point integral.

7.1 Bhabha scattering

As already stated in the introduction, Bhabha scattering is divided into two classes: small-angle Bhabha scattering (SABH) for a scattering angle $1^\circ \lesssim \theta_e \lesssim 6^\circ$ and large angle Bhabha scattering (LABH) for $\theta_e \gtrsim 10^\circ$. The properties of LABH are very different, depending on the energy scale. At LEP1 energies ($E_{cm} = \sqrt{s} \simeq M_Z$) LABH is dominated by the s-channel Z^0 -exchange, so along others, this process was used to determine properties of the Z -boson as well as to measure other important electroweak parameters (for an extensive account of electroweak LEP measurements see [75]). For studying the Z -boson and for precision tests of the Standard Model theoretical higher order QED, EW and QCD corrections have to be evaluated with high precision. For multi-parameter fits the semi-analytic Fortran program ZFITTER [76], [77] was developed.

At LEP2 ($\sqrt{s} \simeq 200$ GeV) LABH is dominated by the t-channel γ -exchange, which in turn means that the QED diagrams give the biggest contribution to the cross section and thus make LEP2 not very useful for testing the EW sector with Bhabha scattering.

In our calculations we will concentrate purely on the QED (γ -mediated) diagrams in leading- and next to leading order (NLO) Bremsstrahlung Bhabha scattering. The QED diagrams not only dominate LABH at LEP2 energies, but even more so for SABH where $\gtrsim 99\%$ of the cross section is given by the pure QED process of the t-channel γ -exchange. For this reason SABH was chosen both at LEP1 and LEP2 for the luminosity monitoring.

The luminosity \mathcal{L} of a collider is the ratio between the event rate dN/dt and the corresponding cross section σ of a given process:

$$\frac{dN}{dt} = \mathcal{L} \sigma, \quad N = \sigma \int dt \mathcal{L} = \sigma L. \quad (130)$$

The error of a luminosity measurement or -calculation thus directly determines the precision of measurement of the cross section and is crucial in the search for *new physics*. From the relation $\sigma = N/L$ it is clear, that the error affecting the luminosity L must be smaller than the experimental error affecting N . The luminosity of a collider depends in a non-trivial way on the machine and beam parameters, by which means L might be calculated. However, this is possible only in a highly inaccurate way and one resorts to a different strategy. To determine the luminosity of an accelerator, one chooses a well known process (i.e. SABH at LEP), which is thought to be not much affected by new physics, and calculates the luminosity according to

$$L = \frac{1}{\sigma_{\text{Bhabha}}} N. \quad (131)$$

This luminosity is then used for the determination of all the experimental cross sections via (130). The main reason why SABH is used for luminosity monitoring is that it is substantially a QED process, dominated by a photon exchange in the t-channel. This in turn implies that its theoretically dominant contribution is in principle calculable by means of perturbative QED at arbitrary precision. Since the Z -exchange in the t-channel and the γ - Z -interferences are very small, a detailed knowledge of the Z -boson properties, which have significantly higher uncertainties than the QED parameters, has negligible influence.

The vast dominance of the t-channel photon exchange can be easily understood by looking at its

massless tree-level differential cross section (which is calculated in section 5)

$$\frac{\sigma^{t,\gamma,Born}}{d\Omega} = \frac{\alpha^2}{4s} \frac{2}{(1 - \cos \theta_e)^2} [4 + (1 + \cos \theta_e)^2], \quad (132)$$

where α is the QED fine structure constant. This cross section becomes infinitely large for $\theta_e \rightarrow 0$.

7.2 Kinematic invariants

We consider the kinematics of single photon Bremsstrahlung corrections to Bhabha scattering. We make the kinematic choice for all momenta to be ingoing:

$$e^-(p_1) + e^+(p_2) \rightarrow e^-(-p_3) + e^+(-p_4) + \gamma(-k). \quad (133)$$

This convention gives the following momentum conservation and mass-shell conditions:

$$\begin{aligned} p_1 + p_2 + p_3 + p_4 + k &= 0, \\ p_1^2 = p_2^2 = p_3^2 = p_4^2 &= m^2, \\ k^2 &= 0. \end{aligned} \quad (134)$$

The Mandelstam invariants are

$$\begin{aligned} s &= (p_1 + p_2)^2, & s' &= (p_3 + p_4)^2, \\ t &= (p_2 + p_4)^2, & t' &= (p_1 + p_3)^2, \\ u &= (p_1 + p_4)^2, & u' &= (p_2 + p_3)^2. \end{aligned} \quad (135)$$

It is clear that, in the IR-limit $k \rightarrow 0$, the primed invariants become equal to the not primed. There are four additional variables that are proportional to the photon momentum

$$\begin{aligned} v_1 &= 2k \cdot p_1, & v_2 &= 2k \cdot p_2, \\ v_3 &= 2k \cdot p_3, & v_4 &= 2k \cdot p_4. \end{aligned} \quad (136)$$

These of course vanish in the IR-limit. Contracting the sum of all five momenta with the photon momentum yields

$$v_1 + v_2 + v_3 + v_4 = 0. \quad (137)$$

The primed and unprimed invariants are related through

$$s = s' + v_3 + v_4, \quad t = t' + v_1 + v_4, \quad u = u' + v_2 + v_3.$$

The sum of the invariants is

$$s + t + u = 4m^2 + v_3, \quad s' + t' + u' = 4m^2 - v_3. \quad (138)$$

It is possible to express all momentum contractions through the invariants s, t and v_i :

$$\begin{aligned} p_1 \cdot p_2 &= (s - 2m^2)/2, & p_3 \cdot p_4 &= (s - 2m^2)/2 - (v_3 + v_4)/2 \\ p_2 \cdot p_4 &= (t - 2m^2)/2, & p_1 \cdot p_3 &= (t - 2m^2)/2 - (v_1 + v_3)/2, \\ p_1 \cdot p_4 &= (-s - t + 2m^2)/2 + v_3/2, & p_2 \cdot p_3 &= (-s - t + 2m^2)/2 - (v_2 + v_3 - v_4)/2. \end{aligned} \quad (139)$$

7.3 Five point topologies

QED corrections to Bhabha scattering are evaluated to NNL order (including the NNLO radiative loop corrections), however not the pentagon functions which motivates their calculation in this thesis.

Figure 6 and Figure 7 show the eight contributing topologies for 5-point Bhabha scattering that interfere with the two radiative Born diagrams. The labels of the diagrams are the following:

$$\begin{aligned}
 c &= \text{crossed}, & uc &= \text{uncrossed} \\
 s &= \text{s-channel}, & t &= \text{t-channel} \\
 r &= \text{final state emission}, & l &= \text{initial state emission}, \\
 u &= \text{electron emission}, & & \text{or positron emission}
 \end{aligned} \tag{140}$$

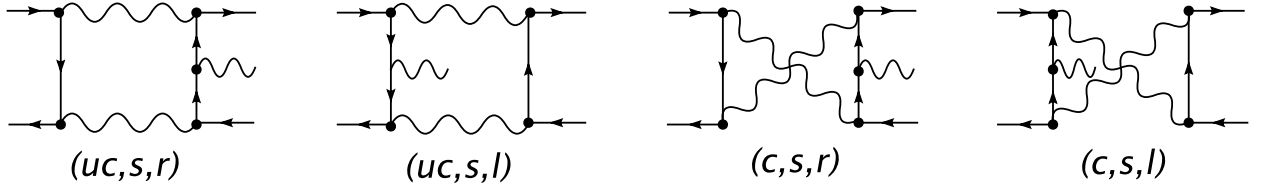


Figure 6: S-channel 5-Point-IR-Box topologies

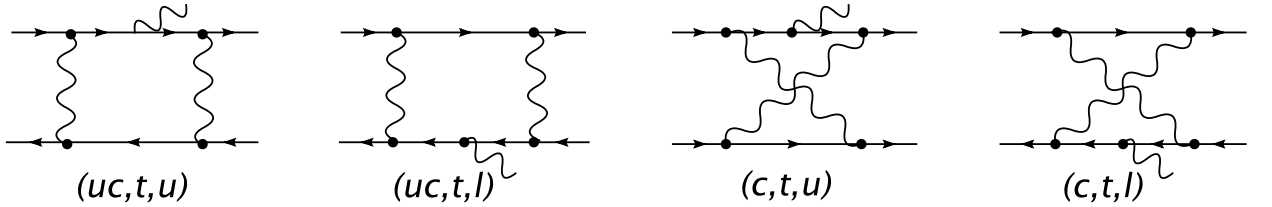


Figure 7: T-channel 5-Point-IR-Box topologies

It turns out however, that we only need to evaluate two of these, since the other ones are either exactly equal or equal up to an interchange of variables.

We take for example the numerator structure of the uncrossed s-channel box diagram with the emission from the right propagator $N_{(uc,s,r)}$ and the uncrossed t-channel diagram with an emission from the lower propagator $N_{(uc,t,l)}$

$$\begin{aligned}
 N_{(uc,s,r)} &= \left[\bar{v}(p_2) \gamma^\beta (\not{q} + \not{p}_1 + m) \gamma^\alpha u(p_1) \right] \left[\bar{u}(-p_3) \gamma^\alpha (\not{q} - \not{p}_3 + m) \gamma^\delta (\not{q} - \not{p}_3 - \not{k} + m) \gamma^\beta v(-p_4) \right] \\
 N_{(uc,t,l)} &= \left[\bar{u}(-p_3) \gamma^\beta (\not{q} + \not{p}_1 + m) \gamma^\alpha u(p_1) \right] \left[\bar{v}(p_2) \gamma^\alpha (\not{q} - \not{p}_2 + m) \gamma^\delta (\not{q} - \not{p}_2 - \not{k} + m) \gamma^\beta v(-p_4) \right]
 \end{aligned} \tag{141}$$

After an interchange $p_2 \leftrightarrow p_3$ these expressions are almost equal, only that we have $\bar{v}(p_2)$ and $\bar{u}(-p_3)$ in $N_{(uc,s,r)}$ but $\bar{u}(-p_2)$ and $\bar{v}(p_3)$ in $N_{(uc,t,l)}(p_2 \leftrightarrow p_3)$. If we take the Born diagrams into

account that these expressions interfere with and sum over the spins – after the interference – we get

$$\begin{aligned}\sum \bar{u}(-p_3)u(-p_3) &= -\sum \bar{v}(p_3)v(p_3) = -\not{p}_3 + m, \\ \sum \bar{u}(p_2)u(p_2) &= -\sum \bar{v}(-p_2)v(-p_2) = \not{p}_2 - m.\end{aligned}\tag{142}$$

The two minus signs cancel and for the interference term we get an exact equality after the interchange $p_2 \leftrightarrow p_3$

$$[\mathcal{M}_{(uc,s,r)} (\mathcal{M}_s + \mathcal{M}_t)^*] = [\mathcal{M}_{(uc,t,l)} (\mathcal{M}_s + \mathcal{M}_t)^*] \begin{pmatrix} s \leftrightarrow t \\ v_2 \leftrightarrow v_3 \end{pmatrix}.\tag{143}$$

This holds for the whole M-matrix, because the denominators of all 8 topologies are equal up to an interchange of momenta. Analogous identities can be found to hold between the other diagrams. We can however not find any identity between the crossed and uncrossed diagrams. This is due to the fact that the crossed diagrams have fermionic propagators that are parallel and others that are anti-parallel to the momentum flow, whereas in the uncrossed diagrams all are either parallel or anti-parallel.

The evaluation of all 5 point topologies thus reduces to the evaluation of one crossed and one uncrossed diagram. For this we choose $\mathcal{M}_{(uc,s,r)}$ and $\mathcal{M}_{(c,s,r)}$. In the IR-limit the total 5-point M-matrix reads

$$\mathcal{M}_{5Point}^{IR} = [\mathcal{M}_{(uc,s,r)} + \mathcal{M}_{(c,s,r)}] + \begin{pmatrix} s \leftrightarrow t \\ v_2 \leftrightarrow v_3 \end{pmatrix} + \begin{pmatrix} s \leftrightarrow t \\ v_1 \leftrightarrow v_4 \end{pmatrix} + \begin{pmatrix} v_2 \leftrightarrow v_3 \\ v_1 \leftrightarrow v_4 \end{pmatrix}.\tag{144}$$

Of course, following the above argument, this identity is to be understood in interference with another M-matrix where the momenta were equally permuted.

7.4 M-matrix and divergence structure of $\mathcal{M}_{(uc,s,r)}$

As already mentioned, among the uncrossed diagrams, we choose to evaluate the 5-Point-IR-Box (uc,s,r) in Figure 8.

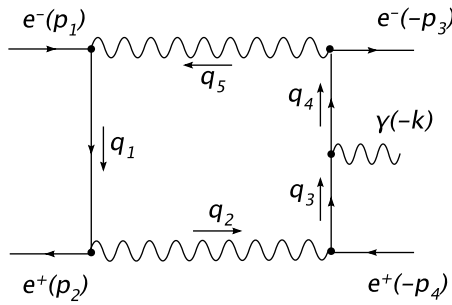


Figure 8: 5-Point-IR-Box (uc,s,r)

The denominators of the propagators are:

$$D_i = [(q - q_i)^2 - m_i^2], \quad i = 1, \dots, 5\tag{145}$$

where the chords of the (uc,s,r)-box q_i are

$$\begin{aligned} q_1 &= -p_1, & q_2 &= -p_1 - p_2, \\ q_3 &= p_3 + k, & q_4 &= p_3, \\ q_5 &= 0. \end{aligned} \tag{146}$$

The masses are

$$(m_1, m_2, m_3, m_4, m_5) = (m, 0, m, m, 0). \tag{147}$$

We have a total of three fermionic propagators in the loop and thus will get tensor integrals up to third order

$$I^{\{0,\mu,\mu\nu,\mu\nu\rho\}} := e^{\epsilon\gamma_E} \int \frac{d^d q}{i\pi^{d/2}} \frac{\{1, q^\mu, q^\mu q^\nu, q^\mu q^\nu q^\rho\}}{D_1 D_2 D_3 D_4 D_5}, \tag{148}$$

The denominators in (145) can be simplified:

$$\begin{aligned} D_1 &= [q^2 + 2p_1 \cdot q], & D_2 &= [q^2 + 2(p_1 + p_2) \cdot q + s], \\ D_3 &= [q^2 - 2(p_3 + k) \cdot q - 2p_3 \cdot k], & D_4 &= [q^2 - 2p_3 \cdot q], \\ D_5 &= [q^2], \end{aligned} \tag{149}$$

yielding for $d = 4$:

$$I^{\overset{q \rightarrow 0}{\infty}} \int_0^\infty dq \frac{\{1, q^\mu, q^\mu q^\nu, q^\mu q^\nu q^\rho\}}{q}, \quad I^{\overset{q \rightarrow \infty}{\infty}} \int_0^\infty dq \frac{\{1, q^\mu, q^\mu q^\nu, q^\mu q^\nu q^\rho\}}{q^7}. \tag{150}$$

We see that \mathcal{M} is UV finite for all numerator structures. However the scalar integral is IR divergent for $q \rightarrow 0$. This singularity is regularized by a tensor structure in the numerator that involves the loop momentum, i.e. the scalar integral is the only one that has an IR-loop singularity at $q = 0$.

A second singularity of the loop integration remains: an IR divergence at $q = q_2$. This can be seen by shifting the integration variable $q \rightarrow q' + q_2$ which gives the same situation as for $q \rightarrow 0$.

For $q \rightarrow q_2$ however also the vector and tensor integrals are IR divergent. Take e.g. the vector integral

$$I^\mu \propto \underbrace{\int \frac{d^d q q^\mu}{D_1 D_2 D_3 D_4 D_5}}_{\text{finite at } q=0} = \underbrace{\int \frac{d^d q (q^\mu - q_2^\mu)}{D_1 D_2 D_3 D_4 D_5}}_{\text{finite at } q=q_2 \text{ divergent at } q=0} + q_2^\mu \underbrace{\int \frac{d^d q}{D_1 D_2 D_3 D_4 D_5}}_{\text{divergent at } q=0 \text{ and } q=q_2}, \tag{151}$$

we conclude that the IR divergences of the two summands at $q = 0$ must cancel each other because I^μ is finite at $q = 0$. This leaves the divergence at $q = q_2$ of the second summand, and we see that indeed the vector integral is IR divergent at $q = q_2$. This is not surprising, because lines five and two are the massless internal lines. Further we note the important fact, that the divergent part of the vector integral I^μ is proportional to q_2^μ and agrees with the scalar one.

An analogous argument for the tensor integral gives the same result, only that now the divergent part is proportional to $q_2^\mu q_2^\nu$. This observation motivates, that for the arising loop integrals $I^{\{0,\mu,\mu\nu,\mu\nu\rho\}}$ we choose to make the ansatz of expanding their solution in the chords:

$$\begin{aligned} I^0 &= I, \\ I^\mu &= q_1^\mu I_1 + q_2^\mu I_2 + q_3^\mu I_3 + q_4^\mu I_4, \\ I^{\mu\nu} &= \sum_{i=1}^4 q_i^\mu q_i^\nu I_{ii} + \sum_{i<j; i,j=1}^4 q_i^\mu q_j^\nu I_{ij} + g^{\mu\nu} I_{00} \\ I^{\mu\nu\rho} &= \sum_{i=1}^4 q_i^\mu q_i^\nu q_i^\rho I_{iii} + \sum_{i<j<k; i,j,k=1}^4 q_i^\mu q_j^\nu q_k^\rho I_{ijk} + g^{\mu\nu} \sum_{i=1}^4 q_i^\rho I_{00i}. \end{aligned} \tag{152}$$

Due to our choice of cords $q_5 = 0$, there can of course be no terms proportional to q_5^μ . In a more general choice where $q_5 \neq 0$ however there would be a q_5^μ contribution, which moreover would also contribute to the divergence, line five being massless.

As an important comment on (151) we would like to state that giving the fact that for tensor integrals we can isolate their divergent part as a scalar integral proportional to q_2^μ , we have to expect that the divergence structure of the tensor integrals is just the same as the one divergence structure of the scalar part. However – as we saw – the scalar integral is divergent both at $q = 0$ and $q = q_2$, but the tensor integral is regularized by its numerator structure at $q = 0$. Therefore we expect only the divergence associates to $q = q_2$ to appear. This qualitative conclusion is mirrored by the results for the divergent parts of the integrals (176).

The above discussion is of course limited to the divergence structure of the loop integrals. As already remarked several times, the photon phase space integrals also diverge. After solving the loop integrals we will get structures proportional to:

$$\frac{1}{v_i}, \quad \frac{\ln(v_i)}{v_i}, \quad (153)$$

which for in IR limit $v_i \rightarrow 0$ give divergent terms proportional to $1/\epsilon$ and $1/\epsilon^2$ respectively.

7.5 The five-point MB-integral

The MB-integrals that were deduced with the package **AMBRE** all have the general structure

$$M = M[Z, A, B, C, D, E, F, G; H] \quad (154)$$

$$M = \int \left[\prod_{i=1}^5 \frac{dr_i}{(2\pi)^5} \right] (-s)^{d/2-r_1-Z} (t)^{r_2} (t')^{r_3} \left(\frac{v_3}{s}\right)^{r_4} \left(\frac{v_4}{s}\right)^{r_5} \frac{\prod_{j=1..14} \Gamma_j}{\prod_{k=15..18} \Gamma_k} \quad (155)$$

with the gamma-functions

$$\begin{aligned} \Gamma_1 &= \Gamma[-r_2], & \Gamma_2 &= \Gamma[-r_3], \\ \Gamma_3 &= \Gamma[-r_4], & \Gamma_4 &= \Gamma[-r_5], \\ \Gamma_5 &= \Gamma[1 + D + r_2 + r_3], & \Gamma_6 &= \Gamma[H - r_1 + r_2 + r_3], \\ \Gamma_7 &= \Gamma[1 + C + r_2 + r_4], & \Gamma_8 &= \Gamma[1 + E + r_3 + r_5], \\ \Gamma_9 &= \Gamma[2 + A + r_2 + 2r_3 + r_5], & \Gamma_{10} &= \Gamma[3 + A + C - 2H + 2r_1 + r_4 + r_5], \\ \Gamma_{11} &= \Gamma[d + 2 + B - 2Z - 2r_1 - r_4 - r_5], & \Gamma_{12} &= \Gamma[d/2 + 1 + G - Z - r_1 - r_4], \\ \Gamma_{13} &= \Gamma[d/2 + 1 + F + 2H - Z - r_1 - r_5], & \Gamma_{14} &= \Gamma[-d/2 + Z + r_1 + r_4 + r_5], \end{aligned} \quad (156)$$

and

$$\begin{aligned} \Gamma_{15} &= \Gamma[2 + D + E + r_2 + 2r_3 + r_5], & \Gamma_{16} &= \Gamma[3 + A + C + 2(r_2 + r_3) + r_4 + r_5], \\ \Gamma_{17} &= \Gamma[d + 2 + F + G - 2Z - 2r_1 - r_4 - r_5], & \Gamma_{18} &= \Gamma[d + 5 + A + B + C - 2Z]. \end{aligned} \quad (157)$$

The Scalar integral is

$$I^0 = M[5, 0, 0, 0, 0, 0, 0, 0; 0], \quad (158)$$

and the vector integrals

$$\begin{aligned}
I_1 &= M[5, 1, 0, 0, 1, 0, 0, 0; 0], & I_2 &= M[5, 0, 1, 0, 0, 0, 0, 1; 0], \\
I_3 &= M[5, 0, 0, 1, 0, 0, 0, 0; 0], & I_4 &= M[5, 1, 0, 0, 0, 1, 0, 0; 0], \\
I_5 &= 0.
\end{aligned} \tag{159}$$

The second rank tensor integrals are

$$\begin{aligned}
I_{11} &= M[5, 2, 0, 0, 2, 0, 0, 0; 0], & I_{22} &= M[5, 0, 2, 0, 0, 0, 0, 2; 0], \\
I_{33} &= M[5, 0, 0, 2, 0, 0, 0, 0; 0], & I_{44} &= M[5, 2, 0, 0, 0, 2, 0, 0; 0], \\
I_{i5} &= 0, \\
I_{12} &= M[5, 1, 1, 0, 1, 0, 0, 1; 0], & I_{13} &= M[5, 1, 0, 1, 1, 0, 0, 0; 0], \\
I_{14} &= M[5, 2, 0, 0, 1, 1, 0, 0; 0], & I_{23} &= M[5, 0, 1, 1, 0, 0, 0, 1; 0], \\
I_{24} &= M[5, 1, 1, 0, 0, 1, 0, 1; 0], & I_{34} &= M[5, 1, 0, 1, 0, 1, 0, 0; 0], \\
I_{00} &= (-1/2)M[4, 0, 0, 0, 0, 0, 0, 0; 0].
\end{aligned} \tag{160}$$

The third rank tensor integrals are

$$\begin{aligned}
I_{111} &= M[5, 3, 0, 0, 3, 0, 0, 0; 0], & I_{222} &= M[5, 0, 3, 0, 0, 0, 0, 3; 0], \\
I_{333} &= M[5, 0, 0, 3, 0, 0, 0, 0; 0], & I_{444} &= M[5, 3, 0, 0, 0, 3, 0, 0; 0], \\
I_{ij5} &= 0, \\
I_{112} &= M[5, 2, 1, 0, 2, 0, 0, 1; 0], & I_{113} &= M[5, 2, 0, 1, 2, 0, 0, 0; 0], \\
I_{114} &= M[5, 3, 0, 0, 2, 1, 0, 0; 0], & I_{221} &= M[5, 1, 2, 0, 1, 0, 0, 2; 0], \\
I_{223} &= M[5, 0, 2, 1, 0, 0, 0, 2; 0], & I_{224} &= M[5, 1, 2, 0, 0, 1, 0, 2; 0], \\
I_{331} &= M[5, 1, 0, 2, 1, 0, 0, 0; 0], & I_{332} &= M[5, 0, 1, 2, 0, 0, 0, 1; 0], \\
I_{334} &= M[5, 1, 0, 2, 0, 1, 0, 0; 0], & I_{441} &= M[5, 3, 0, 0, 1, 2, 0, 0; 0], \\
I_{442} &= M[5, 2, 1, 0, 0, 2, 0, 1; 0], & I_{443} &= M[5, 2, 0, 1, 0, 2, 0, 0; 0], \\
I_{123} &= M[5, 1, 1, 1, 1, 0, 0, 1; 0], & I_{124} &= M[5, 2, 1, 0, 1, 1, 0, 1; 0], \\
I_{134} &= M[5, 2, 0, 1, 1, 1, 0, 0; 0], & I_{234} &= M[5, 1, 1, 1, 0, 1, 0, 1; 0], \\
I_{001} &= (-1/2)M[2, 1, -4, 0, 1, 0, -4, 0; 2], \\
I_{002} &= (-1/2)M[2, 0, -3, 0, 0, 0, -4, 1; 2], \\
I_{003} &= (-1/2)M[2, 0, -4, 1, 0, 0, -4, 0; 2], \\
I_{004} &= (-1/2)M[2, 1, -4, 0, 0, 1, -4, 0; 2].
\end{aligned} \tag{161}$$

As expected, all of these integrals turn out to be finite, except for

$$I, I_2, I_{22}, I_{222}. \tag{162}$$

Where all four functions have a real IR-divergence from the soft Bremsstrahlung. Additionally the scalar integral I^0 has a virtual IR-divergence at $q = 0$ and the tensor integrals in (152) diverge for $q = q_2$.

7.6 The divergent integrals

The scalar integral reads

$$\begin{aligned}
I &= \prod_{j=1}^5 \int_{-i\infty+w_i}^{+i\infty+w_i} \frac{dr_j}{(2\pi)^5} \frac{(-s)^{-\epsilon-r_1-3} (-t)^{r_2} (-t')^{r_3} \left(\frac{v_3}{s}\right)^{r_4} \left(\frac{v_4}{s}\right)^{r_5}}{\Gamma(-2\epsilon-1)\Gamma(2r_2+2r_3+r_4+r_5+3)} \Gamma(-r_2)\Gamma(-r_3)\Gamma(-r_4)\Gamma(-r_5) \\
&\times \Gamma(r_2+r_3+1)\Gamma(-r_1+r_2+r_3)\Gamma(-\epsilon-r_1-r_4-2)\Gamma(r_2+r_4+1)\Gamma(r_3+r_5+1) \\
&\times \Gamma(-\epsilon-r_1-r_5-2)\Gamma(\epsilon+r_1+r_4+r_5+3)\Gamma(2r_1+r_4+r_5+3)
\end{aligned} \tag{163}$$

After a further change of variables in the the single integrals, the scalar pentagon function evaluates to:

$$I = I^{IR}(s, v_4, t, t') + I^{IR}(s, v_3, t', t) + \text{finite terms},$$

$$I^{IR}(s, v_4, t, t') = \frac{1}{2sm^2v_4} \left[\left(\frac{1}{\epsilon} + 2 \ln \frac{t'}{v_4} \right) S_{-1,1}(t) + S_{0,1}(t) - 2S_{0,2}(t, t') \right]. \quad (164)$$

Where the first index of the newly defined S-functions denotes the ϵ -order and the second one the number of MB-integrals. The above S-functions read:

$$S_{-1,1}(t) = \int_{-i\infty+u}^{+i\infty+u} \frac{dr}{2\pi i} \left(-\frac{t}{m^2} \right)^{-1-r} \frac{\Gamma(-r)^3 \Gamma(1+r)}{\Gamma(-2r)}, \quad (165)$$

$$S_{0,1}(t) = \int_{-i\infty+u}^{+i\infty+u} \frac{dr}{2\pi i} \left(-\frac{t}{m^2} \right)^{-1-r} \frac{\Gamma(-r)^3 \Gamma(1+r)}{\Gamma(-2r)} \left[\gamma_E - \log(m^2) - 2\psi^{(0)}(-2r) + 3\psi^{(0)}(-r) \right], \quad (166)$$

$$S_{0,2}(t, t') = \prod_{j=1}^2 \int_{-i\infty+u_j}^{+i\infty+u_j} \frac{dr_j}{(2\pi i)^2} \left(-\frac{t'}{m^2} \right)^{-1-r_1} \left(\frac{t}{t'} \right)^{r_2} \frac{\Gamma(-r_1)^2}{\Gamma(-2r_1)} [\Gamma(-r_1 - r_2 - 1) \Gamma(-r_2) \Gamma(r_2 + 1) \Gamma(r_1 + r_2 + 1)]. \quad (167)$$

With $u, u_j \in (-\frac{1}{2}, 0)$.

These integrals can be represented as sums over residues by making use of the residue theorem,

$$\oint_{\gamma} dz f(z) = 2\pi i \sum_{\text{Res}} \text{Res}[f(z)], \quad (168)$$

which relates the contour integral of $f(z)$ along the curve γ to the sum over the residues $\text{Res}[f(z)]$ enclosed by γ . The above S-functions turn out to all be representable as a combination of inverse binomial sums:

$$\tilde{\Sigma}_{a_1, \dots, a_p; b_1, \dots, b_q}^{i_1, \dots, i_p; j_1, \dots, j_q}(t) := \sum_{n=0}^{\infty} \frac{1}{\binom{2n}{n}} \frac{t^n}{(2n+1)} [S_{a_1}(n)]^{i_1} \dots [S_{a_p}(n)]^{i_p} [S_{b_1}(2n+1)]^{j_1} \dots [S_{b_q}(2n+1)]^{j_q} \quad (169)$$

that were discussed in [83] (see Appendix C.14) where the $S_a(n)$ are harmonic sums (Appendix C)

$$S_a(n) = \sum_{k=1}^n \frac{1}{k^a}. \quad (170)$$

Both $S_{-1,1}(t)$ and $S_{0,1}(t)$ are evaluated by closing the contour to the left. Expressing the sums through the conformal variable y :

$$y(t) = \frac{\sqrt{1-4/t} - 1}{\sqrt{1-4/t} + 1}, \quad t = -\frac{(1-y)^2}{y}, \quad 0 \leq y \leq 1, \quad (171)$$

we get:

$$S_{-1,1}(t) = \tilde{\Sigma}_{-; -}^{-; -}(t) = \sum_{n=0}^{\infty} \frac{t^n}{\binom{2n}{n} (2n+1)} = \frac{2y}{y^2 - 1} \ln(y), \quad (172)$$

$$\begin{aligned}
S_{0,1}(t) &= 3\tilde{\Sigma}_1^1; \bar{\bar{}}(t) - 2\tilde{\Sigma}_-^1; \bar{\bar{}}(t) = \sum_{n=0}^{\infty} \frac{t^n}{\binom{2n}{n} (2n+1)} [3S_1(n) - 2S_1(2n+1)] \\
&= \left(\frac{4y}{y^2-1} \right) \left[-\text{Li}_2[y] - \text{Li}_2[-y] - \ln(y) \left(\ln(1-y^2) - \frac{\ln(y)}{2} \right) + \frac{1}{2}\zeta_2 \right]. \quad (173)
\end{aligned}$$

The S-function $S_{0,2}(t, t')$ can be substantially simplified in the IR limit $t' \rightarrow t$ by applying Barnes' first lemma with respect to r_2 . Naively applying the lemma, however gives rise to a $\Gamma(0)$ divergence due to the two gamma functions $\Gamma(-1-r_1-r_2)$ and $\Gamma(1+r_1+r_2)$. In order for the lemma to yield a finite result we need to introduce an infinitesimal shift in the arguments and later apply analytical continuation. The result then reads:

$$\begin{aligned}
S_{0,2}(t, t) &= \int_{-i\infty+u_1}^{+i\infty+u_1} \frac{dr_1}{(2\pi i)} \left(\frac{-t}{m^2} \right)^{-1-r_1} \frac{\Gamma(-r_1)^3}{\Gamma(-2r_1)} \Gamma(1+r_1) [\gamma_E + \Psi^{(0)}(1+r_1)] \\
&= \ln\left(\frac{-t}{m^2}\right) \tilde{\Sigma}_-^1; \bar{\bar{}}(t) + 3\tilde{\Sigma}_1^1; \bar{\bar{}}(t) - 2\tilde{\Sigma}_-^1; \bar{\bar{}}(t) \\
&= \ln\left(\frac{-t}{m^2}\right) S_{-1,1}(t) + S_{0,1}(t). \quad (174)
\end{aligned}$$

The whole scalar five point integral in the IR limit then becomes

$$\begin{aligned}
I &= I^{IR}(s, v_4, t, t) + I^{IR}(s, v_3, t, t) + \text{finite terms}, \\
I^{IR}(s, v_4, t, t) &= \frac{1}{2sm^2v_4} \left[\left(\frac{1}{\epsilon} - 2 \ln\left(\frac{-v_4}{m^2}\right) \right) S_{-1,1}(t) - S_{0,1}(t) \right], \\
I^{IR}(s, v_4, t, t) &= \frac{1}{sm^2v_4} \left(\frac{y}{y^2-1} \right) \left[\left(\frac{1}{\epsilon} - 2 \ln\left(\frac{-v_4}{m^2}\right) \right) \ln(y) \right. \\
&\quad \left. + 2 \left(\text{Li}_2[y] + \text{Li}_2[-y] + \ln(y) \left(\ln(1-y^2) - \frac{\ln(y)}{2} \right) - \frac{1}{2}\zeta_2 \right) \right]. \quad (175)
\end{aligned}$$

Strictly speaking – due to $0 \leq v_4$ – the expression $\ln(-v_4/m^2)$ is not well defined. This issue is further addressed in (190) by making use of the identity $s = s + i\epsilon$.

Summarizing, the divergent parts of the loop integrals are

$$\begin{aligned}
I &= [I^{IR}(s, v_4, t, t) + I^{IR}(s, v_3, t, t)] + \text{finite terms}, \\
I^\mu &= q_2^\mu [I^{IR}(s, v_4, t, t)] + \text{finite terms}, \\
I^{\mu\nu} &= q_2^\mu q_2^\nu [I^{IR}(s, v_4, t, t)] + \text{finite terms}, \\
I^{\mu\nu\rho} &= q_2^\mu q_2^\nu q_2^\rho [I^{IR}(s, v_4, t, t)] + \text{finite terms}. \quad (176)
\end{aligned}$$

8 The cross section

In this section we calculate the differential cross section $d\sigma/d\cos\theta$ of the interference of all eight 5-point topologies with all eight Born Bremsstrahlung diagrams. To render the phase space integration over the photon momentum feasible, we will change our kinematic convention and later carry out the phase space integrals – using dimensional regularization – in section 9. The spinor and gamma matrix algebra was solved with the program FORM [78]. For general algebraic manipulation the program Mathematica [54] was used.

8.1 Kinematic conventions

First we should note, that our previous kinematic convention for all 4-momenta to be ingoing

$$p_1 + p_2 = -p_3 - p_4 - k, \quad (177)$$

leads e.g. to a negative energy of the final particles. We will thus change our convention when performing the phase space integral to

$$k_1 + k_2 = k_3 + k_4 + k_5, \quad (178)$$

rendering, amongst other things, the energy of all particles strictly positive. These two choices are related through

$$(p_1, p_2, p_3, p_4, k) = (k_1, k_2, -k_3, -k_4, -k_5). \quad (179)$$

The Mandelstam invariants remain unchanged under this transformation, however notice that the IR-invariants v_i do change:

$$(v_1, v_2, v_3, v_4) = (-z_1, -z_2, z_3, z_4) = (-2k_1 \cdot k_5, -2k_2 \cdot k_5, 2k_3 \cdot k_5, 2k_4 \cdot k_5). \quad (180)$$

The Bremsstrahlung Born diagrams contain the eikonal current, which was derived in section 4. Under the sign change of the final momenta, this current also picks up a sign:

$$\left[\frac{e k_1 \cdot \epsilon}{(k_1 \cdot k_5)} - \frac{e k_2 \cdot \epsilon}{(k_2 \cdot k_5)} - \frac{e k_3 \cdot \epsilon}{(k_3 \cdot k_5)} + \frac{e k_4 \cdot \epsilon}{(k_4 \cdot k_5)} \right] = \left[-\frac{e p_1 \cdot \epsilon}{(p_1 \cdot k)} + \frac{e p_2 \cdot \epsilon}{(p_2 \cdot k)} + \frac{e p_3 \cdot \epsilon}{(p_3 \cdot k)} - \frac{e p_4 \cdot \epsilon}{(p_4 \cdot k)} \right]. \quad (181)$$

8.2 The M-matrix

We now turn to the main task of calculating the divergent part of the differential cross section of the interference between the (uc,s,r) diagram in Figure 8 and the Born Bremsstrahlung diagrams (both s- and t-channel). This interference is depicted in Figure 9, however we will evaluate the interference of the (uc,s,r) diagram with Bremsstrahlung diagrams with emissions from all four legs. Due to the simple relation

$$\mathcal{M}_1 \mathcal{M}_2^* + \mathcal{M}_1^* \mathcal{M}_2 = 2\text{Re}[\mathcal{M}_1 \mathcal{M}_2^*], \quad (182)$$

we will only have to calculate one of the interferences:

$$\mathcal{M}^{(2)} = \frac{1}{4} \sum_{\text{spin}} \sum_{\text{pol}} [i\mathcal{M}_{(uc,s,r)}] [i\mathcal{M}_s^{IR} + i\mathcal{M}_t^{IR}]^*. \quad (183)$$

Where we have averaged over the spin of the incoming particles and summed over spin and polarization of the outgoing ones. In the following we will work in the Feynman gauge ($\xi = 1$).

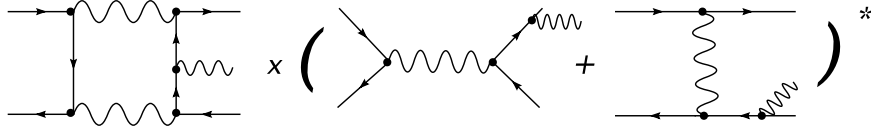


Figure 9: $\mathcal{M}_{(uc,s,r)} \times [\mathcal{M}_s^{IR} + \mathcal{M}_t^{IR}]^*$

The Feynman rules for the (uc,s,r) diagram yield

$$\begin{aligned}
i\mathcal{M}_{(uc,s,r)} &= \int \frac{d^d q}{(2\pi)^d} (i^{10} e^5) \frac{\epsilon_\delta^*(-k)}{D_1 D_2 D_3 D_4 D_5} \left[\bar{v}(p_2) \gamma^\alpha [\not{q} + \not{p}_1 + m] \gamma^\beta u(p_1) \right] \\
&\quad \left[\bar{u}(-p_3) \gamma^\beta [\not{q} - \not{p}_3 + m] \gamma^\delta [\not{q} - \not{p}_3 - \not{k} + m] \gamma^\alpha v(-p_4) \right] \\
&= (2^{-d} \pi^{-d/2}) \int \frac{d^d q}{i\pi^{d/2}} (i^{-i} e^5) \frac{\epsilon_\delta^*(-k)}{D_1 D_2 D_3 D_4 D_5} \left[\bar{v}(p_2) \gamma^\alpha [\not{q} + \not{p}_1 + m] \gamma^\beta u(p_1) \right] \\
&\quad \left[\bar{u}(-p_3) \gamma^\beta [\not{q} - \not{p}_3 + m] \gamma^\delta [\not{q} - \not{p}_3 - \not{k} + m] \gamma^\alpha v(-p_4) \right]. \tag{184}
\end{aligned}$$

Where we have singled out the factor $(i 2^{-d} \pi^{-d/2})$ to obtain the measure $d^d q / (i\pi^{d/2})$ which is implemented in the **Mathematica** package **AMBRE** [55], where for example the command

$$\text{Fullintegral}[\{\mathbf{X}\}, \{\text{PR}[\mathbf{q}, 0, \mathbf{n1}] * \text{PR}[\mathbf{q} + \mathbf{p1}, \mathbf{m}, \mathbf{n2}]\}, \{\mathbf{q}\}],$$

corresponds to

$$\int \frac{d^d q}{i\pi^{d/2}} \frac{X}{(q^2)^{n_1} [(q + p_1)^2 - m^2]^{n_2}}. \tag{185}$$

As further described in Appendix D, the $1/i$ is canceled by an i from the Wick-rotation.

The Feynman rules for the Bremsstrahlung Born diagrams give

$$\begin{aligned}
[i\mathcal{M}_s^{IR} + i\mathcal{M}_t^{IR}]^* &= 2e \left[-\frac{p_1 \cdot \epsilon}{v_1} + \frac{p_2 \cdot \epsilon}{v_2} + \frac{p_3 \cdot \epsilon}{v_3} - \frac{p_4 \cdot \epsilon}{v_4} \right] \left[\frac{(-ie^2)}{s} [\bar{u}(p_1) \gamma^\mu v(p_2)] [\bar{v}(-p_4) \gamma^\mu u(-p_3)] \right. \\
&\quad \left. + \frac{(-ie^2)}{t} [\bar{u}(p_1) \gamma^\mu u(-p_3)] [\bar{v}(-p_4) \gamma^\mu v(p_2)] \right], \tag{186}
\end{aligned}$$

the first two factors being the eikonal current whose factorization was deduced in section 4.

8.3 The loop integral contributions

We use equation (15) of section 2 for $2 \rightarrow 2$ Bhabha scattering, multiply with the additional photon phase space and integrate over the redundant angle (which gives us an extra 2π), and obtain:

$$\frac{d\sigma}{d\cos\theta} = \int \left[\frac{d^{d-1} k_5}{(2\pi)^3 2E_\gamma} \frac{\Theta(\omega - E_\gamma)}{(2\pi\mu)^{d-4}} \right] \frac{2\text{Re}[\mathcal{M}^{(2)}]}{32\pi s}, \tag{187}$$

where $\mathcal{M}^{(2)}$ was defined in (183). In section 7 we deduced $I^{IR}(s, v_4, t, t)$ and gave its result grouped according to the ϵ dependence of the terms. For the phase space integration however it is more desirable to group the terms according to their dependence on the v_j which comprise the soft photon

momentum. Further we will multiply $I^{IR}(s, v_4, t, t)$ with the factor $((4\pi)^{-d/2}) = (4\pi)^{-2}(1+\epsilon \ln(4\pi))$ that we factored out in order to obtain the measure used in **AMBRE**.

$$\tilde{I}^{IR}(s, v_4, t) = \frac{1 + \epsilon \ln(4\pi)}{(4\pi)^2} I^{IR}(s, v_4, t, t) = \frac{1}{(4\pi)^2} \frac{1}{sm^2} \left[\frac{1}{v_4} \tilde{I}_1 - \frac{\ln(v_4)}{v_4} \tilde{I}_2 \right], \quad (188)$$

with

$$\begin{aligned} \tilde{I}_1 &= \left(\frac{y}{y^2 - 1} \right) \left[\frac{\ln(y)}{\epsilon} + 2\pi i + 2 \ln(m^2) \ln(y) + \ln(4\pi) \ln(y) \right. \\ &\quad \left. + 2 \left(\text{Li}_2[y] + \text{Li}_2[-y] + \ln(y) \left(\ln(1 - y^2) - \frac{\ln(y)}{2} \right) - \frac{1}{2} \zeta_2 \right) \right], \\ \tilde{I}_2 &= \left(\frac{y}{y^2 - 1} \right) [2 \ln(y) + \epsilon \ln(4\pi)]. \end{aligned} \quad (189)$$

In \tilde{I}_2 we have kept the constant term in ϵ , because the integration over $\ln(v_4)/(v_i v_4)$ will give rise to a ϵ^{-2} term. We have further inserted the identity

$$\ln(-v_j) = \ln\left(\frac{-v_j}{-s}\right) + \ln(-s - i\epsilon) = \ln\left(\frac{v_j}{s}\right) + \ln(s) - i\pi = \ln(v_j) - i\pi. \quad (190)$$

As we have discussed above, we are interested only in the real part of the M-matrix squared. The summand $2\pi i$ in I_1 will thus drop out.

The appearing quantities in the cross section will then be:

$I_1(y)$	$\left(\frac{y}{y^2 - 1} \right) \left[\frac{\ln(y)}{\epsilon} + 2 \ln(m^2) \ln(y) + \ln(4\pi) \ln(y) \right. \\ \left. + 2 \left(\text{Li}_2[y] + \text{Li}_2[-y] + \ln(y) \left(\ln(1 - y^2) - \frac{\ln(y)}{2} \right) - \frac{1}{2} \zeta_2 \right) \right]$	(191)
$I_2(y)$	$\left(\frac{y}{y^2 - 1} \right) [2 \ln(y) + \epsilon \ln(4\pi)]$	

We now stand facing the photon phase space integration over the two structures

$$\frac{-\ln(v_j)}{v_i v_j}, \quad \frac{1}{v_i v_j}. \quad (192)$$

We saw in section 7 that $j \in \{3, 4\}$. v_j therefore does not change sign when we change our momentum convention like stated above. However the v_i arise from the Born diagrams which have emissions from all four legs, i.e. $i \in \{1, 2, 3, 4\}$. Thus the above structures transform like

$$\left(\frac{-\ln(v_j)}{v_i v_j}, \frac{1}{v_i v_j} \right) \rightarrow \begin{cases} \left(\frac{\ln(z_j)}{z_i z_j}, -\frac{1}{z_i z_j} \right) & \text{if } i \in \{1, 2\} \\ \left(\frac{-\ln(z_j)}{z_i z_j}, \frac{1}{z_i z_j} \right) & \text{if } i \in \{3, 4\}. \end{cases} \quad (193)$$

The explicit integration will be carried out in the next section.

8.4 The cross section

The cross sections for the (uc,s,r)-diagram interfering with the 4 (each one emitting a photon from a different one of the four legs) s-channel and 4 t-channel Bremsstrahlungs Born diagrams are:

$$\begin{aligned} \frac{d\sigma[(uc, s, r); s]}{d \cos \theta} &= \sigma_s \Delta^{uc}(\epsilon^{-1}, \epsilon^{-2}) \\ \frac{d\sigma[(uc, s, r); t]}{d \cos \theta} &= \frac{-\sigma_{st}}{2} \Delta^{uc}(\epsilon^{-1}, \epsilon^{-2}) \end{aligned} \quad (194)$$

with the Born cross sections σ_s and σ_{st} given in (59) and the dimensionless divergent factor

$$\Delta^{uc}(\epsilon^{-1}, \epsilon^{-2}) \left[\frac{e^8(2m^2-t)}{m^2\pi^3} \left(I_2(y(t)) \left[t(P_1^{(14)} + P_1^{(24)}) + (s-2m^2)(P_1^{(14)} - P_1^{(34)}) \right. \right. \right. \\ \left. \left. \left. + 2m^2(P_1^{(44)} - P_1^{(24)}) \right] + I_1(y(t)) \left[t(P_2^{(14)} + P_2^{(24)}) \right. \right. \right. \\ \left. \left. \left. + (s-2m^2)(P_2^{(14)} - P_2^{(34)}) + 2m^2(P_2^{(44)} - P_2^{(24)}) \right] \right) \right] \quad (195)$$

which contains the IR divergent photon phase space integrals

$$P_1^{(ij)} = \int \left[\frac{d^{d-1}k_5}{(2\pi)^3 2E_\gamma} \frac{\Theta(\omega - E_\gamma)}{(2\pi\mu)^{d-4}} \right] \frac{-\ln(z_j)}{z_i z_j}, \quad P_2^{(ij)} = \int \left[\frac{d^{d-1}k_5}{(2\pi)^3 2E_\gamma} \frac{\Theta(\omega - E_\gamma)}{(2\pi\mu)^{d-4}} \right] \frac{1}{z_i z_j}. \quad (196)$$

obaying the following identities

$$P_k^{(ij)} = P_k^{(ji)}, \quad P_k^{(33)} = P_k^{(44)}, \quad P_k^{(13)} = P_k^{(24)}, \quad P_k^{(23)} = P_k^{(14)}, \quad (197)$$

for $k = 1, 2$. The evaluation of these integrals is the object of the next section.

The cross sections for the interference of the crossed 5-point diagram (c,s,r) with the Born Bremsstrahlung diagrams are:

$$\frac{d\sigma[(c, s, r); s]}{d \cos \theta} = \sigma_s \Delta^c(\epsilon^{-1}, \epsilon^{-2}) \\ \frac{d\sigma[(c, s, r); t]}{d \cos \theta} = \frac{-\sigma_{st}}{2} \Delta^c(\epsilon^{-1}, \epsilon^{-2}). \quad (198)$$

They hold a new divergent factor which has the same structure as the first one, only that the u and t are interchanged in $I_{1,2}$ and the global factor is slightly different:

$$\Delta^c(\epsilon^{-1}, \epsilon^{-2}) \left[\frac{e^8(u-2m^2)}{m^2\pi^3} \left(I_2(y(u)) \left[t(P_1^{(14)} + P_1^{(24)}) + (s-2m^2)(P_1^{(14)} - P_1^{(34)}) \right. \right. \right. \\ \left. \left. \left. + 2m^2(P_1^{(44)} - P_1^{(24)}) \right] + I_1(y(u)) \left[t(P_2^{(14)} + P_2^{(24)}) \right. \right. \right. \\ \left. \left. \left. + (s-2m^2)(P_2^{(14)} - P_2^{(34)}) + 2m^2(P_2^{(44)} - P_2^{(24)}) \right] \right) \right] \quad (199)$$

We can now use the crossing symmetry identity (144) to obtain the final result for the interference of all eight 5-point topologies with the eight Born Bremsstrahlung topologies:

$$\frac{d\sigma}{d \cos \theta} = [2\sigma_s - \sigma_{st}] [\Delta^{uc}(\epsilon^{-1}, \epsilon^{-2}) + \Delta^c(\epsilon^{-1}, \epsilon^{-2})] + (s \leftrightarrow t). \quad (200)$$

8.5 Bloch-Nordsieck cancellation

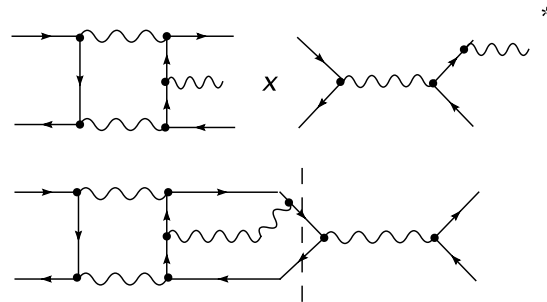


Figure 10: One has to join two diagrams and apply all possible cuts in order to determine the corresponding diagrams for the Bloch-Nordsieck cancellation.

As deduced in section 4, there exist QED diagrams which cancel the divergent part of (200). However these corresponding diagrams include a set of two-loop diagrams, which goes beyond the scope of this thesis. In order to find all possible diagrams that can possibly contribute, one has to flip the conjugated diagram and join the common final particle lines, as shown for the (uc,s,r)-diagram in figure 10. One then has to employ all possible cuts that separate the graph into two new and valid Feynman diagrams. As shown in figure 10, some of the arising diagrams are of next to next to leading order (NNLO), which makes their calculation not feasible for this thesis.

9 The photon phase space integrals

The integral P_2 is the same as in the single photon Born Bremsstrahlung diagram. P_1 is thus the only new integral that we need to evaluate.

9.1 The P_1 integral

In order to be able to calculate the divergent part of the P_1 integral through Feynman parameters, like we did in section 5, we will make use of the following representation of the logarithm

$$-\ln(z_j) = \frac{d}{d\eta} \Big|_{\eta=0} e^{-\eta \ln(z_j)} = \frac{d}{d\eta} \Big|_{\eta=0} (z_j)^{-\eta}, \quad (201)$$

with a real parameter η . This allows us to rewrite P_1 as

$$P_1 = \frac{d}{d\eta} \Big|_{\eta=0} \int \left[\frac{d^{d-1} k_5}{(2\pi)^3 2E_\gamma} \frac{\Theta(\omega - E_\gamma)}{(2\pi\mu)^{d-4}} \right] \frac{1}{z_i z_j^{1+\eta}}. \quad (202)$$

Using the Feynman parameter representation (appendix C)

$$\frac{1}{z_i z_j^{1+\eta}} = \frac{\Gamma[2+\eta]}{\Gamma[1]\Gamma[1+\eta]} \int_0^1 d\alpha \frac{\alpha^\eta}{[\alpha z_j + (1-\alpha)z_i]^{2+\eta}}, \quad (203)$$

we get

$$P_1 = \frac{d}{d\eta} \Big|_{\eta=0} \frac{\Gamma[2+\eta]}{\Gamma[1+\eta]} \int_0^1 d\alpha \int \left[\frac{d^{d-1} k_5}{(2\pi)^3 2E_\gamma} \frac{\Theta(\omega - E_\gamma)}{(2\pi\mu)^{d-4}} \right] \frac{(\alpha/2)^\eta}{4[k_\alpha \cdot k_5]^{2+\eta}}, \quad (204)$$

with the parameter dependent 4 momentum

$$k_\alpha = (\alpha k_j + (1-\alpha)k_i). \quad (205)$$

Like in section 5, we decompose the contraction $k_\alpha \cdot k_5$ as

$$k_\alpha \cdot k_5 = E_\gamma k_\alpha^0 (1 - \beta_\alpha \cos \theta). \quad (206)$$

In d -dimensional polar coordinates ($d^{d-1} k_5 = dE_\gamma E_\gamma^{d-2} d\Omega_{(d-1)}$) this reads

$$P_1 = \frac{d}{d\eta} \Big|_{\eta=0} \frac{\Gamma[2+\eta](2\pi\mu)^{4-d}}{\Gamma[1+\eta]8(2\pi)^3} \int_0^1 d\alpha (\alpha/2)^\eta \int dE_\gamma E_\gamma^{d-5-\eta} \frac{d\Omega_{(d-1)} \Theta(\omega - E_\gamma)}{[k_\alpha^0 (1 - \beta_\alpha \cos \theta)]^{2+\eta}}. \quad (207)$$

Performing all but one of the angular integrations

$$\int d\Omega_{(d-1)} = \int_0^\pi \frac{2\pi^{d/2-1}}{\Gamma[d/2-1]} [\sin^{d-3} \theta d\theta], \quad (208)$$

gives

$$P_1 = \frac{2^{-1-d} \pi^{-d/2}}{\Gamma[d/2-1]} \frac{d}{d\eta} \Big|_{\eta=0} \int_0^1 d\alpha \frac{1}{(k_\alpha^0)^2} \frac{\Gamma[2+\eta](\alpha/2)^\eta}{(k_\alpha^0)^\eta \Gamma[1+\eta]} \int_0^\omega dE_\gamma \frac{E_\gamma^{d-5-\eta}}{\mu^{d-4}} \int_0^\pi d\theta \frac{\sin^{d-3} \theta}{[1 - \beta_\alpha \cos \theta]^{2+\eta}}. \quad (209)$$

The energy integral is easily done, and the remaining angular integral can be simplified:

$$\begin{aligned} \int_0^\omega dE_\gamma \frac{E_\gamma^{d-5-\eta}}{\mu^{d-4}} &= \frac{\omega^{-\eta}}{d-4-\eta} [\omega/\mu]^{d-4}, \\ \int_0^\pi d\theta \frac{\sin^{d-3} \theta}{[1-\beta_\alpha \cos \theta]^{2+\eta}} &= \int_{-1}^{+1} dx \frac{(1-x^2)^{d/2-2}}{(1-\beta_\alpha x)^{2+\eta}}. \end{aligned} \quad (210)$$

Next we collect all the η dependent parts and differentiate

$$\begin{aligned} \left. \frac{d}{d\eta} \right|_{\eta=0} & \frac{\Gamma[2+\eta] (\alpha/k_\alpha^0)^\eta (2\omega)^{-\eta} (1-x^2)^{d/2-2}}{\Gamma[1+\eta] (d-4-\eta) (1-\beta_\alpha x)^{2+\eta}} \\ &= \frac{1}{4\epsilon^2} \frac{1}{(1-\beta_\alpha x)^2} \left[\frac{1}{(1-x^2)^\epsilon} \left[1 - 2\epsilon \left(1 + \ln \left(\frac{\alpha}{2\omega k_\alpha^0} \right) - \ln(1-\beta_\alpha x) \right) \right] \right], \\ &= \frac{1}{4(\beta_\alpha x - 1)^2} \left[\frac{1}{\epsilon^2} - \frac{1}{\epsilon} \left(2 + 2 \ln \left(\frac{\alpha}{2\omega k_\alpha^0} \right) - 2 \ln(1-\beta_\alpha x) + \ln(1-x^2) \right) \right. \\ & \quad \left. + \ln(1-x^2) \left(2 + 2 \ln \left(\frac{\alpha}{2\omega k_\alpha^0} \right) - 2 \ln(1-\beta_\alpha x) + \frac{\ln(1-x^2)}{2} \right) + \mathcal{O}(\epsilon) \right], \end{aligned} \quad (211)$$

where we have inserted $d = 4 - 2\epsilon$ and the Laurent expansion

$$(1-x^2)^{-\epsilon} = 1 - \ln(1-x^2)\epsilon + \frac{\ln^2(1-x^2)}{2}\epsilon^2 + \mathcal{O}(\epsilon^3). \quad (212)$$

We have already encountered the following x -integrals when we calculated the Born Bremsstrahlung phase space in section 5:

$$\int_{-1}^{+1} dx \frac{1}{(1-\beta_\alpha x)^2} = \frac{2}{1-\beta_\alpha^2}, \quad \int_{-1}^{+1} dx \frac{\ln(1-x^2)}{(1-\beta_\alpha x)^2} = \frac{2}{1-\beta_\alpha^2} \left[2 \ln 2 - \frac{1}{\beta_\alpha} \ln \frac{1+\beta_\alpha}{1-\beta_\alpha} \right], \quad (213)$$

for the divergent part one new integral arises, that can however easily be calculated

$$\int_{-1}^{+1} dx \frac{\ln(1-\beta_\alpha x)}{(1-\beta_\alpha x)^2} = \frac{1}{(1-\beta_\alpha^2)} \left[2 + \ln(1-\beta_\alpha^2) + \frac{1}{\beta_\alpha} \ln \left(\frac{1-\beta_\alpha}{1+\beta_\alpha} \right) \right]. \quad (214)$$

There are two more integrals arising

$$\int_{-1}^{+1} dx \frac{\ln^2(1-x^2)}{(1-\beta_\alpha x)^2}, \quad \int_{-1}^{+1} dx \frac{\ln(1-x^2) \ln(1-\beta_\alpha x)}{(1-\beta_\alpha x)^2}, \quad (215)$$

however, both contributing to the constant term in ϵ . We list their results in appendix F. Putting everything together gives

$$\begin{aligned} P_1 &= [\omega/\mu]^{d-4} \frac{2^{-1-d} \pi^{-d/2}}{\Gamma[d/2-1]} \int_0^1 \frac{d\alpha}{(k_\alpha^0)^2} \int_{-1}^{+1} \frac{dx}{(1-\beta_\alpha x)^2} \\ & \frac{1}{4} \left[\frac{1}{\epsilon^2} - \frac{1}{\epsilon} \left(2 + 2 \ln \left(\frac{\alpha}{2\omega k_\alpha^0} \right) - 2 \ln(1-\beta_\alpha x) + \ln(1-x^2) \right) \right. \\ & \quad \left. + \ln(1-x^2) \left(2 + 2 \ln \left(\frac{\alpha}{2\omega k_\alpha^0} \right) - 2 \ln(1-\beta_\alpha x) + \frac{\ln(1-x^2)}{2} \right) + \mathcal{O}(\epsilon) \right], \end{aligned} \quad (216)$$

with the expansion

$$\begin{aligned}
[\omega/\mu]^{d-4} \frac{2^{-1-d} \pi^{-d/2}}{\Gamma[d/2-1]} &= \frac{1}{32\pi^2} [1 + \epsilon (\ln(\pi) - \gamma_E - 2 \ln[\omega/(2\mu)])] \\
&+ \frac{\epsilon^2}{32\pi^2} \left[\frac{\gamma_E^2}{2} - \frac{\pi^2}{12} + \frac{\ln(\pi)^2}{2} + 2 \ln(2)(\ln(2\pi) - \gamma_E - 2 \ln(\omega/\mu)) \right. \\
&+ \left. 2 \ln(\omega/\mu)(\gamma_E + \ln(\omega/\mu)) - \ln(\pi)(\gamma_E + 2 \ln(\omega/\mu)) \right] + \mathcal{O}(\epsilon^3) \quad (217)
\end{aligned}$$

this gives

$$P_1 = \frac{1}{128\pi^2} \left[\frac{1}{\epsilon^2} P_{(\epsilon,2)} - \frac{1}{\epsilon} P_{(\epsilon,1)} + P_{(\epsilon,0)} \right] + \mathcal{O}(\epsilon), \quad (218)$$

with

$$\begin{aligned}
P_{(\epsilon,2)} &= \int_0^1 \frac{d\alpha}{(k_\alpha^0)^2} \int_{-1}^{+1} \frac{dx}{(1 - \beta_\alpha x)^2} = \int_0^1 \frac{d\alpha}{(k_\alpha^0)^2} \frac{2}{1 - \beta_\alpha^2} = 2 \int_0^1 \frac{d\alpha}{(k_\alpha)^2}, \\
P_{(\epsilon,1)} &= \int_0^1 \frac{d\alpha}{(k_\alpha^0)^2} \int_{-1}^{+1} \frac{dx}{(1 - \beta_\alpha x)^2} \left[\ln(1 - x^2) - 2 \ln(1 - \beta_\alpha x) + \gamma_E - \ln(\pi) + 2 + \ln\left(\frac{\alpha}{4\mu k_\alpha^0}\right) \right] \\
&= \int_0^1 \frac{d\alpha}{(k_\alpha^0)^2} \frac{2}{1 - \beta_\alpha^2} [(\gamma_E - \ln(\pi) - 2 \ln(2\mu k_\alpha^0)) + 2 \ln(\alpha) - \ln(1 - \beta_\alpha^2)] \\
&= 2[\gamma_E - \ln(\pi) - 2 \ln(\mu\sqrt{s})] \int_0^1 \frac{d\alpha}{(k_\alpha)^2} + 4 \int_0^1 d\alpha \frac{\ln(\alpha)}{(k_\alpha)^2} - 2 \int_0^1 d\alpha \frac{\ln(1 - \beta_\alpha^2)}{(k_\alpha)^2} \\
P_{(\epsilon,0)} &= \int_0^1 \frac{d\alpha}{(k_\alpha^0)^2} \int_{-1}^{+1} dx \left[\frac{\ln^2(\pi)}{2} - (2 + \gamma_E - 4 \ln(2)) \ln(\pi) + 2 \ln(\alpha)(-\ln(\pi) - \ln(4) + \gamma_E) \right. \\
&+ 2 \ln\left(\frac{\omega}{\mu}\right) \left(2 \ln(\alpha) - \ln(\pi) + \ln\left(\frac{\omega}{\mu}\right) - 4 \ln(2) + \gamma_E + 2 \right) - \frac{\pi^2}{12} + \frac{\gamma_E^2}{2} + 2\gamma_E \\
&- 2 \ln(\sqrt{s}\omega/2) \left(-\ln(\pi) + 2 \ln\left(\frac{\omega}{\mu}\right) - \ln(4) + \gamma_E \right) + 6 \ln^2(2) - 4(1 + \gamma_E) \ln(2) \left. \right] \frac{1}{(1 - \beta_\alpha x)^2} \\
&- 2 \left(-\ln(\pi) + 2 \ln\left(\frac{\omega}{\mu}\right) - \ln(4) + \gamma_E \right) \frac{\ln(1 - \beta_\alpha x)}{(1 - \beta_\alpha x)^2} + (2 \ln(\alpha) - \ln(\pi) - 2 \ln(\sqrt{s}\omega/2) \\
&+ 2 \ln\left(\frac{\omega}{\mu}\right) - 4 \ln(2) + \gamma_E + 2) \frac{\ln(1 - x^2)}{(1 - \beta_\alpha x)^2} - \frac{2 \ln(1 - \beta_\alpha x) \ln(1 - x^2)}{(1 - \beta_\alpha x)^2} + \frac{\ln^2(1 - x^2)}{2(1 - \beta_\alpha x)^2} \quad (219)
\end{aligned}$$

Where we have made use of $(k_\alpha^0)^2(1 - \beta_\alpha^2) = (k_\alpha)^2$ and $(k_\alpha^0) = \sqrt{s}/2$, which follows from the fact that all the particles have the same energy in the cm-system, since they all have the same mass. Note that this simplification would not have been possible, if we had not transformed our momenta, so that they all have positive energy.

We insert the x-integrals out of appendix F into $P_{(\epsilon,0)}$, and are left with the α -integration

$$\begin{aligned}
P_{(\epsilon,0)} = & \int_0^1 d\alpha \left[\left[\frac{\pi^2}{6} + \ln^2(\pi) - 4\gamma_E \ln(s\omega) - 8 \ln(s\omega) \ln\left(\frac{\omega}{\mu}\right) + 4\gamma_E \ln\left(\frac{\omega}{\mu}\right) + \gamma_E^2 \right. \right. \\
& - 2 \ln(\pi) \left(-2 \ln(s\omega) + 2 \ln\left(\frac{\omega}{\mu}\right) + 2 \ln(2) + \gamma_E \right) + 4 \ln\left(\frac{\omega}{\mu}\right) \ln\left(\frac{4\omega}{\mu}\right) + 4\gamma_E \ln(2) \left. \right] \frac{1}{(k_\alpha)^2} \\
& + 4 \left(-\ln(\pi) + 2 \ln\left(\frac{\omega}{\mu}\right) + \gamma_E \right) \frac{\ln(\alpha)}{(k_\alpha)^2} + \left(2 \ln(\pi) - 4 \ln\left(\frac{\omega}{\mu}\right) - 2i\pi - 2\gamma_E \right) \frac{\ln(1 + \beta_\alpha)}{(k_\alpha)^2} \\
& + \left(2 \ln(\pi) - 4 \ln\left(\frac{\omega}{\mu}\right) + 2i\pi - 2\gamma_E \right) \frac{\ln(1 - \beta_\alpha)}{(k_\alpha)^2} \\
& + 2(-2 \ln(s\omega) + 4 \ln(2) + i\pi) \frac{\ln(1 - \beta_\alpha)}{\beta_\alpha (k_\alpha)^2} + 2(2 \log(s\omega) - 4 \ln(2) - i\pi) \frac{\ln(1 + \beta_\alpha)}{\beta_\alpha (k_\alpha)^2} \\
& + 4 \frac{\ln(\alpha) \ln(1 - \beta_\alpha)}{\beta_\alpha (k_\alpha)^2} + 4 \frac{\ln(\beta_\alpha) \ln(1 - \beta_\alpha)}{\beta_\alpha (k_\alpha)^2} - 4 \frac{\ln(\alpha) \ln(1 + \beta_\alpha)}{\beta_\alpha (k_\alpha)^2} - 4 \frac{\ln(\beta_\alpha) \ln(1 + \beta_\alpha)}{\beta_\alpha (k_\alpha)^2} \\
& - \frac{4 \ln^2(1 - \beta_\alpha)}{\beta_\alpha (k_\alpha)^2} - 2 \frac{\ln^2(1 - \beta_\alpha)}{(k_\alpha)^2} + 4 \frac{\ln(1 + \beta_\alpha) \ln(1 - \beta_\alpha)}{(k_\alpha)^2} + \frac{4 \ln^2(1 + \beta_\alpha)}{\beta_\alpha (k_\alpha)^2} - 2 \frac{\ln^2(1 + \beta_\alpha)}{(k_\alpha)^2} \\
& \left. + \frac{2}{\beta_\alpha (k_\alpha)^2} \left(\text{Li}_2 \left[\frac{2\beta_\alpha}{\beta_\alpha - 1} \right] - \text{Li}_2 \left[\frac{2\beta_\alpha}{\beta_\alpha + 1} \right] + (1 + \beta_\alpha) \text{Li}_2 \left[\frac{1 + \beta_\alpha}{1 - \beta_\alpha} \right] - (1 - \beta_\alpha) \text{Li}_2 \left[\frac{1 - \beta_\alpha}{1 + \beta_\alpha} \right] \right) \right] \quad (220)
\end{aligned}$$

The analytic result for the divergent part of the phase space integrals is given at the end of this section, the individual parameter integrals are listed in appendix F.

For the constant term there are a number of new integrals arising including parameter integrals over dilogarithms, that will lead to trilogarithms $\text{Li}_3[x]$. The kernel of the parameter integral of course heavily depends on which leg radiates the soft photon. To make this more explicit, we will give the $P_{(\epsilon,l)}$ two further upper indicies (ij), denoting the different momenta k_i and k_j .

We find the following kinematic identities:

$$\begin{aligned}
(k_\alpha^{(ii)})^2 &= m^2, & (\beta_\alpha^{(ii)})^2 &= \beta^2, \\
(k_\alpha^{(34)})^2 &= (k_\alpha^{(43)})^2 = m^2 + (s - 4m^2)\alpha(1 - \alpha), & (\beta_\alpha^{(34)})^2 &= (\beta_\alpha^{(43)})^2 = \beta^2(1 - 2\alpha)^2, \\
(k_\alpha^{(13)})^2 &= (k_\alpha^{(24)})^2 = m^2 - t\alpha(1 - \alpha), & (\beta_\alpha^{(13)})^2 &= (\beta_\alpha^{(24)})^2 = \frac{4}{s}[m^2 - t\alpha(1 - \alpha)], \\
(k_\alpha^{(23)})^2 &= (k_\alpha^{(14)})^2 = m^2 - u\alpha(1 - \alpha), & (\beta_\alpha^{(23)})^2 &= (\beta_\alpha^{(14)})^2 = \frac{4}{s}[m^2 - u\alpha(1 - \alpha)].
\end{aligned} \quad (221)$$

Integrals for the radiation from the same leg (ij) = (ii) are trivial.

Integrals arising for initial-initial or final-final interference (ij) = (34) are already fairly complex, however all except for three can be solved with **Mathematica** after applying a variable transformation. Due to the length of the results, they are not listed here, but can be found in the file **P1_ALPHA_Integrals.nb**.

Integrals arising for initial-final interference (ij) = (24) are of even higher complexity and have not been evaluated.

9.2 The P_2 integral

The photon phase space integration over the second structure P_2 was already evaluated, however in the Born Bremsstrahlung diagrams, we evaluated them grouped together, we will therefore deduce

their individual results in this section. We are to carry out the integration

$$P_2 = \int \left[\frac{d^{d-1} k_5}{(2\pi)^3 2E_\gamma} \frac{\Theta(\omega - E_\gamma)}{(2\pi\mu)^{d-4}} \right] \frac{1}{z_i z_j}. \quad (222)$$

Following essentially the same steps as in the P_1 case gives

$$\begin{aligned} P_2 &= \frac{[\omega/\mu]^{d-4}}{d-4} \int_0^1 \frac{d\alpha}{(k_\alpha^0)^2} \frac{2^{-1-d} \pi^{-d/2}}{\Gamma[d/2-1]} \int_{-1}^{+1} dx \frac{(1-x^2)^{d/2-2}}{(1-\beta_\alpha x)^2} \\ &= \int_0^1 \frac{d\alpha}{(k_\alpha^0)^2} \int_{-1}^{+1} \frac{dx}{64\pi^2} \left[\left[-\frac{1}{\epsilon} + \left(\gamma_E - \ln(\pi) + 2 \ln\left(\frac{\omega}{2\mu}\right) + \ln(1-x^2) \right) \right] \frac{1}{(1-\beta_\alpha x)^2} \right. \\ &\quad + \epsilon \left[\left[\frac{\pi^2}{12} - \frac{\gamma_E^2}{2} - \frac{\ln^2(\pi)}{2} + 2 \ln(2)(\gamma_E - \ln(2)) \right. \right. \\ &\quad \left. \left. + \ln(\pi) \left(2 \ln\left(\frac{\omega}{2\mu}\right) + \gamma_E \right) - 2 \ln\left(\frac{\omega}{\mu}\right) \left(\ln\left(\frac{\omega}{\mu}\right) - 2 \ln(2) + \gamma_E \right) \right] \frac{1}{(1-\beta_\alpha x)^2} \right. \\ &\quad \left. \left. - \left(2 \ln\left(\frac{\omega}{2\mu}\right) - \ln(\pi) + \gamma_E \right) \frac{\ln(1-x^2)}{(1-\beta_\alpha x)^2} - \frac{\ln^2(1-x^2)}{2(1-\beta_\alpha x)^2} \right] \right] \\ &= \frac{1}{32\pi^2} \int_0^1 \frac{d\alpha}{(k_\alpha)^2} \left[-\frac{1}{\epsilon} + \gamma_E - \ln(\pi) + 2 \ln\left(\frac{\omega}{2\mu}\right) \right] - \frac{1}{32\pi^2} \int_0^1 \frac{d\alpha}{(k_\alpha)^2} \frac{1}{\beta_\alpha} \ln\left(\frac{1+\beta_\alpha}{1-\beta_\alpha}\right) \\ &\quad + \frac{\epsilon}{64\pi^2} \int_0^1 \frac{d\alpha}{(k_\alpha)^2} \left[\left[-4 \ln^2\left(\frac{\omega}{\mu}\right) - 4(\gamma_E - \ln(\pi)) \ln\left(\frac{\omega}{\mu}\right) - \ln^2(\pi) + 2\gamma_E \ln(\pi) \right. \right. \\ &\quad \left. \left. + \frac{8}{3} \ln(2) \ln(8) - 8 \ln^2(2) + \frac{\pi^2}{2} - \gamma_E^2 \right] + 2 \left(2 \ln\left(\frac{\omega}{\mu}\right) - \ln(\pi) + \gamma_E \right) \frac{1}{\beta_\alpha} \ln\left(\frac{1+\beta_\alpha}{1-\beta_\alpha}\right) \right. \\ &\quad \left. \left. - \frac{2}{\beta_\alpha} \left(\text{Li}_2\left[\frac{2\beta_\alpha}{\beta_\alpha+1}\right] - \text{Li}_2\left[\frac{2\beta_\alpha}{\beta_\alpha-1}\right] \right) \right] \right] \end{aligned} \quad (223)$$

All the above parameter integrals we already found in the P_1 case.

9.3 The divergent part

Using (221) the $\mathcal{O}(\epsilon^{-1})$ part of the above deduced integrals evaluates to:

$P_1^{(33)}$	$\frac{1}{128\pi^2} \frac{2}{m^2} \left[\frac{1}{\epsilon^2} - \frac{1}{\epsilon} (\gamma_E - \ln(\pi) - 2 \ln(\mu\sqrt{s}) - 2 - \ln(1 - \beta^2)) \right]$
$P_1^{(34)}$	$\frac{1}{128\pi^2} \frac{4}{s\beta} \left[\frac{1}{\epsilon^2} \ln\left(\frac{1+\beta}{1-\beta}\right) - \frac{1}{\epsilon} \left[\ln\left(\frac{1+\beta}{1-\beta}\right) (\gamma_E - \ln(\pi) - 2 \ln(\mu\sqrt{s})) + \text{Li}_2\left[\frac{-2\beta}{1-\beta}\right] \right. \right.$ $\left. \left. - \text{Li}_2\left[\frac{2\beta}{1+\beta}\right] - \frac{1}{2} \ln\left(\frac{1+\beta}{1-\beta}\right) \ln(4(1 - \beta^2)) - \text{Li}_2\left[\frac{1-\beta}{2}\right] + \text{Li}_2\left[\frac{1+\beta}{2}\right] \right] \right]$
$P_1^{(13)}$	$\frac{1}{128\pi^2} \frac{4}{\sqrt{t(t-4m^2)}} \left[\frac{1}{\epsilon^2} \ln\left(\frac{\sqrt{4m^2-t}+\sqrt{-t}}{\sqrt{4m^2-t}-\sqrt{-t}}\right) \right.$ $\left. - \frac{1}{\epsilon} \left[(\gamma_E - \ln(\pi) - 2 \ln(\mu\sqrt{s})) \ln\left(\frac{\sqrt{4m^2-t}+\sqrt{-t}}{\sqrt{4m^2-t}-\sqrt{-t}}\right) \right. \right.$ $+ \text{Li}_2\left[\frac{2\sqrt{-t}}{\sqrt{-t}-\sqrt{4m^2-t}}\right] - \text{Li}_2\left[\frac{2\sqrt{-t}}{\sqrt{-t}+\sqrt{4m^2-t}}\right] - \text{Li}_2\left[\frac{\sqrt{u}+\sqrt{-t}}{\sqrt{u}-\sqrt{4m^2-t}}\right]$ $\left. - \text{Li}_2\left[\frac{\sqrt{u}-\sqrt{-t}}{\sqrt{u}+\sqrt{4m^2-t}}\right] - \text{Li}_2\left[\frac{\sqrt{u}+\sqrt{-t}}{\sqrt{u}+\sqrt{4m^2-t}}\right] + \text{Li}_2\left[\frac{\sqrt{u}-\sqrt{-t}}{\sqrt{u}+\sqrt{4m^2-t}}\right] \right.$ $\left. + \ln(\beta^2) \ln\left(\frac{\sqrt{4m^2-t}+\sqrt{-t}}{\sqrt{4m^2-t}-\sqrt{-t}}\right) + \ln\left(\frac{\sqrt{u}+\sqrt{-t}}{\sqrt{u}-\sqrt{-t}}\right) \ln\left(\frac{\sqrt{4m^2-t}+\sqrt{u}}{\sqrt{4m^2-t}-\sqrt{u}}\right) \right]$
$P_1^{(23)}$	$P_1^{(13)}(t \leftrightarrow u)$
$P_2^{(33)}$	$\frac{1}{32\pi^2} \frac{1}{m^2} \left[-\frac{1}{\epsilon} + (\gamma_E - \ln(\pi) + 2 \ln[\omega/\mu] - \frac{1}{\beta} \ln\left(\frac{1+\beta}{1-\beta}\right)) \right]$
$P_2^{(34)}$	$\frac{1}{32\pi^2} \frac{2}{s\beta} \left[-\frac{1}{\epsilon} + \gamma_E - \ln(\pi) + 2 \ln[\omega/\mu] \ln\left(\frac{1+\beta}{1-\beta}\right) - \frac{1}{32\pi^2} \frac{2}{s\beta} [2\text{Li}_2[\beta] - 2\text{Li}_2[-\beta]] \right.$ $\left. + \text{Li}_2\left[\frac{1-\beta}{2}\right] - \text{Li}_2\left[\frac{1+\beta}{2}\right] + \frac{1}{2} \ln^2\left(\frac{1-\beta}{2}\right) - \frac{1}{2} \ln^2\left(\frac{1+\beta}{2}\right) \right]$
$P_2^{(13)}$	$\frac{1}{32\pi^2} \frac{2}{(4m^2-t)} \left[\left(-\frac{1}{\epsilon} + \gamma_E - \ln(\pi) + 2 \ln[\omega/\mu]\right) \left[\frac{\sqrt{4m^2-t}}{\sqrt{-t}} \ln\left(\frac{\sqrt{4m^2-t}+\sqrt{-t}}{\sqrt{4m^2-t}-\sqrt{-t}}\right) \right] \right.$ $\left. - \frac{\sqrt{s}}{m} \ln\left(\frac{\sqrt{s}+2m}{\sqrt{s}-2m}\right) + \frac{2\sqrt{u}}{\sqrt{-t}} \ln\left(\frac{\sqrt{u}+\sqrt{-t}}{\sqrt{u}-\sqrt{-t}}\right) - \frac{2\sqrt{4m^2-t}}{\sqrt{-t}} \ln\left(\frac{\sqrt{4m^2-t}+\sqrt{-t}}{\sqrt{4m^2-t}-\sqrt{-t}}\right) \right]$
$P_2^{(23)}$	$P_2^{(13)}(t \leftrightarrow u)$

(224)

The individual integrals leading to these results are listed in appendix F.

10 Summary and Results

The central result of this thesis is the QED cross section (200) in section 8 for the interference of all eight pentagon $e^+e^- \rightarrow e^+e^-\gamma$ Bremsstrahlung diagrams with all eight Born level Bremsstrahlung topologies:

$$\boxed{\frac{d\sigma}{d\cos\theta} = [2\sigma_s - \sigma_{st}] [\Delta^{uc}(\epsilon^{-1}, \epsilon^{-2}) + \Delta^c(\epsilon^{-1}, \epsilon^{-2})] + (s \leftrightarrow t)}. \quad (225)$$

The Born cross sections σ_s and σ_{st} were calculated in section 5 and are given in equation (59):

$$\begin{aligned} \sigma_s &= \frac{1}{8s^3} \left[\frac{s^2}{2} + st + (2m^2 - t)^2 \right], \\ \sigma_{st} &= \frac{1}{8s^2t} [(s+t)^2 - 4m^4]. \end{aligned} \quad (226)$$

The divergent expressions $\Delta^{uc}(\epsilon^{-1}, \epsilon^{-2})$ and $\Delta^c(\epsilon^{-1}, \epsilon^{-2})$ were given in section 8 equations (195) and (199):

$$\begin{aligned} \Delta^{uc}(\epsilon^{-1}, \epsilon^{-2}) &= \left[\frac{e^8(2m^2 - t)}{m^2\pi^3} \right] \left(I_2(y(t)) \left[t(P_1^{(14)} + P_1^{(24)}) + (s - 2m^2)(P_1^{(14)} - P_1^{(34)}) \right. \right. \\ &\quad \left. \left. + 2m^2(P_1^{(44)} - P_1^{(24)}) \right] + I_1(y(t)) \left[t(P_2^{(14)} + P_2^{(24)}) \right. \right. \\ &\quad \left. \left. + (s - 2m^2)(P_2^{(14)} - P_2^{(34)}) + 2m^2(P_2^{(44)} - P_2^{(24)}) \right] \right), \\ \Delta^c(\epsilon^{-1}, \epsilon^{-2}) &= \left[\frac{e^8(u - 2m^2)}{m^2\pi^3} \right] \left(I_2(y(u)) \left[t(P_1^{(14)} + P_1^{(24)}) + (s - 2m^2)(P_1^{(14)} - P_1^{(34)}) \right. \right. \\ &\quad \left. \left. + 2m^2(P_1^{(44)} - P_1^{(24)}) \right] + I_1(y(u)) \left[t(P_2^{(14)} + P_2^{(24)}) \right. \right. \\ &\quad \left. \left. + (s - 2m^2)(P_2^{(14)} - P_2^{(34)}) + 2m^2(P_2^{(44)} - P_2^{(24)}) \right] \right). \end{aligned} \quad (227)$$

Where the $P_k^{(ij)}$ are the divergent photon phase space integrals that were solved in section 9 and the $I_k(y)$ arise from the divergent loop integrals deduced in section 7. They are explicitly listed in (191):

$$\begin{aligned} I_1(y) &= \left(\frac{y}{y^2 - 1} \right) \left[\frac{\ln(y)}{\epsilon} + 2 \ln(m^2) \ln(y) + \ln(4\pi) \ln(y) \right. \\ &\quad \left. + 2 \left(\text{Li}_2[y] + \text{Li}_2[-y] + \ln(y) \left(\ln(1 - y^2) - \frac{\ln(y)}{2} \right) - \frac{1}{2} \zeta_2 \right) \right], \\ I_2(y) &= \left(\frac{y}{y^2 - 1} \right) [2 \ln(y) + \epsilon \ln(4\pi)]. \end{aligned} \quad (228)$$

Mellin-Barnes representations for all the loop integrals were deduced in section 7 and are given in equations (159)-(161). They are all of the form (155). Out of these integrals the divergent part was extracted and treated in dimensional regularisation which, after applying the residue theorem, lead to (191).

The divergent parts of the phase space integrals were completely solved and are listed in section 9 expression (224). The class of functions found is similar to the one arising from the Born Bremsstrahlung phase space integration performed in section 5.

The constant terms of the photon phase space integration were reduced to the parameter integrals in section 9. The pending integrals are given in (220) and (223). Their complexity depends heavily on which legs radiate the soft photon. Radiation from the same leg yields trivial integrals that can

easily be solved. All integrals for initial-initial and final-final radiation interference except for three could be evaluated using variable transformations and `Mathematica`. Their results are given in the file `P1_ALPHA_Integrals.nb`. The class of the arising functions is more complicated and include i.e. trilog since we have to integrate over dilogarithms in (220) and (223). Integrals for initial-final interference were not solved.

An obvious next step would be to evaluate all pending phase space integrals and therewith complete the $\mathcal{O}(\epsilon^0)$ evaluation of the phase space integrals. Even though the deduced MB-integrals for the Feynman loops can be integrated using Monte-Carlo methods, it would also be desirable to analytically solve them up to $\mathcal{O}(\epsilon^0)$. This might also give rise to new phase space integrals. Further, as for all IR-problems, it needs to be shown that the deduced expression cancels against the IR-divergences of other graphs.

11 Appendix

A Conventions

We use natural units

$$\hbar = 1, \quad c = 1, \quad \epsilon_0 = 1, \quad (\text{A.1})$$

where \hbar denotes Planck's constant, c the vacuum speed of light and ϵ_0 the permittivity of free space. The electromagnetic fine-structure constant α is then given by

$$\alpha = \alpha'(\mu^2 = 0) = \frac{e^2}{4\pi\epsilon_0\hbar c} = \frac{e^2}{4\pi} \approx \frac{1}{137.03599911(46)}. \quad (\text{A.2})$$

In this convention, energies and momenta are given in the same units, electron volt (eV). The space-time dimension is taken to be d and the metric tensor $g_{\mu\nu}$ in Minkowski-space is defined as

$$g_{00} = 1, \quad g_{ii} = -1, \quad i = 1 \dots d-1, \quad g_{ij} = 0, \quad i \neq j. \quad (\text{A.3})$$

Einstein's summation convention is used, i.e.

$$x_\mu y^\mu := \sum_{\mu=1}^d x_\mu y^\mu. \quad (\text{A.4})$$

Bold-faced symbols represent $d-1$ -dimensional spatial vectors:

$$x = (x_0, \mathbf{x}). \quad (\text{A.5})$$

If not stated otherwise, Greek indexes refer to the d -component space-time vector and Latin ones to the $d-1$ spatial components only. The dot product of two vectors is defined by

$$p \cdot q = p_0 q_0 - \sum_{i=1}^{d-1} p_i q_i. \quad (\text{A.6})$$

The γ -matrices γ_μ are taken to be of dimension d and fulfill the anti-commutation relation

$$\{\gamma_\mu, \gamma_\nu\} = 2g_{\mu\nu}. \quad (\text{A.7})$$

It follows that

$$\gamma_\mu \gamma^\mu = d \quad (\text{A.8})$$

$$\text{Tr}(\gamma_\mu \gamma_\nu) = 4g_{\mu\nu} \quad (\text{A.9})$$

$$\text{Tr}(\gamma_\mu \gamma_\nu \gamma_\alpha \gamma_\beta) = 4[g_{\mu\nu} g_{\alpha\beta} + g_{\mu\beta} g_{\nu\alpha} - g_{\mu\alpha} g_{\nu\beta}]. \quad (\text{A.10})$$

The dagger-symbol for a d -momentum p is defined by

$$\not{p} := \gamma_\mu p^\mu. \quad (\text{A.11})$$

The conjugate of a bi-spinor u of a particle is given by

$$\bar{u} = u^\dagger \gamma_0, \quad (\text{A.12})$$

where \dagger denotes Hermitian and $*$ complex conjugation, respectively. The bi-spinor u and v fulfill the Dirac-equation,

$$(\not{p} - m)u(p) = 0, \quad \bar{u}(p)(\not{p} - m) = 0 \quad (\text{A.13})$$

$$(\not{p} + m)v(p) = 0, \quad \bar{v}(p)(\not{p} + m) = 0. \quad (\text{A.14})$$

Bi-spinors and polarization vectors are normalized to

$$\sum_{\sigma} u(p, \sigma) \bar{u}(p, \sigma) = \not{p} + m \quad (\text{A.15})$$

$$\sum_{\sigma} v(p, \sigma) \bar{v}(p, \sigma) = \not{p} - m \quad (\text{A.16})$$

$$\sum_{\lambda} \epsilon^{\mu}(k, \lambda) \epsilon^{\nu}(k, \lambda) = -g^{\mu\nu}, \quad (\text{A.17})$$

where λ and σ represent the spin.

The commonly used caret “^” to signify an operator, e.g. \hat{O} , is omitted if confusion is not to be expected.

B Feynman Rules of QED

The following rules are to be associated with Feynman diagrams and yield the analytic expression for $i\mathcal{M}$.

B.1 General rules

- Write down the Dirac spinor and -matrices in the order that is obtained by following the fermionic lines through the diagram in the opposite direction of the fermionic flow.
- 4-momentum conservation must be respected at each vertex.
- Associate an integral $(2\pi)^{-4} \int d^4q$ with every closed loop having the loop momentum q^μ .
- Multiply by a symmetry factor $1/n!$ for any n equivalent final states.
- Due to anti-commutativity, every closed fermionic line gets a factor -1 .

B.2 Free particles

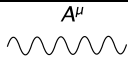
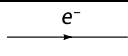
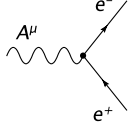
Associate to incoming electron, positron, photon

$$u(p), \quad \bar{v}(p), \quad \epsilon_\mu(k).$$

Associate to outgoing electron, positron, photon

$$\bar{u}(p), \quad v(p), \quad \epsilon_\mu^*(k).$$

B.3 Propagators and vertex

photon propagator		$\frac{-ig^{\mu\nu} + i(1-\xi)(k^\mu k^\nu / k^2)}{k^2}$
electron propagator		$\frac{i(\not{p} + m)}{p^2 - m^2}$
electron photon vertex		$ie\gamma^\mu$

- In the fermion propagator, if the momentum flow and the fermionic flow are antiparallel: $\not{p} \rightarrow -\not{p}$.
- Common gauges are:

$$\begin{aligned} \xi = 0 & \quad \text{Landau gauge} \\ \xi = 1 & \quad \text{Feynman gauge} \\ \xi = 3 & \quad \text{Yennie gauge} \\ \xi = \infty & \quad \text{Unitary gauge} \end{aligned}$$

C Functions and sums

In the following we summarize definitions and elementary relations of special functions and sums frequently encountered in QFT.

C.1 Gamma function

Mathematica symbol: `Gamma[x]`.

$$\Gamma(x) = \int_0^{\infty} dt t^{x-1} e^{-t} \quad (\text{C.1})$$

$$\Gamma(x) = \lim_{n \rightarrow \infty} n^x \frac{n!}{x(x+1) \cdots (x+n)}, \quad \frac{1}{\Gamma(x)} = x e^{x\gamma_E} \prod_{n=1}^{\infty} \left[e^{-x/n} \left(1 + \frac{x}{n} \right) \right] \quad (\text{C.2})$$

Where the Euler-Mascheroni γ_E constant is approximately $\gamma_E = 0.577215665$.
Some algebraic relations

$$\begin{aligned} \Gamma(n+1) &= n! \quad \text{for } n \in \mathbb{N} \\ \Gamma(1+x) &= x\Gamma(x) \\ \Gamma(2x) &= \Gamma(x)\Gamma(x+1/2)(2\pi)^{-1/2} 2^{2x-1/2} \\ \frac{\Gamma(n+1+\epsilon)}{\Gamma(n+1)} &= \Gamma(1+\epsilon) \exp \left[- \sum_{k=1}^{\infty} \frac{(-\epsilon)^k}{k} S_k(n) \right] \end{aligned} \quad (\text{C.3})$$

Parametrization

$$\frac{1}{A^x} = \frac{1}{\Gamma(x)} \int_0^{\infty} dt t^{x-1} e^{-At} \quad (\text{C.4})$$

Residues

$$\text{Res}[\Gamma(a-x); a+n] = \frac{(-1)^{n+1}}{n!} \quad \text{Res}[\Gamma(a+x); -a-n] = \frac{(-1)^n}{n!} \quad (\text{C.5})$$

Laurent series expansion

$$\Gamma(\epsilon) = \frac{1}{\epsilon} - \gamma_E + \frac{1}{2} \left(\gamma_E^2 + \frac{\pi^2}{6} \right) \epsilon + \mathcal{O}(\epsilon^2) \quad (\text{C.6})$$

C.2 Feynman parameter representations

$$\begin{aligned} \frac{1}{A^a B^b} &= \frac{\Gamma[a+b]}{\Gamma[a]\Gamma[b]} \int_0^1 dx \frac{x^{a-1} (1-x)^{b-1}}{[xA + (1-x)B]^{a+b}} \\ \frac{1}{A^a B^b C^c} &= \frac{\Gamma[a+b+c]}{\Gamma[a]\Gamma[b]\Gamma[c]} \int_0^1 dx \int_0^1 dy \frac{(xy)^{a-1} (x(1-y))^{b-1} (1-x)^{c-1}}{[(xy)A + (x(1-y))B + (1-x)C]^{a+b+c}} \\ \frac{1}{A_1^{\alpha_1} \cdots A_n^{\alpha_n}} &= \frac{\Gamma[\sum_i \alpha_i]}{\Gamma[\alpha_1] \cdots \Gamma[\alpha_n]} \int_0^1 \left[\prod_i dx_i x_i^{\alpha_i-1} \right] \frac{\delta(\sum_i x_i - 1)}{[x_1 A_1 + \cdots + x_n A_n]^{\sum_i \alpha_i}} \end{aligned} \quad (\text{C.7})$$

C.3 Pochhammer symbol

Mathematica symbol: `Pochhammer[a, n]`.

$$(a)_n = \frac{\Gamma(a+n)}{\Gamma(a)} = (a+n-1) \cdots (a+1)(a) \quad (\text{C.8})$$

C.4 Beta function

Mathematica symbol: `Beta[a, b]`.

$$\begin{aligned} B(p, q) &= \int_0^\infty dt \frac{t^{p-1}}{(1+t)^{p+q}} = \int_0^1 dt t^{p-1} (1-t)^{q-1} = 2 \int_0^{\pi/2} d\theta \sin^{2q-1} \theta \cos^{2p-1} \theta \\ &= \frac{\Gamma(p)\Gamma(q)}{\Gamma(p+q)} \end{aligned} \quad (\text{C.9})$$

Some algebraic relations

$$\begin{aligned} B(p, q) &= B(p+1, q) + B(p, q+1) \\ B(p, q+1) &= \frac{q}{p} B(p+1, q) \\ B(p, q) &= \frac{p+q}{q} B(p, q+1) \end{aligned} \quad (\text{C.10})$$

C.5 Polygamma function

Mathematica symbol: `PolyGamma[n, x]`.

$$\begin{aligned} \psi^{(n)}(x) &= \frac{d^{n+1}}{dx^{n+1}} \ln[\Gamma(x)] = \frac{d^n}{dx^n} \psi(x) \\ \psi(x) &= \psi^0(x) = \frac{\Gamma'(x)}{\Gamma(x)} \end{aligned} \quad (\text{C.11})$$

Useful representations

$$\begin{aligned} \psi^{(n)}(x+1) &= \psi^{(n)}(x) + x^{-n-1} (-1)^n n! \\ \psi^{(n)}(x) &= (-1)^{n+1} n! \sum_{k=0}^{\infty} \frac{1}{(x+k)^{n+1}} \end{aligned} \quad (\text{C.12})$$

Integral representation for $n > 0$, $\Re e(x) > 0$:

$$\psi^{(n)}(x) = (-1)^{(n+1)} \int_0^\infty dt \frac{t^n e^{-xt}}{1-e^{-t}} \quad (\text{C.13})$$

Due to the identity $\psi^0(m) = S_1(m-1) - \gamma_E$, we also have an integral representation for $n = 0$ and $m \in \mathbb{N}$ given by (C.21).

Residues

$$\text{Res}[\psi(x); -n] = -1, \quad \text{Res}[\psi^{(m)}(x); -n] = 0 \quad \text{for } m \geq 1 \quad (\text{C.14})$$

C.6 Polylogarithms

Mathematica symbol: `PolyLog[n, x]`.

$$\begin{aligned} \text{Li}_n[x] &= \sum_{k=1}^{\infty} \frac{x^k}{k^n} = \int_0^x dt \frac{\text{Li}_{n-1}[t]}{t} \\ \text{Li}_0[x] &= \frac{x}{1-x}, \quad \text{Li}_1[x] = -\ln(1-x) \\ \text{Li}_n[x^2] &= 2^{n-1} [\text{Li}_n[x] + \text{Li}_n[-x]] \end{aligned} \quad (\text{C.15})$$

C.7 Nielsen integrals

Mathematica symbol: `PolyLog[a, b, x]`.

$$\begin{aligned} S_{a,b}(x) &= \frac{(-1)^{a+b-1}}{(a-1)!b!} \int_0^1 dz \frac{\log^{a-1}(z) \log^b(1-zx)}{z} \\ \text{Li}_n[x] &= \frac{d\text{Li}_{n+1}[x]}{d\log(x)} = S_{n-1,1}(x) \end{aligned} \quad (\text{C.16})$$

C.8 Harmonic sums

Mathematica symbol: `HarmonicNumber[n, a]`. For $a > 0$:

$$S_a(n) = \sum_{k=1}^n \frac{1}{k^a}, \quad S_{-a}(n) = \sum_{k=1}^n \frac{(-1)^k}{k^a}, \quad S_a(0) = 0 \quad (\text{C.17})$$

$$S_{a,a_1\dots a_i}(n) = \sum_{k=1}^n \frac{S_{a_1,\dots,a_i}(k)}{k^a}, \quad S_{-a,a_1,\dots,a_i}(n) = \sum_{k=1}^n \frac{(-1)^k S_{a_1,\dots,a_i}(k)}{k^a} \quad (\text{C.18})$$

The permutation relation

$$\begin{aligned} S_{m,n} + S_{n,m} &= S_m S_n + S_{\text{sign}(m)\text{sign}(n)[|m|+|n|]} := S_m S_n + S_{m \wedge n} \\ S_{1,-1} + S_{-1,1} &= S_1 S_{-1} + S_{-2} \end{aligned} \quad (\text{C.19})$$

Relations to other functions

$$\begin{aligned} S_a(n) &= \frac{(-1)^{a-1}}{\Gamma(a)} \psi^{(a-1)}(n+1) + \zeta_a, \quad a \geq 2 \\ S_1(n) &= \psi(n+1) + \gamma_E \\ S_2(n) &= \zeta_2 - \psi^{(1)}(n+1) \end{aligned} \quad (\text{C.20})$$

Integral representation

$$S_{\pm a}(n) = \frac{(-1)^{a-1}}{(a-1)!} \int_0^1 dx \log^{a-1}(x) \frac{(\pm x)^n - 1}{x \mp 1}, \quad S_{\pm 1}(n) = \int_0^1 dx \frac{(\pm x)^n - 1}{x \mp 1} \quad (\text{C.21})$$

C.9 σ -values

$$\sigma_{a_1\dots a_i} = S_{a_1,\dots,a_i}(\infty), \quad \sigma_0 = \sum_{k=1}^{\infty} 1 \quad (\text{C.22})$$

There is a strong connection between finite σ -values and the multiple ζ -values. However there is no general formula that relates the two. Some of the basic relations are:

$$\sigma_{11} = \frac{1}{2}\zeta_2 + \frac{1}{2}\sigma_1^2, \quad \sigma_{-3} = -\frac{3}{4}\zeta_3, \quad \sigma_{12} = -\zeta_3 + \sigma_1\zeta_2 \quad (\text{C.23})$$

$$\sigma_{21} = 2\zeta_3, \quad \sigma_{2-1} = -\frac{3}{2}\zeta_2 \ln(2) + \frac{1}{4}\zeta_3, \quad \sigma_{-21} = -\frac{5}{8}\zeta_3 \quad (\text{C.24})$$

C.10 Riemann zeta function

Mathematica symbol: `Zeta[a]`.

$$\zeta_a = \sum_{k=1}^{\infty} \frac{1}{k^a} = \sigma_a = S_a(\infty) = \text{Li}_a[1], \quad a > 0 \quad (\text{C.25})$$

Integral representation

$$\zeta_a = \frac{1}{\Gamma(a)} \int_0^{\infty} dx \frac{x^{a-1}}{e^x - 1} \quad (\text{C.26})$$

Zeta values of even weight, are proportional to π to that power:

$$\zeta_1 = \infty, \quad \zeta_2 = \frac{\pi^2}{6}, \quad \zeta_3 = 1,202057, \quad \zeta_4 = \frac{\pi^4}{90}, \quad \zeta_6 = \frac{\pi^6}{945}, \quad \zeta_8 = \frac{\pi^8}{9450} \quad (\text{C.27})$$

C.11 Hypergeometric series

Mathematica symbol: `HypergeometricPFQ[{a1, ..., ap}, {b1, ..., bq}, x]`.

$$\begin{aligned} {}_pF_q \left[\begin{matrix} a_1, \dots, a_p \\ b_1, \dots, b_q \end{matrix}; x \right] &= \sum_{k=0}^{\infty} \frac{(a_1)_k \dots (a_p)_k x^k}{(b_1)_k \dots (b_q)_k k!} \\ {}_2F_1 \left[\begin{matrix} a, b \\ b \end{matrix}; x \right] &= {}_2F_1[a, b; b; x] = \sum_{k=0}^{\infty} \frac{\Gamma(a+k) x^k}{\Gamma(a) k!} = \frac{1}{(1-x)^a} \\ &= \frac{1}{2\pi i} \frac{1}{\Gamma(a)} \int_{-i\infty}^{+i\infty} dz (-x)^z \Gamma(a+z) \Gamma(-z) \end{aligned} \quad (\text{C.28})$$

C.12 Mellin transform

$$\mathbf{M}[f](N) = \int_0^1 dx x^{N-1} f(x) \quad (\text{C.29})$$

Mellin-convolution

$$\begin{aligned} [A \otimes B](x) &= \int_0^1 dx_1 \int_0^1 dx_2 \delta(x - x_1 x_2) A(x_1) B(x_2) \\ \mathbf{M}[A \otimes B](N) &= \mathbf{M}[A](N) \cdot \mathbf{M}[B](N) \end{aligned} \quad (\text{C.30})$$

An important example

$$(-1)^{a-1} \Gamma(a) \cdot \mathbf{M}[(x^M \log^{a-1}(x))](N) = \frac{1}{(N+M)^a} \quad (\text{C.31})$$

C.13 Harmonic polylogarithms

For $\vec{m}_w \neq \vec{0}_w$ and $\vec{m}_w = (a, \vec{m}_{w-1})$:

$$\begin{aligned} \text{H}[\vec{m}_w; x] &= \int_0^x f(a; x') \text{H}[\vec{m}_{w-1}; x'], \\ \frac{d}{dx} \text{H}[\vec{m}_w; x] &= f(a; x) \text{H}[\vec{m}_{w-1}; x]. \end{aligned} \quad (\text{C.32})$$

$$\begin{aligned}
\mathbb{H}[0; x] &= \ln x, & f(0; x) &= \frac{1}{x}, \\
\mathbb{H}[1; x] &= \int_0^x \frac{dx'}{1-x'} = -\ln(1-x), & f(1; x) &= \frac{1}{1-x}, \\
\mathbb{H}[-1; x] &= \int_0^x \frac{dx'}{1+x'} = \ln(1+x), & f(-1; x) &= \frac{1}{1+x}
\end{aligned} \tag{C.33}$$

Product algebra

$$\mathbb{H}[\vec{0}_w; x] = \frac{1}{w!} \ln^w x, \quad \mathbb{H}[\vec{1}_w; x] = \frac{1}{w!} (-\ln(1-x))^w, \quad \mathbb{H}[(\vec{-1})_w; x] = \frac{1}{w!} \ln^w(1+x),$$

$$\mathbb{H}[\vec{p}; x] \mathbb{H}[\vec{q}; x] = \sum_{\vec{r} \in \vec{p} \uplus \vec{q}} \mathbb{H}[\vec{r}; x]. \tag{C.34}$$

The sum is understood to be over all permutations of indices that do not change the original internal order of the respective index vector. For example if we take $\vec{p} = (a, b)$ and $\vec{q} = (c, d)$ we get

$$\begin{aligned}
\mathbb{H}[a, b; x] \mathbb{H}[c, d; x] &= \mathbb{H}[a, b, c, d; x] + \mathbb{H}[a, c, b, d; x] \\
&\quad + \mathbb{H}[a, c, d, b; x] + \mathbb{H}[c, a, b, d; x] \\
&\quad + \mathbb{H}[c, a, d, b; x] + \mathbb{H}[c, d, a, b; x].
\end{aligned} \tag{C.35}$$

a can interchange freely with c and d, so can b. a however always has to be listed before b. c always has to be listed before d.

C.14 Inverse binomial sums

The appearing sums in section 7 are in direct correspondence to the class of inverse binomial sums discussed in [83]

$$\Sigma_{a_1, \dots, a_p; b_1, \dots, b_q; c}^{i_1, \dots, i_p; j_1, \dots, j_q}(u) \equiv \sum_{j=1}^{\infty} \frac{1}{\binom{2j}{j}} \frac{u^j}{j^c} [S_{a_1}(j-1)]^{i_1} \dots [S_{a_p}(j-1)]^{i_p} [S_{b_1}(2j-1)]^{j_1} \dots [S_{b_q}(2j-1)]^{j_q}. \tag{C.36}$$

Our sums are of a slightly different form compared to (C.36), namely

$$\tilde{\Sigma}_{a_1, \dots, a_p; b_1, \dots, b_q}^{i_1, \dots, i_p; j_1, \dots, j_q}(u) \equiv \sum_{n=0}^{\infty} \frac{1}{\binom{2n}{n}} \frac{u^n}{(2n+1)} [S_{a_1}(n)]^{i_1} \dots [S_{a_p}(n)]^{i_p} [S_{b_1}(2n+1)]^{j_1} \dots [S_{b_q}(2n+1)]^{j_q}. \tag{C.37}$$

These two classes are of course related. By setting $n = j - 1$ and using

$$\frac{1}{\binom{2j-2}{j-1}} = \frac{2(2j-1)}{j} \frac{1}{\binom{2j}{j}}, \tag{C.38}$$

we find the relation

$$\tilde{\Sigma}_{a_1, \dots, a_p; b_1, \dots, b_q}^{i_1, \dots, i_p; j_1, \dots, j_q}(u) = \frac{2}{u} \cdot \Sigma_{a_1, \dots, a_p; b_1, \dots, b_q; 1}^{i_1, \dots, i_p; j_1, \dots, j_q}(u). \tag{C.39}$$

Note that a correspondence of this form holds only for $c = 1$ in (C.36).

The results for all the sums appearing in our calculations are listed in [83], where they can be found in Table 1 of Appendix D. Expressing the sums through the conformal variable y :

$$y = \frac{\sqrt{1-4/u}-1}{\sqrt{1-4/u}+1}, \quad u = -\frac{(1-y)^2}{y}, \quad (\text{C.40})$$

we get:

$$\tilde{\Sigma}_{-; -}^{-}(u) = \sum_{n=0}^{\infty} \frac{u^n}{\binom{2n}{n} (2n+1)} = \frac{y}{y^2-1} 2 \ln(y), \quad (\text{C.41})$$

$$\begin{aligned} \tilde{\Sigma}_{1; -}^{1; -}(u) &= \sum_{n=0}^{\infty} \frac{u^n}{\binom{2n}{n} (2n+1)} S_1(n) = \frac{y}{y^2-1} [-4\text{Li}_2[-y] - 4 \ln(y) \ln(1+y) \\ &\quad + \ln^2(y) - 2\zeta_2], \end{aligned} \quad (\text{C.42})$$

$$\begin{aligned} \tilde{\Sigma}_{-; 1}^{-; 1}(u) &= \sum_{n=0}^{\infty} \frac{u^n}{\binom{2n}{n} (2n+1)} S_1(2n+1) = \frac{y}{y^2-1} \left[2\text{Li}_2[y] - 4\text{Li}_2[-y] - 4 \ln(y) \ln(1+y) \right. \\ &\quad \left. + 2 \ln(y) \ln(1-y) + \frac{1}{2} \ln^2(y) - 4\zeta_2 \right], \end{aligned} \quad (\text{C.43})$$

$$\begin{aligned} \tilde{\Sigma}_{1; -}^{2; -}(u) &= \sum_{n=0}^{\infty} \frac{u^n}{\binom{2n}{n} (2n+1)} S_1(n)^2 = \frac{y}{y^2-1} \left[16S_{1,2}(-y) - 8\text{Li}_3[-y] + 16\text{Li}_2[-y] \ln(1+y) \right. \\ &\quad \left. + 8 \ln^2(1+y) \ln(y) - 4 \ln(1+y) \ln^2(y) + \frac{1}{3} \ln^3(y) + 8\zeta_2 \ln(1+y) \right. \\ &\quad \left. - 4\zeta_2 \ln(y) - 8\zeta_3 \right], \end{aligned} \quad (\text{C.44})$$

$$\tilde{\Sigma}_{2; -}^{1; -}(u) = \sum_{n=0}^{\infty} \frac{u^n}{\binom{2n}{n} (2n+1)} S_2(n) = -\frac{y}{3(y^2-1)} \ln^3(y), \quad (\text{C.45})$$

$$\begin{aligned} \tilde{\Sigma}_{1; -}^{3; -}(u) &= \sum_{n=0}^{\infty} \frac{u^n}{\binom{2n}{n} (2n+1)} S_1(n)^3 = \frac{y}{y^2-1} \left[-96S_{1,2}(-y) \ln(1+y) - 96S_{1,3}(-y) \right. \\ &\quad \left. + 48S_{2,2}(-y) - 24\zeta_2 \ln^2(1+y) - 48 \ln^2(1+y) \text{Li}_2[-y] + 48\zeta_3 \ln(1+y) \right. \\ &\quad \left. + 48 \ln(1+y) \text{Li}_3[-y] - 16 \ln(y) \ln^3(1+y) + 24\zeta_2 \ln(y) \ln(1+y) \right. \\ &\quad \left. + 12 \ln^2(y) \ln^2(1+y) - 2 \ln^3(y) \ln(1+y) + \frac{1}{12} \ln^4(y) - 3\zeta_2 \ln^2(y) \right. \\ &\quad \left. + 6 \ln^2(y) \text{Li}_2[-y] + 2 \ln^2(y) \text{Li}_2[y] - 10\zeta_3 \ln(y) - 24 \ln(y) \text{Li}_3[-y] \right. \\ &\quad \left. - 8 \ln(y) \text{Li}_3[y] + 3\zeta_4 + 24\text{Li}_4[-y] + 12\text{Li}_4[y] \right], \end{aligned} \quad (\text{C.46})$$

$$\begin{aligned} \tilde{\Sigma}_{3; -}^{1; -}(u) &= \sum_{n=0}^{\infty} \frac{u^n}{\binom{2n}{n} (2n+1)} S_3(n) = \frac{y}{y^2-1} \left[\frac{1}{12} \ln^4(y) + 12\text{Li}_4[y] + 2 \ln^2(y) \text{Li}_2[y] \right. \\ &\quad \left. - 4\zeta_3 \ln(y) - 8 \ln(y) \text{Li}_3[y] - 12\zeta_4 \right], \end{aligned} \quad (\text{C.47})$$

$$\begin{aligned} \tilde{\Sigma}_{1,2; -}^{1,1; -}(u) &= \sum_{n=0}^{\infty} \frac{u^n}{\binom{2n}{n} (2n+1)} S_1(n) S_2(n) = \frac{y}{y^2-1} \left[\frac{2}{3} \ln^3(y) \ln(1+y) - \frac{1}{12} \ln^4(y) + \zeta_2 \ln^2(y) \right. \\ &\quad \left. + 2 \ln^2(y) \text{Li}_2[-y] + 2 \ln^2(y) \text{Li}_2[y] + 2\zeta_3 \ln(y) - 8 \ln(y) \text{Li}_3[-y] - 8 \ln(y) \text{Li}_3[y] \right. \\ &\quad \left. + 2\zeta_4 + 16\text{Li}_4[-y] + 12\text{Li}_4[y] \right]. \end{aligned} \quad (\text{C.48})$$

Some of the above results have been published in [79].

D Integration of L-loop, N-point functions

D.1 General setup

We consider the L-loop, N-point function

$$G(X) \equiv \int \frac{[Dk_1 \cdots Dk_L] \cdot X}{D_1^{n_1} \cdots D_N^{n_N}} \quad (\text{D.49})$$

with the measure $Dk_i \equiv (-i\pi^{-d/2})d^d k_i$, the scalar propagators $D_i \equiv [q_i^2 - m_i^2]$ and a numerator structure $X \equiv X(k_1^{\mu_1}, \dots, k_L^{\mu_L})$. The q_i in the propagators are of course sums of the loop and external momenta.

In the following we will simplify the integral $G(X)$ in several steps.

- **Feynman parameters**

$$G(X) = \Gamma[N_n] \int \frac{[Dk_1 \cdots Dk_L] \cdot X}{\Gamma[n_1] \cdots \Gamma[n_N]} \int_0^1 \prod_{j=1}^N [dx_j x_j^{n_j-1}] \frac{\delta(1 - x_1 \cdots - x_N)}{(x_1 D_1 + \cdots + x_N D_N)^{N_n}} \quad (\text{D.50})$$

with $N_n = n_1 + \cdots + n_N$. Interchanging the integrals, we are now dealing with the expression

$$G(X) = \frac{\Gamma[N_n]}{\Gamma[n_1] \cdots \Gamma[n_N]} \int_0^1 \prod_{j=1}^N [dx_j x_j^{n_j-1}] I_L(X) \delta(1 - x_1 \cdots - x_N), \quad (\text{D.51})$$

with

$$I_L(X) \equiv \int \frac{[Dk_1 \cdots Dk_L] \cdot X}{(x_1 D_1 + \cdots + x_N D_N)^{N_n}}. \quad (\text{D.52})$$

- **L-vector notation**

Each propagator D_i is a polynomial of second order in the momenta. Because the whole denominator is a sum of the D_i , it itself is also a polynomial of second order in the momenta and can therefore be written as

$$\frac{1}{(x_1 D_1 + \cdots + x_N D_N)^{N_n}} = \frac{1}{(kMk - 2Qk + J)^{N_n}}. \quad (\text{D.53})$$

In the above notation k is a L-vector that has the loop momenta k_1, \dots, k_L as entries. M is a (L×L)-matrix and $Q = Q(x_i, p_e)$ as well as $J = J(x_i x_j, m_i^2, p_{e_i} p_{e_j})$ are also L-vectors. The momentum integration is now much simpler.

- **Momentum shift**

By shifting the momenta, we can get rid of the linear momentum term

$$\begin{aligned} k &= \bar{k} + M^{-1}Q, \\ kMk - 2Qk + J &= \bar{k}M\bar{k} - QM^{-1}Q + J. \end{aligned} \quad (\text{D.54})$$

Shifts, of course leave the measure unchanged. Renaming $\bar{k} \rightarrow k$ we have

$$I_L(X) = \int \frac{[Dk_1 \cdots Dk_L] \cdot X}{(kMk - QM^{-1}Q + J)^{N_n}}. \quad (\text{D.55})$$

- **Wick Rotation**

In order to evaluate integrals in Minkowski space, we perform the Wick Rotation

$$k^0 \rightarrow ik_E^0, \quad Dk_i \rightarrow iDk_{Ei}, \quad k^2 \rightarrow -k_E^2, \quad (\text{D.56})$$

which gives us (renaming $k_E \rightarrow k$)

$$I_L(X) = (-1)^{N_n} (i)^L \int \frac{[Dk_1 \cdots Dk_L] \cdot X}{(kMk + \mu^2)^{N_n}}, \quad (\text{D.57})$$

with

$$\mu^2 \equiv -(J - QM^{-1}Q). \quad (\text{D.58})$$

- **Diagonalization of the Matrix M**

Note that M is a symmetric matrix and as such, can always be diagonalized by a rotation rotation V :

$$kMk = \underbrace{k[V^\dagger (V^{-1})^\dagger]}_{k'} \underbrace{M[V^{-1} V]}_{M_{diag}} \underbrace{k}_{k'} = k' M_{diag} k' \equiv \sum_i \alpha_i k_i'^2. \quad (\text{D.59})$$

Where the α_i are the eigenvalues of M_{diag} :

$$M_{diag} = \text{diag}[\alpha_1, \dots, \alpha_L]. \quad (\text{D.60})$$

Since the Jacobian $J[V]$ for the change of variables $k' = Vk$ is one:

$$\det V = 1, \quad \Rightarrow V^{-1} = V^\top, \quad \Rightarrow J[V] = \det V^\top = \det V = 1, \quad (\text{D.61})$$

the diagonalization leaves both the measure and the integral invariant. Renaming $k' \rightarrow k$ now yields

$$I_L(X) = (-1)^{N_n} (i)^L \int \frac{[Dk_1 \cdots Dk_L] \cdot X}{(\sum_i \alpha_i k_i^2 + \mu^2)^{N_n}}. \quad (\text{D.62})$$

- **Rescaling k**

$$\bar{k}_i = \sqrt{\alpha_i} k_i, \quad Dk_i = (\alpha_i)^{-d/2} D\bar{k}_i, \quad (\text{D.63})$$

and using

$$\prod_{i=1}^L \alpha_i = \det M, \quad (\text{D.64})$$

gives (renaming $\bar{k} \rightarrow k$)

$$\begin{aligned} I_L(X) &= (-1)^{N_n} (i)^L (\det M)^{-d/2} \int \frac{[Dk_1 \cdots Dk_L] \cdot X}{(k_1^2 + \cdots + k_L^2 + \mu^2)^{N_n}} \\ &= (\det M)^{-d/2} \frac{(-1)^{N_n}}{\pi^{Ld/2}} \int \frac{[d^d k_1 \cdots d^d k_L] \cdot X}{(k_1^2 + \cdots + k_L^2 + \mu^2)^{N_n}}. \end{aligned} \quad (\text{D.65})$$

Note that after having done the Wick rotation, (D.65) is now a euclidean integral.

D.2 Concrete evaluation

We will now evaluate the L-loop integral of the form (D.65). For this however, we need to first focus on the one-loop case.

• One Loop, $X = 1$

Consider the euclidean one loop integral

$$\bar{I}_1(1) \equiv \int \frac{d^d k_E}{(k_E^2 + \mu^2)^N} = i(-1)^{N+1} \int \frac{d^d k}{(k^2 - \mu^2)^N}. \quad (\text{D.66})$$

Using d-dimensional polar coordinates and integrating over the angles, we get (renaming $k_E \rightarrow k$)

$$\bar{I}_1(1) = \left[\frac{2\pi^{d/2}}{\Gamma[d/2]} \right] \int_0^\infty \frac{dk \cdot k^{d-1}}{(k^2 + \mu^2)^N} = \left[\frac{2\pi^{d/2}}{\Gamma[d/2]} \right] \frac{1}{2(\mu^2)^{N-1}} \int_0^\infty \frac{[2k/\mu^2 dk] k^{d-2}}{(k^2/\mu^2 + 1)^N}. \quad (\text{D.67})$$

Changing the variable

$$q \equiv k^2/\mu^2, \quad dq = (2k/\mu^2) dk, \quad (\text{D.68})$$

we get

$$\bar{I}_1(1) = \left[\frac{2\pi^{d/2}}{\Gamma[d/2]} \right] \frac{1}{2(\mu^2)^{N-d/2}} \int_0^\infty \frac{dq \cdot q^{d/2-1}}{(q+1)^N} = \left[\frac{2\pi^{d/2}}{\Gamma[d/2]} \right] \frac{B(d/2, N-d/2)}{2(\mu^2)^{N-d/2}}, \quad (\text{D.69})$$

where we have made use of the integral representation of the Beta function. Rewriting the Beta function as a combination of Gamma functions, we find the final result

$$\bar{I}_1(1) \equiv \int \frac{d^d k_E}{(k_E^2 + \mu^2)^N} = \left[\frac{\pi^{d/2}}{(\mu^2)^{N-d/2}} \right] \frac{\Gamma[N-d/2]}{\Gamma[N]}. \quad (\text{D.70})$$

• L-Loop, $X = 1$

It is easy to generalize the one loop result to L-loops. Consider the euclidean L-loop integral

$$\bar{I}_L(1) \equiv \int \frac{d^d k_{E1} \cdots d^d k_{EL}}{(k_{E1}^2 + \cdots + k_{EL}^2 + \mu^2)^N} = i^L (-1)^{N+L} \int \frac{d^d k_1 \cdots d^d k_L}{(k_1^2 + \cdots + k_L^2 - \mu^2)^N}. \quad (\text{D.71})$$

We can now rewrite this integral as (renaming $k_E \rightarrow k$)

$$\bar{I}_L(1) = \int d^d k_1 \cdots d^d k_{L-1} \int \frac{d^d k_L}{(k_L^2 + M_{L-1})^N}, \quad (\text{D.72})$$

with $M_{L-1} \equiv (k_1^2 + \cdots + k_{L-1}^2 + \mu^2)$. This form of course allows us to apply the one loop result, which in fact can be done in the same matter for all L-loop integrations. We thus get

$$\begin{aligned} \bar{I}_L(1) &= \int \frac{d^d k_1 \cdots d^d k_{L-1}}{(k_1^2 + \cdots + k_{L-1}^2 + \mu^2)^{N-d/2}} \frac{\pi^{d/2} \Gamma[N-d/2]}{\Gamma[N]} \\ &= \frac{\pi^{Ld/2}}{(\mu^2)^{N-Ld/2}} \left[\frac{\Gamma[N-d/2]}{\Gamma[N]} \right] \left[\frac{\Gamma[(N-d/2)-d/2]}{\Gamma[N-d/2]} \right] \cdots \left[\frac{\Gamma[N-Ld/2]}{\Gamma[N-(L-1)d/2]} \right]. \end{aligned} \quad (\text{D.73})$$

Canceling each of the first $L-1$ numerators with the denominator of the following factor, we get the final result

$$\bar{I}_L(1) \equiv \int \frac{d^d k_{E1} \cdots d^d k_{EL}}{(k_{E1}^2 + \cdots + k_{EL}^2 + \mu^2)^N} = \frac{\pi^{Ld/2}}{(\mu^2)^{N-Ld/2}} \left[\frac{\Gamma[N - Ld/2]}{\Gamma[N]} \right]. \quad (\text{D.74})$$

• **One Loop**, $X = k^2$

Consider the euclidean one loop integral

$$\bar{I}_1(k^2) \equiv \int \frac{d^d k_E \cdot k_E^2}{(k_E^2 + \mu^2)^N} = i(-1)^N \int \frac{d^d k \cdot k^2}{(k^2 - \mu^2)^N}. \quad (\text{D.75})$$

The calculation of the $X = k^2$ case is completely analogous to the $X = 1$ case. We make the same change of variables (renaming $k_E \rightarrow k$)

$$\begin{aligned} \bar{I}_1(k^2) &= \left[\frac{2\pi^{d/2}}{\Gamma[d/2]} \right] \frac{1}{2(\mu^2)^{N-1}} \int_0^\infty \frac{[2k/\mu^2 dk] k^d}{(k^2/\mu^2 + 1)^N} = \left[\frac{2\pi^{d/2}}{\Gamma[d/2]} \right] \frac{1}{2(\mu^2)^{N-1-d/2}} \int_0^\infty \frac{dq \cdot q^{d/2}}{(q+1)^N} \\ &= \left[\frac{\pi^{d/2}}{\Gamma[d/2]} \right] \frac{B(d/2 + 1, N - 1 - d/2)}{(\mu^2)^{N-1-d/2}} \\ &= \frac{d}{2} \frac{\pi^{d/2}}{(\mu^2)^{N-1-d/2}} \frac{\Gamma[N - 1 - d/2]}{\Gamma[N]}. \end{aligned} \quad (\text{D.76})$$

• **L-Loop**, $X = k_i^2$

With the already obtained results, the evaluation of the $X = k_i^2$ L-loop case is elementary. The result reads

$$\begin{aligned} \bar{I}_1(k^2) &\equiv \int \frac{d^d k_{E1} \cdots d^d k_{EL} \cdot k_{Ei}^2}{(k_{E1}^2 + \cdots + k_{EL}^2 + \mu^2)^N} = i^L (-1)^{N+L+1} \int \frac{d^d k_1 \cdots d^d k_L \cdot k_E^2}{(k_1^2 + \cdots + k_L^2 - \mu^2)^N} \\ &= \frac{d}{2} \frac{\pi^{Ld/2}}{(\mu^2)^{N-1-Ld/2}} \frac{\Gamma[N - 1 - Ld/2]}{\Gamma[N]}. \end{aligned} \quad (\text{D.77})$$

• $G(1)$

Inserting (D.74) into

$$I_L(1) = (\det M)^{-d/2} \frac{(-1)^{N_n}}{\pi^{Ld/2}} \bar{I}_L(1), \quad (\text{D.78})$$

gives us

$$I_L(1) = (\det M)^{-d/2} \frac{(-1)^{N_n}}{(\mu^2)^{N_n-Ld/2}} \left[\frac{\Gamma[N_n - Ld/2]}{\Gamma[N_n]} \right], \quad (\text{D.79})$$

inserting this into (D.51), we get

$$\begin{aligned} G(1) &= \frac{(-1)^{N_n}}{(\mu^2)^{N_n-Ld/2}} \frac{\Gamma[N_n - Ld/2]}{\Gamma[n_1] \cdots \Gamma[n_N]} \int_0^1 \prod_{j=1}^N [dx_j x_j^{n_j-1}] (\det M)^{-d/2} \delta(1 - x_1 \cdots - x_N) \\ &= (-1)^{N_n} \frac{\Gamma[N_n - Ld/2]}{\Gamma[n_1] \cdots \Gamma[n_N]} \int_0^1 \prod_{j=1}^N [dx_j x_j^{n_j-1}] \delta(1 - x_1 \cdots - x_N) \frac{U(x)^{N_n-d/2(L+1)}}{F(x)^{N_n-d/2L}}. \end{aligned} \quad (\text{D.80})$$

Where we have introduced the F- and U-Form:

$$U(x) \equiv \det M, \quad F(x) \equiv (\det M)\mu^2. \quad (\text{D.81})$$

It is worth noting, that in the one loop case M is one. For L=1 we thus have the following situation:

$$M = U(x) = 1, \quad F(x) = \mu^2. \quad (\text{D.82})$$

This is easily understood, since for L=1, M is just the coefficient of the k^2 term in the denominator ($x_1 D_1 + \dots + x_N D_N$). Each D_i has the loop momentum squared with the coefficient one as a summand. The overall coefficient is then the sum of all the Feynman parameters, which is put to one under the integral by the delta distribution. In two and higher loop cases this is no longer the case, since M will also have entries for the product of different momenta.

- $G(k_1^\alpha)$

In the steps that led to (D.65) we transformed the integration momenta three times

$$k_i = \bar{k}_i + M_{il}^{-1} Q^l, \quad \bar{k}_i = V_{il} \bar{k}^l, \quad \bar{\bar{k}}_i = \sqrt{\alpha_i} \bar{\bar{k}}^i. \quad (\text{D.83})$$

Note that in this notation k_i is the i th entry of the L-vector k , so k_i is itself a 4-vector and should be denoted as k_i^α . Inverting the last two transformations and inserting them into the first, leads to the overall transformation

$$k_i = \frac{1}{\sqrt{\alpha_l}} (V_{il})^{-1} \bar{\bar{k}}^l + M_{il}^{-1} Q^l, \quad (\text{D.84})$$

where we implicitly sum over the index l . We need to take this transformation into account when evaluating $G(X)$ for non trivial X. After renaming $\bar{\bar{k}}_i \rightarrow k$ we have

$$I_L(k_1^\alpha) \equiv (\det M)^{-d/2} \frac{(-1)^{N_n}}{\pi^{Ld/2}} \int \frac{[d^d k_1 \dots d^d k_L] \left[\frac{1}{\sqrt{\alpha_l}} (V_{1l})^{-1} k_l^\alpha + [M_{1l}^{-1} Q^l]^\alpha \right]}{(k_1^2 + \dots + k_L^2 + \mu^2)^N}. \quad (\text{D.85})$$

The linear term in k vanishes due to

$$\int d^d k f(k^2) k^\alpha = 0. \quad (\text{D.86})$$

This leaves only the constant term

$$I_L(k_1^\alpha) = [M_{1l}^{-1} Q^l]^\alpha \cdot I_L(1) = [M_{1l}^\top Q^l]^\alpha (\det M)^{-1} \cdot I_L(1) \quad (\text{D.87})$$

which yields

$$G(k_1^\alpha) = (-1)^{N_n} \frac{\Gamma[N_n - Ld/2]}{\Gamma[n_1] \dots \Gamma[n_N]} \int_0^1 \prod_{j=1}^N [dx_j x_j^{n_j-1}] \delta(1 - x_1 \dots - x_N) \frac{U(x)^{N_n - 1 - d/2(L+1)}}{F(x)^{N_n - d/2L}} [M_{1l}^\top Q^l]^\alpha. \quad (\text{D.88})$$

- $G(k_1^\alpha k_2^\beta)$

When evaluating L-loop, N-point functions with two momenta in the numerator, the transformation (D.84) gives us quadratic, linear and constant terms in the momenta. The linear terms vanishes as before, and we are left with

$$I_L(k_1^\alpha k_2^\beta) = (\det M)^{-2} [M_{1l}^\top Q^l]^\alpha [M_{2l}^\top Q^l]^\beta I_L(1) + (\det M)^{-d/2} I_L^{\alpha\beta}, \quad (\text{D.89})$$

where

$$\begin{aligned}
I_L^{\alpha\beta} &\equiv \frac{(-1)^{N_n}}{\pi^{Ld/2}} \int \frac{[d^d k_1 \cdots d^d k_L] \left[\frac{1}{\sqrt{\alpha_l \alpha_k}} [k_l^\alpha (V_{1l}^{-1})^\dagger V_{2k}^{-1} k_k^\beta] \right]}{(k_1^2 + \cdots + k_L^2 + \mu^2)^N} \\
&= \frac{(V_{1l}^{-1})^\dagger V_{2l}^{-1}}{\alpha_l} \frac{(-1)^{N_n}}{\pi^{Ld/2}} \int \frac{[d^d k_1 \cdots d^d k_L] k_l^\alpha k_l^\beta}{(k_1^2 + \cdots + k_L^2 + \mu^2)^N}.
\end{aligned} \tag{D.90}$$

$I_L^{\alpha\beta}$ can be simplified in the above way, because it is only non linear (i.e. non vanishing) for $k = l$. We now make the ansatz

$$I_L^{\alpha\beta} = g^{\alpha\beta} \cdot I. \tag{D.91}$$

If we contract both sides with $g^{\alpha\beta}$, we get

$$\begin{aligned}
I &= \frac{1}{d} \frac{(V_{1l}^{-1})^\dagger V_{2l}^{-1}}{\alpha_l} \frac{(-1)^{N_n}}{\pi^{Ld/2}} \int \frac{[d^d k_1 \cdots d^d k_L] k_l^2}{(k_1^2 + \cdots + k_L^2 + \mu^2)^N} \\
&= \frac{1}{2} \frac{(V_{1l}^{-1})^\dagger V_{2l}^{-1}}{\alpha_l} \frac{(-1)^{N_n}}{(\mu^2)^{N-1-Ld/2}} \frac{\Gamma[N-1-Ld/2]}{\Gamma[N]}
\end{aligned} \tag{D.92}$$

where we have used (D.77). Putting all the partial results together, we get the final result

$$\begin{aligned}
G(k_1^\alpha k_2^\beta) &= (-1)^{N_n} \frac{\Gamma[N_n - Ld/2]}{\Gamma[n_1] \cdots \Gamma[n_N]} \int_0^1 \prod_{j=1}^N [dx_j x_j^{n_j-1}] \delta(1 - x_1 \cdots - x_N) \frac{U(x)^{N_n-2-d/2(L+1)}}{F(x)^{N_n-d/2L}} \\
&\times \left[[M_{1l}^\top Q^l]^\alpha [M_{2l}^\top Q^l]^\beta - \frac{g^{\alpha\beta}}{2} U(x) \cdot F(x) \frac{(V_{1l}^{-1})^\dagger V_{2l}^{-1}}{\alpha_l} \frac{\Gamma[N-1-Ld/2]}{\Gamma[N-Ld/2]} \right].
\end{aligned} \tag{D.93}$$

E Phase space

E.1 Two particle phase space

We will first look at the case of a two-body phase space:

$$d\mathcal{PS}(1, 2) = (2\pi)^4 \delta^4(p_{12} - p_1 - p_2) \frac{d^3 p_1}{(2\pi)^3 2E_1} \frac{d^3 p_2}{(2\pi)^3 2E_2}, \quad (\text{E.1})$$

$$\begin{aligned} d\Phi(1, 2) &= \delta^4(p_{12} - p_1 - p_2) \frac{d^3 p_1}{2E_1} \frac{d^3 p_2}{2E_2} \\ &= \delta^1(E_{12} - E_1 - E_2) \frac{1}{2E_2} \cdot \frac{d^3 p_1}{2E_1}, \end{aligned} \quad (\text{E.2})$$

where the four momentum of the initial particles is p_{12}^μ .

We now use properties of the Dirac distribution to rewrite it

$$\underbrace{\delta[E_{12}^2 - 2E_{12}E_1 + E_1^2 - E_2^2]}_{\text{zero at } E_1=(E_{12}-E_2)} = \frac{1}{|-2E_{12} + 2(E_{12} - E_2)|} \delta[E_1 - (E_{12} - E_2)]. \quad (\text{E.3})$$

\Rightarrow

$$\begin{aligned} \delta[E_1 - (E_{12} - E_2)] &= 2E_2 \delta[E_{12}^2 - 2E_{12}E_1 + E_1^2 - E_2^2] \\ &\stackrel{(*)}{=} 2E_2 \delta[p_{12} \cdot p_{12} - 2p_{12} \cdot p_1 + p_1 \cdot p_1 - p_2 \cdot p_2] \\ &= 2E_2 \delta[m_{12}^2 + m_1^2 - m_2^2 - 2m_{12}E_1] \end{aligned} \quad (\text{E.4})$$

The equality (*) holds because of three momentum conservation. Using this representation of the Dirac distribution we get

$$d\Phi(1, 2) = \delta[m_{12}^2 + m_1^2 - m_2^2 - 2m_{12}E_1] \frac{d^3 p_1}{2E_1}. \quad (\text{E.5})$$

Now we rewrite the differential in polar coordinates:

$$\frac{d^3 p_1}{E_1} = \frac{1}{E_1} d\Omega |\vec{p}_1|^2 d|\vec{p}_1| = |\vec{p}_1| d\Omega dE_1. \quad (\text{E.6})$$

The last equality holds because of $dm_1^2 = 0 = dE_1^2 - d|\vec{p}_1|^2 = 2E_1 dE_1 - 2|\vec{p}_1| d|\vec{p}_1|$. From this it follows that $E_1 dE_1 = |\vec{p}_1| d|\vec{p}_1|$, which reduces the phase space to

$$d\Phi(1, 2) = \delta[m_{12}^2 + m_1^2 - m_2^2 - 2m_{12}E_1] \frac{|\vec{p}_1|}{2} d\Omega dE_1 = \frac{|\vec{p}_1|}{2} \frac{1}{|-2m_{12}|} d\Omega. \quad (\text{E.7})$$

Using $|\vec{p}_1| = \lambda^{1/2}(m_{12}^2, m_1^2, m_2^2)/(2m_{12})$, this can be reformulated as

$$d\Phi(1, 2) = \frac{1}{4m_{12}} \frac{\lambda^{1/2}(m_{12}^2, m_1^2, m_2^2)}{2m_{12}} d\Omega. \quad (\text{E.8})$$

The Källén function $\lambda(a, b, c)$ is defined as $\lambda(a, b, c) = a^2 + b^2 + c^2 - 2ab - 2bc - 2ca = (a - b - c)^2 - 4bc$. Integrating the phase space over the azimuthal angle gives a factor 2π , and the final result reads

$$d\Phi(1, 2) = \frac{\pi}{4} \frac{\lambda^{1/2}(m_{12}^2, m_1^2, m_2^2)}{m_{12}^2} d\cos\theta. \quad (\text{E.9})$$

E.2 Three particle phase space

Now we are considering the three-body phase space which we need since the muon is decaying into three particles. Once again we only consider the reduced phase space

$$d\Phi(1, 2, 3) = \delta^4[p_{123} - p_1 - p_2 - p_3] \frac{d^3 p_1}{2E_1} \frac{d^3 p_2}{2E_2} \frac{d^3 p_3}{2E_3}. \quad (\text{E.10})$$

We multiply with

$$1 = d^4 p_{12} \delta^4[p_{12} - p_1 - p_2] \quad (\text{E.11})$$

resulting in

$$\begin{aligned} d\Phi(1, 2, 3) &= \underbrace{\left[\frac{d^3 p_1}{2E_1} \frac{d^3 p_2}{2E_2} \delta^4[p_{12} - p_1 - p_2] \right]}_{=d\Phi(1,2)} \frac{d^3 p_3}{2E_3} d^4 p_{12} \delta^4[p_{123} \underbrace{-p_1 - p_2}_{=-p_{12}} - p_3] \\ &= d\Phi(1, 2) \frac{d^3 p_3}{2E_3} d^3 p_{12} \delta^4[p_{123} - p_{12} - p_3] dE_{12}. \end{aligned} \quad (\text{E.12})$$

We multiply, this time with

$$1 = dm_{12}^2 \delta^1[p_{12} \cdot p_{12} - m_{12}^2] = dm_{12}^2 \delta^1[E_{12}^2 - |\vec{p}_{12}|^2 - m_{12}^2] \quad (\text{E.13})$$

which gives

$$d\Phi(1, 2, 3) = d\Phi(1, 2) \frac{d^3 p_3}{2E_3} d^3 p_{12} \delta^4[p_{123} - p_{12} - p_3] dm_{12}^2 dE_{12} \delta^1[E_{12}^2 - |\vec{p}_{12}|^2 - m_{12}^2]. \quad (\text{E.14})$$

If we understand E_{12} as the integration variable, the argument of the last Dirac distribution vanishes for $E_{12} = \sqrt{|\vec{p}_{12}|^2 + m_{12}^2}$, giving rise to

$$dE_{12} \delta[E_{12}^2 - |\vec{p}_{12}|^2 - m_{12}^2] = \frac{dE_{12}}{|2\sqrt{|\vec{p}_{12}|^2 + m_{12}^2}|} \delta[E_{12} - \sqrt{|\vec{p}_{12}|^2 + m_{12}^2}] = \frac{1}{2E_{12}}. \quad (\text{E.15})$$

Inserting this gives the final result

$$\begin{aligned} d\Phi(1, 2, 3) &= d\Phi(1, 2) \underbrace{\frac{d^3 p_3}{2E_3} \frac{d^3 p_{12}}{2E_{12}} \delta^4[p_{123} - p_{12} - p_3]}_{=d\Phi(12,3)} dm_{12}^2 \\ d\Phi(1, 2, 3) &= d\Phi(1, 2) d\Phi(12, 3) ds'. \quad s' \equiv m_{12}^2 \end{aligned} \quad (\text{E.16})$$

From its definition (E.10) it is clear that $d\Phi(1, 2, 3)$ is totally symmetric in its entries - that is to say the following holds as well:

$$d\Phi(1, 2, 3) = d\Phi(2, 3, 1) = d\Phi(2, 3) d\Phi(23, 1) ds'. \quad (\text{E.17})$$

For the evaluation of the three particle phase space of the Bremsstrahlung diagrams, we made use of (E.16).

F Bhabha phase space integrals

F.1 Further x-integrals for section 9

The x-integrals for the constant term

$$\int_{-1}^{+1} dx \frac{\ln(1-x^2)^2}{(1-\beta_\alpha x)^2} = \frac{2}{\beta_\alpha(1-\beta_\alpha^2)} \left[\beta_\alpha \left(4 \ln^2(2) - \frac{\pi^2}{3} \right) - 4 \ln(2) \ln \left(\frac{1+\beta_\alpha}{1-\beta_\alpha} \right) - 2 \text{Li}_2 \left[\frac{2\beta_\alpha}{\beta_\alpha-1} \right] + 2 \text{Li}_2 \left[\frac{2\beta_\alpha}{\beta_\alpha+1} \right] \right] \quad (\text{F.18})$$

$$\begin{aligned} \int_{-1}^{+1} dx \frac{\ln(1-x^2) \ln(1-\beta_\alpha x)}{(1-\beta_\alpha x)^2} &= \frac{1}{\beta_\alpha(1-\beta_\alpha^2)} \left[\beta_\alpha \left(2 \ln(2) \ln(1-\beta_\alpha^2) + 4 \ln(2) + \frac{\pi^2}{3} + \ln^2 \left(\frac{1+\beta_\alpha}{1-\beta_\alpha} \right) \right) \right. \\ &+ 2 \ln^2(1-\beta_\alpha) - 2 \ln^2(\beta_\alpha+1) - (2-2 \ln(\beta_\alpha) - i\pi(1+\beta_\alpha)) \ln \left(\frac{1+\beta_\alpha}{1-\beta_\alpha} \right) \\ &\left. + (\beta_\alpha-1) \text{Li}_2 \left[\frac{1-\beta_\alpha}{1+\beta_\alpha} \right] + (\beta_\alpha+1) \text{Li}_2 \left[\frac{1+\beta_\alpha}{1-\beta_\alpha} \right] \right] \end{aligned} \quad (\text{F.19})$$

F.2 Feynman parameter integrals for section 9

Parameter Integrals for the divergent part and final state radiation from the same leg:

$$\begin{aligned} \int_0^1 \frac{d\alpha}{m^2 + (s-4m^2)\alpha(1-\alpha)} &= \frac{2}{s\beta} \ln \left(\frac{1+\beta}{1-\beta} \right), \\ \int_0^1 \frac{d\alpha \ln(\alpha)}{m^2 + (s-4m^2)\alpha(1-\alpha)} &= \frac{1}{s\beta} \left[\text{Li}_2 \left[\frac{-2\beta}{1-\beta} \right] - \text{Li}_2 \left[\frac{2\beta}{1+\beta} \right] \right] \\ \int_0^1 \frac{d\alpha \ln(1-\beta^2(1-2\alpha)^2)}{m^2 + (s-4m^2)\alpha(1-\alpha)} &= \frac{1}{s\beta} \left[\ln \left(\frac{1+\beta}{1-\beta} \right) \ln(4(1-\beta^2)) + 2 \text{Li}_2 \left[\frac{1-\beta}{2} \right] - 2 \text{Li}_2 \left[\frac{1+\beta}{2} \right] \right]. \end{aligned} \quad (\text{F.20})$$

Parameter Integrals for the divergent part and initial-final state interference

$$\begin{aligned} \int_0^1 \frac{d\alpha}{m^2 - t\alpha(1-\alpha)} &= \frac{2}{\sqrt{t(t-4m^2)}} \ln \left(\frac{\sqrt{4m^2-t} + \sqrt{-t}}{\sqrt{4m^2-t} - \sqrt{-t}} \right), \\ \int_0^1 \frac{d\alpha \ln(\alpha)}{m^2 - t\alpha(1-\alpha)} &= \frac{1}{\sqrt{t(t-4m^2)}} \left[\text{Li}_2 \left[\frac{2\sqrt{-t}}{\sqrt{-t} - \sqrt{4m^2-t}} \right] - \text{Li}_2 \left[\frac{2\sqrt{-t}}{\sqrt{-t} + \sqrt{4m^2-t}} \right] \right], \\ \int_0^1 \frac{d\alpha \ln \left(1 - \frac{4}{s}(m^2 - t\alpha(1-\alpha)) \right)}{m^2 - t\alpha(1-\alpha)} &= \frac{2}{\sqrt{t(t-4m^2)}} \left[\text{Li}_2 \left[\frac{\sqrt{u} + \sqrt{-t}}{\sqrt{u} - \sqrt{4m^2-t}} \right] \right. \\ &- \text{Li}_2 \left[\frac{\sqrt{u} - \sqrt{-t}}{\sqrt{u} - \sqrt{4m^2-t}} \right] - \text{Li}_2 \left[\frac{\sqrt{u} + \sqrt{-t}}{\sqrt{u} + \sqrt{4m^2-t}} \right] + \text{Li}_2 \left[\frac{\sqrt{u} - \sqrt{-t}}{\sqrt{u} + \sqrt{4m^2-t}} \right] \\ &\left. + \ln(\beta^2) \ln \left(\frac{\sqrt{4m^2-t} + \sqrt{-t}}{\sqrt{4m^2-t} - \sqrt{-t}} \right) + \ln \left(\frac{\sqrt{u} + \sqrt{-t}}{\sqrt{u} - \sqrt{-t}} \right) \ln \left(\frac{\sqrt{4m^2-t} + \sqrt{u}}{\sqrt{4m^2-t} - \sqrt{u}} \right) \right]. \end{aligned} \quad (\text{F.21})$$

Parameter integrals for the divergent part and final-final state radiation from different legs

$$\begin{aligned}
\int_0^1 \frac{d\alpha}{[m^2 - (4m^2 - s)\alpha(1 - \alpha)]} &= \frac{2}{s\beta} \ln \left(\frac{1 + \beta}{1 - \beta} \right), \\
\int_0^1 \frac{d\alpha}{\beta\sqrt{(1 - 2\alpha)^2} (s - 4m^2)\alpha(1 - \alpha) + m^2} \frac{\ln \frac{1 - \beta\sqrt{(1 - 2\alpha)^2}}{1 + \beta\sqrt{(1 - 2\alpha)^2}}}{\beta\sqrt{(1 - 2\alpha)^2} (s - 4m^2)\alpha(1 - \alpha) + m^2} &= \frac{2}{s\beta} \left[2\text{Li}_2[\beta] - 2\text{Li}_2[-\beta] + \text{Li}_2\left[\frac{1 - \beta}{2}\right] - \text{Li}_2\left[\frac{1 + \beta}{2}\right] \right. \\
&\quad \left. + \frac{1}{2} \ln^2\left(\frac{1 - \beta}{2}\right) - \frac{1}{2} \ln^2\left(\frac{1 + \beta}{2}\right) \right]. \tag{F.22}
\end{aligned}$$

Parameter integrals for the divergent part and initial-final state radiation

$$\begin{aligned}
\int_0^1 \frac{d\alpha \ln \left[\frac{\sqrt{s} + 2\sqrt{m^2 - t\alpha(1 - \alpha)}}{\sqrt{s} - 2\sqrt{m^2 - t\alpha(1 - \alpha)}} \right]}{(2/\sqrt{s})[m^2 - t\alpha(1 - \alpha)]^{3/2}} &= \frac{4}{(4m^2 - t)} \left[\frac{\sqrt{s}}{2m} \ln \left(\frac{\sqrt{s} + 2m}{\sqrt{s} - 2m} \right) - \frac{\sqrt{u}}{\sqrt{-t}} \ln \left(\frac{\sqrt{u} + \sqrt{-t}}{\sqrt{u} - \sqrt{-t}} \right) \right. \\
&\quad \left. + \frac{\sqrt{4m^2 - t}}{\sqrt{-t}} \ln \left(\frac{\sqrt{4m^2 - t} + \sqrt{-t}}{\sqrt{4m^2 - t} - \sqrt{-t}} \right) \right]. \tag{F.23}
\end{aligned}$$

G Muon decay

In this section we will analytically calculate the muon decay rate (see Figure 11) in two different ways. First we calculate it directly by doing the s integration in a convenient frame and second we change the s integration to an integration over the electron energy.

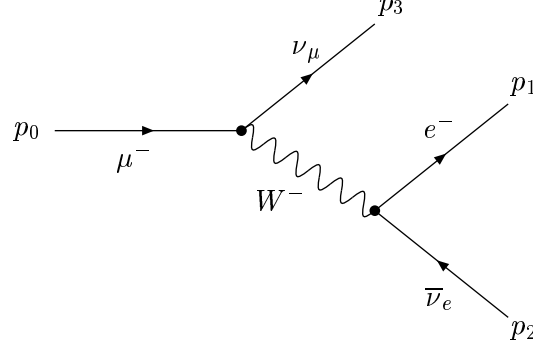


Figure 11: muon decay $\mu^- \rightarrow e^- \nu_\mu \bar{\nu}_e$

The focus hereby lies on the formal aspects of the second calculation, where we first approximate the denominator of the W propagator to then solve the neutrino phase space integrals using tensor integration. Tensor Integrals are of the type

$$\int d^4 p p^{\mu_1} \dots p^{\mu_n} f(p), \quad (\text{G.1})$$

where $f(p)$ is any scalar function, which might also depend on p . Tensor integrals arise naturally in loop calculations, when integrating the numerator of the gauge boson propagator, which has a tensor structure involving the integration variable (i.e., the loop momentum).

G.1 Feynman rules

For the process under consideration, we will use the following Feynman rules:
The W^- -fermion-(anti-)fermion vertex

$$\left[-i \frac{G_F M_W^2}{\sqrt{2}} \right]^{1/2} \gamma_\mu (1 - \gamma_5) \quad (\text{G.2})$$

and the W^- -gauge boson propagator

$$\frac{-i}{k^2 - M_W^2} \left[g_{\mu\nu} - \frac{k_\mu k_\nu}{k^2 - \xi M_W^2} (1 - \xi) \right] = \frac{-i}{k^2 - M_W^2} \left[g_{\mu\nu} - \frac{k_\mu k_\nu}{\alpha k^2 - M_W^2} (\alpha - 1) \right]. \quad (\text{G.3})$$

Where $\xi = 1/\alpha$ is a gauge parameter, G_F is the Fermi constant and M_W is the W^- -mass. In our further calculation, we will always use the unitary gauge:

$$-i \frac{g_{\mu\nu} + k_\mu k_\nu / M_W^2}{k^2 - M_W^2}. \quad (\text{G.4})$$

In the muon decay all external particles are fermions. The incoming muon is associated with the spinor u , while outgoing antifermions (i.e., the electron neutrino) with v and outgoing particles are associated with the spinor conjugate \bar{u} .

G.2 M-matrix

The above rules give the following expression for the M-matrix:

$$\mathcal{M} = -\frac{G_F M_W^2}{\sqrt{2}} [\bar{u}_3 \gamma_\mu (1 - \gamma_5) u_0] [\bar{u}_1 \gamma_\nu (1 - \gamma_5) v_2] \frac{g_{\mu\nu} + k_\mu k_\nu / M_W^2}{k^2 - M_W^2}. \quad (\text{G.5})$$

The complex conjugate reads

$$\mathcal{M}^* = -\frac{G_F M_W^2}{\sqrt{2}} [\bar{u}_0 \gamma_\beta (1 - \gamma_5) u_3] [\bar{v}_2 \gamma_\alpha (1 - \gamma_5) u_1] \frac{g_{\alpha\beta} + k_\alpha k_\beta / M_W^2}{k^2 - M_W^2}. \quad (\text{G.6})$$

The expressions between the square brackets form scalars. We can thus arrange them, without having to worry about γ -algebra, in the following order:

$$|\mathcal{M}|^2 \propto [\bar{u}_0 \gamma_\beta (1 - \gamma_5) u_3 \bar{u}_3 \gamma_\mu (1 - \gamma_5) u_0] [\bar{u}_1 \gamma_\nu (1 - \gamma_5) v_2 \bar{v}_2 \gamma_\alpha (1 - \gamma_5) u_1]. \quad (\text{G.7})$$

Next we sum over the particle spin components. This summation gives rise to the usual trace expressions:

$$\sum_{\text{spin}} |\mathcal{M}|^2 \propto \text{Tr} [\bar{u}_0 \gamma_\beta (1 - \gamma_5) u_3 \bar{u}_3 \gamma_\mu (1 - \gamma_5) u_0] \text{Tr} [\bar{u}_1 \gamma_\nu (1 - \gamma_5) v_2 \bar{v}_2 \gamma_\alpha (1 - \gamma_5) u_1]. \quad (\text{G.8})$$

Like always, we make use of the cyclic property of the trace as well as the Dirac equation for the expressions $u_i \bar{u}_i$ and $v_i \bar{v}_i$, resulting in

$$\sum_{\text{spin}} |\mathcal{M}|^2 \propto \text{Tr} [(\not{p}_0 + m_\mu) \gamma_\beta (1 - \gamma_5) \not{p}_3 \gamma_\mu (1 - \gamma_5)] \text{Tr} [(\not{p}_1 + m_e) \gamma_\nu (1 - \gamma_5) \not{p}_2 \gamma_\alpha (1 - \gamma_5)], \quad (\text{G.9})$$

where the neutrino masses are set to zero. Inserting the constant and boson propagators that we have been omitting so far, we get

$$\begin{aligned} \frac{1}{2} \sum_{\text{spin}} |\mathcal{M}|^2 &= \frac{1}{2} \frac{G_F^2 M_W^4}{2} \text{Tr} [(\not{p}_0 + m_\mu) \gamma_\beta (1 - \gamma_5) \not{p}_3 \gamma_\mu (1 - \gamma_5)] \\ &\cdot \text{Tr} [(\not{p}_1 + m_e) \gamma_\nu (1 - \gamma_5) \not{p}_2 \gamma_\alpha (1 - \gamma_5)] \\ &\cdot \frac{g_{\alpha\beta} + k_\alpha k_\beta / M_W^2}{k^2 - M_W^2} \frac{g_{\mu\nu} + k_\mu k_\nu / M_W^2}{k^2 - M_W^2}. \end{aligned} \quad (\text{G.10})$$

This expression for the squared M-Matrix can be solved, making use of the γ -trace identities. In our calculations we used the program FORM, yielding:

$$\begin{aligned} \frac{1}{2} \sum_{\text{spin}} |\mathcal{M}|^2 &= \frac{32 G_F^2 m_\mu^2}{(M_W^2 - k^2)^2} [p_0.p_1 p_0.p_2 p_0.p_3 - p_0.p_1 p_0.p_3 p_2.p_3 + p_0.p_1 p_2.p_3 (M_W^2) \\ &- p_0.p_2 p_0.p_3 p_1.p_3 + p_0.p_2 p_1.p_3 (M_W^2 + 2 \frac{M_W^4}{m_\mu^2}) - p_0.p_3 p_1.p_2 (M_W^2 + \frac{m_\mu^2}{2}) \\ &+ p_0.p_3 p_1.p_3 p_2.p_3 + p_0.p_3 p_0.p_3 p_1.p_2 - p_1.p_3 p_2.p_3 (2M_W^2)]. \end{aligned} \quad (\text{G.11})$$

Where $a.b$ is the Minkowski scalar product of two four vectors.

From here we have two possibilities of calculating the total decay rate:

- 1.) We can fix the kinematics of the decay in a convenient way and then integrate over one angle and s .
- 2.) We can approximate the boson propagator, integrate over the neutrino phase space, using tensor integrals and integrate over the energy of the electron.

G.3 The kinematic approach

Using the expression for the three-body phase space, derived in the appendix E:

$$d\mathcal{P}\mathcal{S}(1, 2, 3) = \frac{1}{(2\pi)^5} d\Phi(1, 2) d\Phi(12, 3) ds, \quad s = m_{12}^2 \quad (\text{G.12})$$

we can rewrite the two-particle phase spaces as:

$$\begin{aligned} d\Phi(1, 2) &= \frac{\pi}{4} \frac{s - m_e^2}{s} d\cos\theta_e \\ d\Phi(12, 3) &= \frac{\pi}{2} \frac{m_\mu^2 - s}{m_\mu^2}. \end{aligned} \quad (\text{G.13})$$

Where we have integrated over $d\cos\theta_{\nu_\mu}$. The angle θ_{ν_μ} is the angle between the muon and the muon neutrino, θ_e is the angle between the electron and the electron antineutrino. The differential cross section now reads:

$$d\Gamma = \frac{1}{64m_\mu^3} \frac{1}{(2\pi)^3} \cdot \left[\frac{1}{2} |\mathcal{M}|^2 \right] \cdot \frac{(m_\mu^2 - s)(s - m_e^2)}{s} d\cos\theta_e ds. \quad (\text{G.14})$$

At this point we turn back to the expression (G.11) and express all contracted momentum pairs through the Mandelstam variables, which are defined as follows:

$$\begin{aligned} s &= (p_0 - p_3)^2 = (p_1 + p_2)^2 \\ t &= (p_0 - p_1)^2 = (p_2 + p_3)^2 \\ u &= (p_0 - p_2)^2 = (p_1 + p_3)^2. \end{aligned} \quad (\text{G.15})$$

Any possible contraction of the momenta in (G.11) can now be expressed via these three variables:

$$\begin{aligned} p_0 \cdot p_1 &= \frac{m_\mu^2 + m_e^2 - t}{2} & p_0 \cdot p_2 &= \frac{m_\mu^2 - u}{2} \\ p_0 \cdot p_3 &= \frac{m_\mu^2 - s}{2} & p_1 \cdot p_2 &= \frac{s - m_e^2}{2} \\ p_1 \cdot p_3 &= \frac{u - m_e^2}{2} & p_2 \cdot p_3 &= \frac{t}{2}. \end{aligned} \quad (\text{G.16})$$

Using `MATHEMATICA`, we rewrite $\sum |\mathcal{M}|^2$ purely in Mandelstam variables:

$$\begin{aligned} \frac{1}{2} \sum_{\text{spin}} |\mathcal{M}|^2 &= \frac{4G_F^2}{(M_W^2 - s)^2} [-m_e^4 m_\mu^4 - 4m_e^2 M_W^4 m_\mu^2 + m_e^2 (m_e^2 + m_\mu^2 - s) s m_\mu^2 \\ &+ (4m_e^2 M_W^2 m_\mu^2) t + 4M_W^4 (m_e^2 + m_\mu^2 - u) u]. \end{aligned} \quad (\text{G.17})$$

The expression (G.17) depends only on s , t and u , but we have to integrate over s and $\cos\theta_e$. This means we need to express t and u in terms of $\cos\theta_e$. We are able to do this by choosing the W boson rest frame:

$$\begin{aligned} k &= (\sqrt{s}, 0, 0, 0) \\ p_0 &= \left(\frac{s + m_\mu^2}{2\sqrt{s}}, 0, 0, \frac{m_\mu^2 - s}{2\sqrt{s}} \right) \\ p_3 &= \frac{m_\mu^2 - s}{2\sqrt{s}} (1, 0, 0, 1) \\ p_1 &= \left(\frac{s + m_e^2}{2\sqrt{s}}, \frac{s - m_e^2}{2\sqrt{s}} \sin\theta_e \cos\phi, \frac{s - m_e^2}{2\sqrt{s}} \sin\theta_e \sin\phi, \frac{s - m_e^2}{2\sqrt{s}} \cos\theta_e \right) \\ p_2 &= \frac{s - m_e^2}{2\sqrt{s}} (1, -\sin\theta_e \cos\phi, -\sin\theta_e \sin\phi, -\cos\theta_e). \end{aligned} \quad (\text{G.18})$$

Where we have also made use of the freedom to choose the direction of the muon momentum. It can be easily seen, that the above choice respects the momentum conservation $p_0 = p_1 + p_2 + p_3$, the on-shell condition $p_i^2 = m_i^2$, as well as all the identities in (G.16).

For further calculation, we have to get rid of the variable u using the following property of s, t and u :

$$s + t + u = m_\mu^2 + m_e^2. \quad (\text{G.19})$$

leaving dependence only on s and t , where t can be expressed in terms of $\cos \theta_e$ using (G.18):

$$t = 2p_2 \cdot p_3 \stackrel{(\text{G.18})}{=} \frac{(m_\mu^2 - s)(s - m_e^2)(\cos \theta_e + 1)}{2s}. \quad (\text{G.20})$$

Multiplying $\sum |\mathcal{M}|^2$ with the other factors out of (G.14) and doing the $\cos \theta_e$ integration, we get the differential decay rate:

$$\begin{aligned} \frac{d\Gamma}{ds} &= \frac{G_F^2 (m_e^2 - s)^2 (m_\mu^2 - s)^2}{192 m_\mu^3 \pi^3 (s - M_W^2)^2 s^3} [2M_W^4 s (m_\mu^2 + 2s) \\ &+ (2M_W^4 s + m_\mu^2 (4M_W^4 + 6sM_W^2 + 3s^2)) m_e^2]. \end{aligned} \quad (\text{G.21})$$

The limit of infinite W mass and vanishing electron mass

$$\lim_{\substack{M_W \rightarrow \infty \\ m_e \rightarrow 0}} \frac{d\Gamma}{ds} = \frac{G_F^2 (m_\mu^2 - s)(m_\mu^2 + 2s)^2}{96 m_\mu^3 \pi^3}, \quad (\text{G.22})$$

yields the correct zeroth order result:

$$\int_0^{m_\mu^2} ds \frac{G_F^2 (m_\mu^2 - s)(m_\mu^2 + 2s)^2}{96 m_\mu^3 \pi^3} = \frac{G_F^2 m_\mu^5}{192 \pi^3}. \quad (\text{G.23})$$

The s integration of the whole expression is a little more involved, since we encounter the following integrals:

$$\int ds \frac{s^n}{(M_W^2 - s)^2}, \quad n = 0, \pm 1, \pm 2, \pm 3 \quad (\text{G.24})$$

We get undefined expressions, if we for example do the following integral:

$$\int ds \frac{s}{(M_W^2 - s)^2} = \frac{M_W^2}{M_W^2 - s} + \ln(M_W^2 - s), \quad (\text{G.25})$$

which has a dimension-full expression in the argument of the logarithm! To prevent this situation, we scale the integration variable with the W mass. The new integration variable is the dimensionless quantity $z = s/M_W^2$. With the original integration range

$$m_e^2 \leq s \leq m_\mu^2, \quad (\text{G.26})$$

our integrals become:

$$\int_{m_e^2}^{m_\mu^2} ds \frac{s^n}{(M_W^2 - s)^2} = M_W^{(2n-4)} \int_{m_e^2}^{m_\mu^2} ds \frac{\left(\frac{s}{M_W^2}\right)^n}{\left(\left(\frac{M_W}{M_W}\right)^2 - \frac{s}{M_W^2}\right)^2} = M_W^{(2n-2)} \int_{m_e^2/M_W^2}^{m_\mu^2/M_W^2} dz \frac{z^n}{(1-z)^2}. \quad (\text{G.27})$$

Using the integrals listed in G.8, we find the expression:

$$\begin{aligned}
\Gamma(\mu^- \rightarrow e^- \nu_\mu \bar{\nu}_e) &= \frac{G_F^2 m_\mu^5}{192\pi^3} [\ln(x) (-12x^2 + (24x^3 + 24x^2)y - 27x^3y^2) \\
&+ \frac{12 - 12x}{y^3} + \frac{6x^2 - 6}{y^2} + \frac{2x^3 - 27x^2 + 27x - 2}{y} \\
&+ \left(\frac{39x^3}{2} - \frac{39x}{2}\right) + (27x^2 - 27x^3)y \\
&+ \ln\left(\frac{1-y}{1-xy}\right) \left(\frac{12}{y^4} + \frac{-12x-12}{y^3} + \frac{33x}{y^2} + \frac{-24x^2-24x}{y}\right) \\
&+ (3x^3 + 3x) + (24x^3 + 24x^2)y - 27x^3y^2], \tag{G.28}
\end{aligned}$$

with

$$x = \frac{m_e^2}{m_\mu^2}, \quad y = \frac{m_\mu^2}{M_W^2}. \tag{G.29}$$

This expression gives the following value for the total decay rate:

$$\Gamma(\mu^- \rightarrow e^- \nu_\mu \bar{\nu}_e) = 3.008728 \cdot 10^{-19} \text{ GeV}, \tag{G.30}$$

which agrees well with the experimental value $2.995917 \cdot 10^{-19} \text{ GeV}$ [92].

G.4 M-matrix with tensor integrals

As mentioned in the introduction, we will also approximate the denominator of the propagator to simplify the integrand, i.e. $\sum |\mathcal{M}|^2$, for the phase space integration. Making use of $k = p_0 - p_3$ and letting the muon-neutrino mass vanish (i.e., $p_3^2 = 0$), we rewrite the squared denominator of the W-propagator as follows:

$$\frac{1}{(M_W^2 - k^2)^2} = \frac{1}{(M_W^2 - m_\mu^2 + 2p_0 \cdot p_3)^2} = \left(\frac{1}{M_W^4}\right) \frac{1}{(1 - (m_\mu^2 - 2p_0 \cdot p_3)/M_W^2)^2}. \tag{G.31}$$

The expression $(m_\mu^2 - 2p_0 \cdot p_3)/M_W^2$ is small compared to 1. We therefore use the approximation

$$\left(\frac{1}{1-\epsilon}\right)^2 = (1 + \epsilon + \epsilon^2 + \dots)^2 \approx 1 + 2\epsilon, \tag{G.32}$$

which is valid for small ϵ and gives

$$\left(\frac{1}{M_W^4}\right) \frac{1}{(1 - (m_\mu^2 - 2p_0 \cdot p_3)/M_W^2)^2} \approx \frac{1}{M_W^4} (1 + 2(m_\mu^2 - 2p_0 \cdot p_3)/M_W^2). \tag{G.33}$$

Using this and letting all M_W^n with $n \leq -4$ equal to zero, we find the result

$$\begin{aligned}
\sum_{\text{spin}} |\mathcal{M}|^2 &= p_0 \cdot p_1 p_2 \cdot p_3 (64G_F^2 m_\mu^2 / M_W^2) \\
&+ p_0 \cdot p_2 p_0 \cdot p_3 p_1 \cdot p_3 (-512G_F^2 / M_W^2) \\
&+ p_0 \cdot p_2 p_1 \cdot p_3 (320G_F^2 m_\mu^2 / M_W^2 + 128G_F^2) \\
&+ p_0 \cdot p_3 p_1 \cdot p_2 (-64G_F^2 m_\mu^2 / M_W^2) \\
&+ p_1 \cdot p_3 p_2 \cdot p_3 (-128G_F^2 m_\mu^2 / M_W^2). \tag{G.34}
\end{aligned}$$

Only considering the zeroth order in M_W , only one term contributes:

$$\sum_{\text{spin}} |\mathcal{M}^{(0)}|^2 = (128G_F^2) p_0 \cdot p_2 \ p_1 \cdot p_3. \quad (\text{G.35})$$

Using the third equality in (G.37), this is relatively easy to solve and gives the short expression frequently to be found in textbooks (i.e. [1]):

$$\Gamma^{(0)}(\mu^- \rightarrow e^- \nu_\mu \bar{\nu}_e) = \frac{G_F^2 m_\mu^5 (1 - \frac{8m_e^2}{m_\mu^2})}{192\pi^3}. \quad (\text{G.36})$$

Where m_e^n for $n \geq 4$ was also neglected. In our further calculation, we will consider the full expression (G.34). To obtain the total decay rate, we are now left to integrate over the three particle phase space $d\mathcal{PS}(1, 2, 3)$.

G.5 Phase space tensor integrals

We can now integrate (G.34) over the separated phase space of the two neutrinos $d\Phi(2, 3)$ (see appendix A.2 for its derivation). We see that we have to integrate over expressions involving two and three muon momenta p_2 and p_3 all being contracted either with one another or with momenta that we do not integrate over. We separate the scalar products in the following way:

$$\begin{aligned} \int d\Phi(2, 3) p_0 \cdot p_1 \ p_2 \cdot p_3 &= p_0 \cdot p_1 \ g_{\mu\nu} \ I^{\mu\nu} \\ \int d\Phi(2, 3) p_0 \cdot p_2 \ p_0 \cdot p_3 \ p_1 \cdot p_3 &= p_{0\alpha} \ p_{0\beta} \ p_{1\gamma} \ I^{\alpha\beta\gamma} \\ \int d\Phi(2, 3) p_0 \cdot p_2 \ p_1 \cdot p_3 &= p_{1\mu} \ p_{0\nu} \ I^{\mu\nu} \\ \int d\Phi(2, 3) p_0 \cdot p_3 \ p_1 \cdot p_2 &= p_{0\mu} \ p_{1\nu} \ I^{\mu\nu} \\ \int d\Phi(2, 3) p_1 \cdot p_3 \ p_2 \cdot p_3 &= p_{1\beta} \ g_{\alpha\gamma} \ I^{\alpha\beta\gamma}. \end{aligned} \quad (\text{G.37})$$

Where $I^{\mu\nu}$ and $I^{\alpha\beta\gamma}$ are the tensor integrals:

$$I^{\mu\nu} \equiv \int d\Phi(2, 3) p_2^\mu p_3^\nu \quad (\text{G.38})$$

$$I^{\alpha\beta\gamma} \equiv \int d\Phi(2, 3) p_2^\alpha p_3^\beta p_3^\gamma. \quad (\text{G.39})$$

In the two body phase space of the muons, these are the only integrals that we will have to compute. We will first treat the simpler case (G.39) and make the following ansatz for the tensor structure of the solution:

$$I^{\mu\nu} = \int d\Phi(2, 3) p_2^\mu p_3^\nu = Ag^{\mu\nu} + BP^\mu P^\nu, \quad (\text{G.40})$$

where $P^\mu = (p_3 + p_2)^\mu$ and $P^2 = t \equiv s' = 2p_2 p_3$. Note that s' differs from s used in the kinematic approach! Further A and B are constants to be determined through contracting $I^{\mu\nu}$ with $g^{\mu\nu}$ and $P^\mu P^\nu$. We have to contract twice, as we need two equations to determine our two constants A and B :

$$\begin{aligned} g^{\mu\nu} I_{\mu\nu} &= \int d\Phi(2, 3) p_2 \cdot p_3 = \int d\Phi(2, 3) \frac{s'}{2} \\ &= \int d\cos\theta \left[\frac{\pi \lambda^{1/2}(s', 0, 0)}{4 s'} \right] \frac{s'}{2} = \frac{\pi}{8} s' \int d\cos\theta = \frac{\pi}{4} s' \\ &= 4A + P^2 B = 4A + s' B \end{aligned} \quad (\text{G.41})$$

$$\begin{aligned}
P^\mu P^\nu I_{\mu\nu} &\stackrel{(**)}{=} \int d\Phi(2,3) p_{2\mu} (p_3 + p_2)^\mu p_{3\nu} (p_3 + p_2)^\nu = \int d\Phi(2,3) (p_2 \cdot p_3)^2 \\
&= \int d\Phi(2,3) \frac{s'^2}{4} = \frac{\pi}{8} s'^2 \\
&= P^2 A + P^2 P^2 B = s' A + s'^2 B.
\end{aligned} \tag{G.42}$$

The equality $(**)$ might seem awkward, since we are pulling the factor $P^\mu = (p_3 + p_2)^\mu$ under an integral which is over the $d\Phi(2,3)$ phase space. However, the kinematic fact $(p_3 + p_2)^\mu = (p_0 - p_1)^\mu$ shows that P^μ is a constant under the $d\Phi(2,3)$ integration.

Finally solving (G.41) and (G.42) for A and B gives the tensor Integral

$$I^{\mu\nu} = \int d\Phi(2,3) p_2^\mu p_3^\nu = \frac{\pi}{24} s' g^{\mu\nu} + \frac{\pi}{12} P^\mu P^\nu. \tag{G.43}$$

The calculation of the tensor integral over three momenta will not be carried out in detail as it is analogous to the calculation of (G.40). The ansatz reads

$$I^{\alpha(\beta\gamma)} = \int d\Phi(2,3) p_2^\alpha p_3^\beta p_3^\gamma = AP^\alpha P^\beta P^\gamma + BP^\alpha g^{\beta\gamma} + C(P^\beta g^{\alpha\gamma} + P^\gamma g^{\alpha\beta}). \tag{G.44}$$

Round brackets around a group of indices signal that the expression is symmetric in these indices. Since $I^{\alpha(\beta\gamma)}$ is symmetric in β and γ , we choose an ansatz which is also symmetric in these indices. We now have to contract $I^{\alpha(\beta\gamma)}$ three times in order to obtain the three constants A , B and C . We contract with $g^{\alpha\beta} P^\gamma$, $g^{\beta\gamma} P^\alpha$ and $P^\alpha P^\beta P^\gamma$, solve the resulting equations and get

$$I^{\alpha(\beta\gamma)} = \int d\Phi(2,3) p_2^\alpha p_3^\beta p_3^\gamma = \frac{\pi}{24} P^\alpha P^\beta P^\gamma + \frac{\pi}{48} s' (P^\beta g^{\alpha\gamma} + P^\gamma g^{\alpha\beta} - P^\alpha g^{\beta\gamma}). \tag{G.45}$$

G.6 Energy spectrum

Having performed the tensor integration over the neutrino phase spaces $d\Phi(2,3)$ from our original expression of the three-body phase space

$$d\mathcal{PS}(1,2,3) = \frac{1}{(2\pi)^5} d\Phi(2,3) d\Phi(23,1) ds', \tag{G.46}$$

we are left to integrate over $d\Phi(23,1) ds'$. With

$$s' = (p_2 + p_3)^2 = m_{23}^2 = m_\mu^2 + m_e^2 - 2m_\mu E_e, \quad \hat{s} = m_{123}^2 = (p_1 + p_2 + p_3)^2 = m_\mu^2 \tag{G.47}$$

and

$$d\Phi(23,1) ds' = \frac{\pi}{4} \frac{\lambda^{1/2}(\hat{s}, s', m_e^2)}{\hat{s}} d\cos\theta ds' \tag{G.48}$$

we can integrate over $d\cos\theta$ which gives rise to a factor 2 since our integrand is independent of $\cos\theta$. The only integration left is over ds' , which we will rewrite as an integration over the electron energy E_e :

$$ds' = -2m_\mu dE_e. \tag{G.49}$$

It is very important to consider the range of integration, when changing the variables. The s' range is:

$$0 \leq s' \leq (m_\mu - m_e)^2. \tag{G.50}$$

With

$$E_e(s') = \frac{m_\mu^2 + m_e^2 - s'}{2m_\mu} \quad (\text{G.51})$$

it follows that

$$E_e(0) = \frac{m_\mu^2 + m_e^2}{2m_\mu}, \quad E_e((m_\mu - m_e)^2) = m_e. \quad (\text{G.52})$$

The upper bound for the variable s' is the lower bound for E_e and vice versa. In order to incorporate this fact in $d\Gamma$, we need to change the integration limits, making the lower limit the lower bound and the upper limit the upper bound:

$$\int_0^{(m_\mu - m_e)^2} ds' = \int_{\frac{m_\mu^2 + m_e^2}{2m_\mu}}^{m_e} (-2m_\mu dE_e) = 2m_\mu \int_{m_e}^{\frac{m_\mu^2 + m_e^2}{2m_\mu}} dE_e. \quad (\text{G.53})$$

As we see the minus sign of the energy measure is compensated by changing the integration limits. Now rewriting the full phase space in terms of E_e gives:

$$d\Phi(23, 1) ds' = +2\pi \sqrt{E_e^2 - m_e^2} dE_e. \quad (\text{G.54})$$

After integrating (G.34) over the neutrino phase space, we rewrite the result in terms of E_e . Incorporating the change of variable according to (G.53), multiplying it by the factors $(2\pi)^{-4} \sqrt{E_e^2 - m_e^2} dE_e$ and $1/2m_\mu$ and using the definition:

$$d\Gamma = \frac{1}{2m_\mu} \left[\frac{1}{2} \sum_{spin} |\mathcal{M}|^2 \right] d\mathcal{P}\mathcal{S}(1, 2, 3), \quad (\text{G.55})$$

this leads to the following result for the energy spectrum:

$$\begin{aligned} \frac{d\Gamma}{dE_e} &= \frac{1}{2m_\mu} \left[E_e^3 \sqrt{E_e^2 - m_e^2} G_F^2 \left(\frac{-2m_\mu^3}{3M_W^2 \pi^3} \right) \right. \\ &+ E_e^2 \sqrt{E_e^2 - m_e^2} G_F^2 \left(\frac{2m_\mu^4}{3M_W^2 \pi^3} - \frac{2m_\mu^2}{3\pi^3} + \frac{2m_e^2 m_\mu^2}{3M_W^2 \pi^3} \right) \\ &+ E_e \sqrt{E_e^2 - m_e^2} G_F^2 \left(\frac{m_\mu^3}{2\pi^3} - \frac{7m_e^2 m_\mu^3}{3M_W^2 \pi^3} + \frac{m_e^2 m_\mu}{2\pi^3} \right) \\ &\left. + \sqrt{E_e^2 - m_e^2} G_F^2 \left(+ \frac{5m_\mu^2 m_e^4}{6M_W^2 \pi^3} - \frac{m_\mu^2 m_e^2}{3\pi^3} + \frac{5m_\mu^4 m_e^2}{6M_W^2 \pi^3} \right) \right]. \quad (\text{G.56}) \end{aligned}$$

In the limit of infinite W mass and vanishing electron mass this becomes:

$$\lim_{\substack{M_W \rightarrow \infty \\ m_e \rightarrow 0}} \frac{d\Gamma}{dE_e} = \frac{G_F^2 m_\mu}{3\pi^3} E_e^2 \left(\frac{3}{4} m_\mu - E_e \right). \quad (\text{G.57})$$

It is easy to check that in lowest order

$$\int_{m_e}^{\frac{m_\mu^2 + m_e^2}{2m_\mu}} dE_e \rightarrow \int_0^{\frac{m_\mu}{2}} dE_e \quad (\text{G.58})$$

this gives the correct result for the total decay rate:

$$\int_0^{\frac{m_\mu}{2}} dE_e \left[\frac{G_F^2 m_\mu}{3\pi^3} E_e^2 \left(\frac{3}{4} m_\mu - E_e \right) \right] = \frac{G_F^2}{12\pi^3} (m_\mu^2 E_e^3 - m_\mu E_e^4) \Big|_0^{\frac{m_\mu}{2}} = \frac{G_F^2 m_\mu^5}{192\pi^3}. \quad (\text{G.59})$$

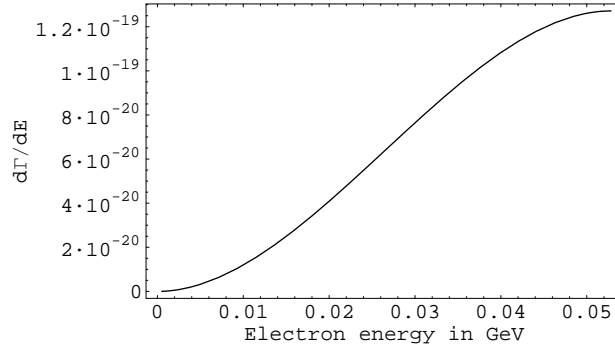


Figure 12: The physical region $m_e \leq E_e \leq \frac{m_\mu^2 + m_e^2}{2m_\mu}$ of the electron energy spectrum

G.7 Total decay rate

The energy integration, just like the s integration in the kinematic approach, has to be handled with caution. If we were to integrate the above expression we would for example encounter the integral:

$$\int dE_e \sqrt{E_e^2 - m_e^2} = \frac{E_e}{2} \sqrt{E_e^2 - m_e^2} - \frac{m_e^2}{2} \ln \left(E_e + \sqrt{E_e^2 - m_e^2} \right), \quad (\text{G.60})$$

which once again has a dimension-full expression in the argument of the logarithm. To prevent this situation, we scale the integration variable E_e with the muon mass, so that the new integration variable becomes $x \equiv E_e/m_\mu$:

$$\begin{aligned} \int_a^b dE_e E_e^n \sqrt{E_e^2 - m_e^2} &= m_\mu^{n+1} \int_a^b dE_e \left(\frac{E_e}{m_\mu} \right)^n \sqrt{\left(\frac{E_e}{m_\mu} \right)^2 - \left(\frac{m_e}{m_\mu} \right)^2}, \\ &= m_\mu^{n+2} \int_{a/m_\mu}^{b/m_\mu} dx x^n \sqrt{x^2 - A^2}. \end{aligned} \quad (\text{G.61})$$

Where $A = m_e/m_\mu$. The new integral is now entirely dimensionless and we no longer encounter any problems with the dimension of the logarithm argument. Using the integrals evaluated in appendix A.3, we reproduce the zeroth order $\Gamma^{(0)}$ in M_W plus additional terms. As already stated in (G.36) the zeroth order reads:

$$\Gamma^{(0)} = \frac{G_F^2 m_\mu^5 \left(1 - \frac{8m_e^2}{m_\mu^2}\right)}{192\pi^3}. \quad (\text{G.62})$$

Its numerical value is:

$$\Gamma^{(0)} = 3.0087246 \cdot 10^{-19} \text{ GeV}. \quad (\text{G.63})$$

The whole expression for the total decay rate reads:

$$\begin{aligned} \Gamma(\mu^- \rightarrow e^- \nu_\mu \bar{\nu}_e) &= \frac{G_F^2}{960 m_\mu^3 M_W^2 \pi^3} \left[\left(\ln \left(\frac{m_e}{m_\mu} \right) - \ln \left(\frac{m_e^2}{m_\mu^2} \right) \right) \right. \\ &\quad \times (120 m_\mu^4 m_e^4 (2m_e^2 + 2m_\mu^2 - M_W^2)) \\ &\quad + (m_e^2 - m_\mu^2) \left((8m_\mu^6 - 35m_\mu^4 M_W^2) m_e^2 + 3m_\mu^8 + 5m_\mu^6 M_W^2 \right. \\ &\quad \left. \left. + (3m_e^8 + (8m_\mu^2 + 5M_W^2) m_e^6 + (218m_\mu^4 - 35m_\mu^2 M_W^2) m_e^4) \right) \right]. \end{aligned} \quad (\text{G.64})$$

Which evaluates to:

$$\Gamma(\mu^- \rightarrow e^- \nu_\mu \bar{\nu}_e) = 3.0087279 \cdot 10^{-19} \text{ GeV}. \quad (\text{G.65})$$

This is the same value already found in the kinematic approach in chapter 5. In the limit of infinite W mass and vanishing electron mass, we once again find the well known zeroth order:

$$\lim_{\substack{M_W \rightarrow \infty \\ m_e \rightarrow 0}} \Gamma = \lim_{m_e \rightarrow 0} \Gamma^{(0)} = \frac{G_F^2 m_\mu^5}{192\pi^3}. \quad (\text{G.66})$$

Who's value is:

$$\lim_{\substack{M_W \rightarrow \infty \\ m_e \rightarrow 0}} \Gamma(\mu^- \rightarrow e^- \nu_\mu \bar{\nu}_e) = 3.0092877 \cdot 10^{-19} \text{ GeV}. \quad (\text{G.67})$$

The mean lifetime τ of a particle is defined as the inverse of its total decay rate. Inserting the value (G.65) yields:

$$\begin{aligned} \tau &\equiv \frac{1}{\Gamma} = \frac{1}{3.0087279 \cdot 10^{-10} \text{ eV}} = \frac{1}{(3.0087279 \cdot 10^{-10} \text{ eV})(1.5192675 \cdot 10^{15} \text{ eV}^{-1} \text{ s}^{-1})} \\ \tau &= 2.1876752 \cdot 10^{-6} \text{ s}. \end{aligned} \quad (\text{G.68})$$

Since the decay $\mu^- \rightarrow e^- \nu_\mu \bar{\nu}_e$ is the vastly dominant decay channel, the value (G.68) gives a good prediction for experimental results [92]:

$$\tau^{(\text{exp})} = 2.19703 \cdot 10^{-6} \text{ s}. \quad (\text{G.69})$$

G.8 Integrals

The following integrals were used for our calculations: In section 5:

$$\begin{aligned} \int dx \frac{x^3}{(1-x)^2} &= \frac{1}{1-x} + 3 \ln(1-x) + 2x + \frac{x^2}{2} \\ \int dx \frac{x^2}{(1-x)^2} &= \frac{1}{1-x} + 2 \ln(1-x) + x \\ \int dx \frac{x}{(1-x)^2} &= \frac{1}{1-x} + \ln(1-x) \\ \int dx \frac{1}{(1-x)^2} &= \frac{1}{1-x} \\ \int dx \frac{1}{x(1-x)^2} &= \frac{1}{1-x} - \ln(1-x) + \ln(x) \\ \int dx \frac{1}{x^2(1-x)^2} &= \left(\frac{1}{1-x} - \frac{1}{x} \right) + 2 \ln(x) - 2 \ln(1-x) \\ \int dx \frac{1}{x^3(1-x)^2} &= 3 \ln(x) - 3 \ln(1-x) - \frac{2}{x} + \frac{1}{1-x} - \frac{1}{2x^2}, \end{aligned} \quad (\text{G.70})$$

in section 9:

$$\begin{aligned} \int dx \sqrt{x^2 - A^2} &= \frac{x}{2} \sqrt{x^2 - A^2} - \frac{A^2}{2} \ln(x + \sqrt{x^2 - A^2}), \\ \int dx x \sqrt{x^2 - A^2} &= \frac{1}{3} (\sqrt{x^2 - A^2})^3, \\ \int dx x^2 \sqrt{x^2 - A^2} &= \frac{x}{4} (\sqrt{x^2 - A^2})^3 + \frac{A^2 x}{8} \sqrt{x^2 - A^2} - \frac{A^4}{8} \ln(x + \sqrt{x^2 - A^2}), \\ \int dx x^3 \sqrt{x^2 - A^2} &= \frac{1}{5} (\sqrt{x^2 - A^2})^5 + \frac{A^2}{3} (\sqrt{x^2 - A^2})^3. \end{aligned} \quad (\text{G.71})$$

G.9 Numerical input

In our calculations we used the following numerical Input out of [92]:

$$\begin{aligned}m_e &= 0.000511 \text{ GeV} \\m_\mu &= 105.6584 \text{ GeV} \\M_W &= 80.403 \text{ GeV} \\G_F &= 1.16639 \cdot 10^{-5} \text{ GeV}^{-2}\end{aligned}\tag{G.72}$$

As well as the conversion constant that connects energy in natural units to inverse time in SI units:

$$1 \text{ eV} = 1.5192675 \text{ s}^{-1}.\tag{G.73}$$

H W^+W^- production

In this section we calculate the σ_{CC3} contribution to the $W^{+*}W^{-*}$ production process. The σ_{CC3} contribution contains only s-channel diagrams of the crayfish type, a t-channel crab diagram (see figure 13) and their interferences. Contributions of deer diagrams (figure 2 in [88]) are not considered.

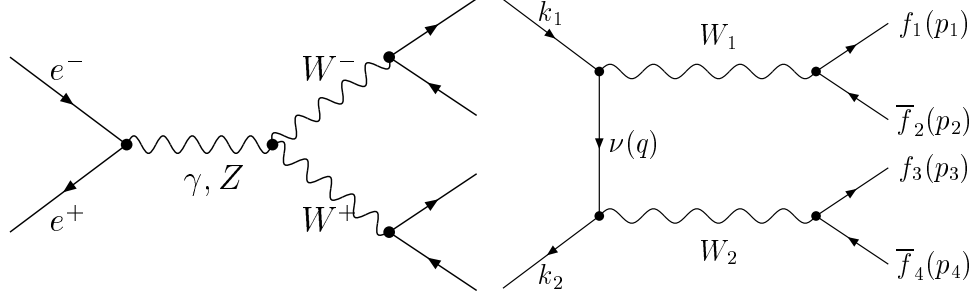


Figure 13: s-channel crayfish (left) and t-channel crab (right) of the $W^{+*}W^{-*}$ production process $e^+e^- \rightarrow W^{+*}W^{-*} \rightarrow 4f$

H.1 M-matrix

The M-matrix is a sum of the three diagrams in Figure 1. Moreover, the W^\pm -propagators and the W decay products \mathcal{M}_{12}^β and \mathcal{M}_{34}^α appear in every diagram, they can therefore be factorized in the following way:

$$\begin{aligned} \mathcal{M} &= \mathcal{M}_\nu + \mathcal{M}_\gamma + \mathcal{M}_Z \\ &= \left[\left(\frac{e}{\sqrt{2}s_w} \right)^2 \frac{1}{(s_1 - M_W^2 + i\sqrt{s_1}\Gamma_W(s_1))} \frac{1}{(s_2 - M_W^2 + i\sqrt{s_2}\Gamma_W(s_2))} \mathcal{M}_{12}^\beta \mathcal{M}_{34}^\alpha \right] \\ &\times \left[-i \left(\frac{e}{\sqrt{2}s_w} \right)^2 B_t^{\alpha\beta} + \sum_{j=\gamma,Z} (ie) \frac{-i}{(s - M_j^2 + i\sqrt{s}\Gamma_j(s))} (ieC(j)V^{\gamma\alpha\beta}) B_j^\gamma \right]. \end{aligned} \quad (\text{H.1})$$

M_j ($j = \gamma, Z$) are the Z-boson and photon masses, M_W the W-boson mass. Γ_j ($j = \gamma, Z$) are the Z-boson and photon decay width, Γ_W the W-boson decay widths. s_w, c_w is the sine and cosine of the Weinberg angle. Finally

$$\begin{aligned} s &\equiv (k_1 + k_2)^2 = 2k_1k_2 \\ s_1 &\equiv (p_1 + p_2)^2 = 2p_1p_2, \quad s_2 \equiv (p_3 + p_4)^2 = 2p_3p_4. \end{aligned} \quad (\text{H.2})$$

In all of the calculations we take the fermions to be massless, since their masses are very small compared to the W pair production threshold $\sqrt{s} = 2M_W$. Further, the summand proportional to B_t is the t-channel part and the ones proportional to B_j ($j = \gamma, Z$) are the two s-channel contributions. They are

$$\begin{aligned} \mathcal{M}_{ij}^\alpha &= \bar{u}(p_i)\gamma_\alpha \frac{1 - \gamma_5}{2} u(p_j) \\ B_t^{\alpha\beta} &= \bar{u}(k_2)\gamma_\alpha \frac{1 - \gamma_5}{2} \not{t} \gamma_\beta u(k_1) \\ B_j^\gamma &= \bar{u}(k_2)\gamma_\gamma \left(L(j) \frac{1 - \gamma_5}{2} + R(j) \frac{1 + \gamma_5}{2} \right) u(k_1) \\ V^{\gamma\alpha\beta} &= g^{\alpha\beta}(W_1 - W_2)^\gamma - 2g^{\beta\gamma}W_1^\alpha + 2g^{\alpha\gamma}W_2^\beta. \end{aligned} \quad (\text{H.3})$$

With the couplings

$$\begin{aligned} L(Z) &= \left(\frac{-1/2 + s_w^2}{s_w c_w} \right), & R(Z) &= \frac{s_w}{c_w}, & C(Z) &= -\frac{c_w}{s_w} \\ L(\gamma) &= R(\gamma) = C(\gamma) = 1 \end{aligned} \quad (\text{H.4})$$

It might seem surprising that there is apparently no numerator structure of the W-Propagators in (1). To clarify this point, one has to look at the Feynman rules. For the W-propagator (in its gauge invariant form) and the coupling to its decay products, they are

$$\left(\frac{ie}{\sqrt{2}s_w} \right) \left(-i \frac{g^{\beta\beta'} - W_1^\beta W_1^{\beta'} (1 - \xi)/(W_1^2 - \xi M_W^2)}{(W_1^2 - M_W^2 + i\sqrt{s_1}\Gamma_W(s_1))} \right) \left[\bar{u}(p_1)\gamma_{\beta'} \frac{1 - \gamma_5}{2} u(p_2) \right] \quad (\text{H.5})$$

It is easy to see, that the gauge dependent term vanishes when we contract it with $\gamma_{\beta'}$

$$\begin{aligned} W_1^\beta W_1^{\beta'} \mathcal{M}_{12}^{\beta'} &= W_1^\beta W_1^{\beta'} [\bar{u}(p_1)\gamma_{\beta'} \frac{1 - \gamma_5}{2} u(p_2)] \\ &= W_1^\beta [\bar{u}(p_1)(\not{p}_1 + \not{p}_2) \frac{1 - \gamma_5}{2} u(p_2)] \\ &= W_1^\beta [\underbrace{\bar{u}(p_1)\not{p}_1}_{=0} \frac{1 - \gamma_5}{2} u(p_2)] + W_1^\beta [\bar{u}(p_1) \frac{1 + \gamma_5}{2} \underbrace{\not{p}_2 u(p_2)}_{=0}]. \end{aligned} \quad (\text{H.6})$$

Where we have made use of $W_1 = p_1 + p_2$ and the Dirac equation $\not{p}u(p) = 0$ for massless fermions. This means that in contraction with $\mathcal{M}_{12}^{\beta'}$

$$-i \frac{g^{\beta\beta'} - W_1^\beta W_1^{\beta'} (1 - \xi)/(W_1^2 - \xi M_W^2)}{(W_1^2 - M_W^2 + i\sqrt{s_1}\Gamma_W(s_1))} \rightarrow -i \frac{g^{\beta\beta'}}{(W_1^2 - M_W^2 + i\sqrt{s_1}\Gamma_W(s_1))}. \quad (\text{H.7})$$

After performing the contraction of $g^{\beta\beta'}$ with $\gamma_{\beta'}$ one arrives at the propagator and indices structure of (1). The numerator structure of the Z- and γ -propagator in (1) is to be explained in direct analogue to the structure of the W-propagator above.

H.2 Squaring \mathcal{M}

The s-channel fermion-fermion-vector coupling B_j^γ has a left- and a right-handed part

$$\begin{aligned} B_j^\gamma &= L(j)B_L^\gamma + R(j)B_R^\gamma \\ B_L^\gamma &= \bar{u}(k_2)\gamma_\gamma \frac{1 - \gamma_5}{2} u(k_1) \\ B_R^\gamma &= \bar{u}(k_2)\gamma_\gamma \frac{1 + \gamma_5}{2} u(k_1). \end{aligned} \quad (\text{H.8})$$

In this decomposition the squared M-Matrix reads

$$\begin{aligned} |\mathcal{M}|^2 &= \left[\left(\frac{e}{\sqrt{2}s_w} \right)^4 \frac{1}{|s_1 - M_W^2 + i\sqrt{s_1}\Gamma_W(s_1)|^2} \frac{1}{|s_2 - M_W^2 + i\sqrt{s_2}\Gamma_W(s_2)|^2} |\mathcal{M}_{12}|^{2\bar{\beta}\beta} |\mathcal{M}_{34}|^{2\bar{\alpha}\alpha} \right] \\ &\times \left[\left(\frac{e}{\sqrt{2}s_w} \right)^4 |B_t|^{2\alpha\beta\bar{\alpha}\bar{\beta}} + \sum_{j=\gamma,Z} 2\Re \left[\frac{-e^4}{2s_w^2} \frac{C(j)L(j)}{(s - M_j^2 - i\sqrt{s}\Gamma_j(s))} V^{\gamma\bar{\alpha}\bar{\beta}} (B_t^{\alpha\beta} B_L^{*\bar{\gamma}}) \right] \right] \\ &+ \sum_{i,j=\gamma,Z} \left(\frac{e^4 C(j)C(i)[L(i)L(j) + R(i)R(j)]}{(s - M_i^2 + i\sqrt{s}\Gamma_i(s))(s - M_j^2 - i\sqrt{s}\Gamma_j(s))} (V^{\gamma\alpha\beta} V^{\bar{\gamma}\bar{\alpha}\bar{\beta}}) \right) |B_L|^{2\gamma\bar{\gamma}}. \end{aligned} \quad (\text{H.9})$$

Not overlined Minkowski indices stem from \mathcal{M} , overlined ones from \mathcal{M}^* .

The appearance of the expression $2\Re[\dots]$ is due to the simple equality $ab^* + a^*b = 2\Re[ab^*]$. Further, in order to obtain the above form, we used $|B_L|^{2\gamma\bar{\gamma}} = |B_R|^{2\gamma\bar{\gamma}}$ which follows from a straight forward calculation.

The phase space of a four particle final state

$$d\Gamma_4 \equiv \prod_{i=1}^4 \frac{d^3 p_i}{2p_i^0} \times \delta^4(k_1 + k_2 - \sum_{i=1}^4 p_i) \quad (\text{H.10})$$

decomposes into

$$d\Gamma_4 = ds_1 ds_2 d\Gamma(12, 34) d\Gamma(1, 2) d\Gamma(3, 4). \quad (\text{H.11})$$

Where the generalized two particle phase space is given by

$$d\Gamma(a, b) = \frac{\pi}{4} \frac{\sqrt{\lambda(m_{ab}^2, m_a^2, m_b^2)}}{m_{ab}^2} d\cos\theta, \quad (\text{H.12})$$

with the usual definitions

$$\begin{aligned} m_{ab}^2 &= (p_a + p_b)^2 \\ \lambda(a, b, c) &= a^2 + b^2 + c^2 - 2ab - 2ac - 2bc \\ \lambda &\equiv \lambda(s, s_1, s_2). \end{aligned} \quad (\text{H.13})$$

In $|\mathcal{M}|^2$ the only p_i ($i=1, \dots, 4$) dependent parts are $|\mathcal{M}_{12}|^{2\bar{\beta}\beta}$ and $|\mathcal{M}_{34}|^{2\bar{\alpha}\alpha}$ respectively. The integration over $d\Gamma(1, 2)$ and $d\Gamma(3, 4)$ can therefore be performed easily.

$$\begin{aligned} \sum_{\text{spin}} \int |\mathcal{M}_{12}|^{2\bar{\beta}\beta} d\Gamma(1, 2) &= \sum_{\text{spin}} \int \bar{u}(p_1) \gamma_\beta \frac{1 - \gamma_5}{2} u(p_2) \bar{u}(p_2) \gamma_{\bar{\beta}} \frac{1 - \gamma_5}{2} u(p_1) d\Gamma(1, 2) \\ &= \frac{1}{2} \int \text{tr}[\not{p}_1 \gamma_\beta \not{p}_2 \gamma_{\bar{\beta}} (1 - \gamma_5)] d\Gamma(1, 2) \\ &= \frac{1}{2} \int [4(p_1^\beta p_2^{\bar{\beta}} - p_1 p_2 g^{\beta\bar{\beta}} + p_1^{\bar{\beta}} p_2^\beta) + \epsilon^{\nu\beta\mu\bar{\beta}} p_1^\nu p_2^\mu] d\Gamma(1, 2) \end{aligned} \quad (\text{H.14})$$

With $s_1 \equiv (p_1 + p_2)^2 = 2p_1 p_2$ and the identities

$$\int d\Gamma(1, 2) = \frac{\pi}{2}, \quad (\text{H.15})$$

$$\int d\Gamma(1, 2) p_1^\nu p_2^\mu = \frac{\pi}{12} \left(\frac{s_1}{2} g^{\mu\nu} + W_1^\nu W_1^\mu \right), \quad (\text{H.16})$$

we get

$$\sum_{\text{spin}} \int |\mathcal{M}_{12}|^{2\bar{\beta}\beta} d\Gamma(1, 2) = \frac{\pi}{3} [-s_1 g^{\beta\bar{\beta}} + W_1^\beta W_1^{\bar{\beta}}]. \quad (\text{H.17})$$

An analogous expression holds for $|\mathcal{M}_{34}|^{2\bar{\alpha}\alpha} d\Gamma(3, 4)$.

H.3 Rewriting $|\mathcal{M}|^2$

The above M-Matrix can further be rewritten as a combination of six generic functions. Three functions $\tilde{\mathcal{C}}^{ab}$ ($a, b=s, t$) describing the couplings and three dynamic functions \mathcal{G}^{ab} .

$$\sum_{\text{spin}} |\mathcal{M}|^2 d\Gamma(1, 2) d\Gamma(3, 4) = \tilde{\mathcal{C}}^{tt} \mathcal{G}^{tt} + \tilde{\mathcal{C}}^{st} \mathcal{G}^{st} + \tilde{\mathcal{C}}^{ss} \mathcal{G}^{ss} \quad (\text{H.18})$$

The three coupling functions are

$$\begin{aligned}
\tilde{C}^{tt} &\equiv \frac{\pi^2}{9} A(s_1, s_2) \left(\frac{e}{\sqrt{2s_w}} \right)^4, \\
\tilde{C}^{ss} &\equiv \frac{\pi^2}{9} A(s_1, s_2) \sum_{i,j=\gamma,Z} \left(\frac{e^4 C(i)C(j)[L(i)L(j) + R(i)R(j)]}{(s - M_i^2 + i\sqrt{s}\Gamma_i(s))(s - M_j^2 - i\sqrt{s}\Gamma_j(s))} \right), \\
\tilde{C}^{st} &\equiv \frac{\pi^2}{9} A(s_1, s_2) \sum_{j=\gamma,Z} \left(\frac{-e^4}{2s_w^2} \right) 2\Re e \left[\frac{C(j)L(j)}{s - M_j^2 + i\sqrt{s}\Gamma_j(s)} \right], \tag{H.19}
\end{aligned}$$

with the factor

$$A(s_1, s_2) \equiv \left[\left(\frac{e}{\sqrt{2s_w}} \right)^4 \frac{1}{|s_1 - M_W^2 + i\sqrt{s_1}\Gamma_W(s_1)|^2} \frac{1}{|s_2 - M_W^2 + i\sqrt{s_2}\Gamma_W(s_2)|^2} \right]. \tag{H.20}$$

Using the two particle phase space integrations

$$\begin{aligned}
|\mathcal{M}_{12}|^{2\bar{\beta}\beta} d\Gamma(1, 2) &= \frac{\pi}{3} [-s_1 g^{\beta\bar{\beta}} + W_1^\beta W_1^{\bar{\beta}}] \\
|\mathcal{M}_{34}|^{2\bar{\alpha}\alpha} d\Gamma(3, 4) &= \frac{\pi}{3} [-s_2 g^{\alpha\bar{\alpha}} + W_2^\alpha W_2^{\bar{\alpha}}] \tag{H.21}
\end{aligned}$$

The dynamic functions become

$$\begin{aligned}
\mathcal{G}^{tt}(\cos\theta) &\equiv [-s_1 g^{\beta\bar{\beta}} + W_1^\beta W_1^{\bar{\beta}}] [-s_2 g^{\alpha\bar{\alpha}} + W_2^\alpha W_2^{\bar{\alpha}}] |B_t|^{2\alpha\beta\bar{\alpha}\bar{\beta}} \\
\mathcal{G}^{ss}(\cos\theta) &\equiv [-s_1 g^{\beta\bar{\beta}} + W_1^\beta W_1^{\bar{\beta}}] [-s_2 g^{\alpha\bar{\alpha}} + W_2^\alpha W_2^{\bar{\alpha}}] (V^{\gamma\alpha\beta} V^{\gamma\bar{\alpha}\bar{\beta}}) |B_L|^{2\gamma\bar{\gamma}} \\
\mathcal{G}^{st}(\cos\theta) &\equiv [-s_1 g^{\beta\bar{\beta}} + W_1^\beta W_1^{\bar{\beta}}] [-s_2 g^{\alpha\bar{\alpha}} + W_2^\alpha W_2^{\bar{\alpha}}] (V^{\gamma\bar{\alpha}\bar{\beta}}) B_t^{\alpha\beta} B_L^{*\bar{\gamma}}. \tag{H.22}
\end{aligned}$$

H.4 Cross section

The unpolarized differential cross section is

$$d\sigma \equiv \frac{1}{4} \sum_{\text{spin}} |\mathcal{M}|^2 \left(\frac{(2\pi)^4}{4k_1 k_2} \right) \left(\frac{1}{(2\pi)^3} \right)^4 d\Gamma_4. \tag{H.23}$$

Inserting the expression for $d\Gamma_4$ yields σ_{cc3} out of [1]

$$\begin{aligned}
\frac{d\sigma_{\text{cc3}}}{d\cos\theta} &\equiv \frac{d\sigma}{ds_1 ds_2 d\cos\theta} = \left(\frac{\sqrt{\lambda}}{s^2 \pi} \right) \left(\frac{1}{32(2\pi)^6} \right) \left[\frac{1}{4} \sum_{\text{spin}} |\mathcal{M}|^2 d\Gamma(1, 2) d\Gamma(3, 4) \right] \\
&= \left(\frac{\sqrt{\lambda}}{s^2 \pi} \right) \left(\frac{1}{128(2\pi)^6} \right) \left[\tilde{C}^{tt} \mathcal{G}^{tt} + \tilde{C}^{st} \mathcal{G}^{st} + \tilde{C}^{ss} \mathcal{G}^{ss} \right]. \tag{H.24}
\end{aligned}$$

H.5 Breit-Wigner factors

The above coupling functions \tilde{C}^{ab} all contain the factor $A(s_1, s_2)$ which might be rewritten as

$$\begin{aligned}
A(s_1, s_2) &= \underbrace{\left(\frac{e^2}{2s_w^2} \right)}_{24\pi\Gamma_W(s_1)/\sqrt{s_1}} \frac{1}{|s_1 - M_W^2 + i\sqrt{s_1}\Gamma_W(s_1)|^2} \underbrace{\left(\frac{e^2}{2s_w^2} \right)}_{24\pi\Gamma_W(s_2)/\sqrt{s_2}} \frac{1}{|s_2 - M_W^2 + i\sqrt{s_2}\Gamma_W(s_2)|^2} \\
&= \frac{24\pi^2}{s_1} \frac{24\pi^2}{s_2} \rho(s_1) \rho(s_2), \tag{H.25}
\end{aligned}$$

where the Breit-Wigner factors $\rho(s_i)$ are:

$$\rho(s_i) = \frac{1}{\pi} \frac{\sqrt{s_i} \Gamma_W(s_i)}{|s_i - M_W^2 + i\sqrt{s_i} \Gamma_W(s_i)|^2}. \quad (\text{H.26})$$

with the off shell W decay rate

$$\Gamma_W(s_i) \equiv \frac{e^2}{48\pi s_w^2} \sqrt{s_i}. \quad (\text{H.27})$$

The Breit-Wigner factors are normalized such that

$$\lim_{\Gamma_W \rightarrow 0} \rho(s_i) = \delta(s_i - M_W^2). \quad (\text{H.28})$$

It is evident, that

$$\lim_{\Gamma_W \rightarrow 0} \rho(s) \rightarrow 0 \quad \text{for } s \neq M_W^2, \quad (\text{H.29})$$

but we do not know what happens at $s = M_W^2$. To analyze this, we integrate over $\lim_{\Gamma_W \rightarrow 0} \rho(s)$.

$$\begin{aligned} \rho(s) &= \frac{1}{2\pi i} \left(\frac{1}{s - M_W^2 - i\sqrt{s}\Gamma_W} - \frac{1}{s - M_W^2 + i\sqrt{s}\Gamma_W} \right) \\ \lim_{\Gamma_W \rightarrow 0} \int ds \rho(s) &= \lim_{\Gamma_W \rightarrow 0} \frac{1}{2\pi i} [\ln(s - M_W^2 - i\sqrt{s}\Gamma_W) - \ln(s - M_W^2 + i\sqrt{s}\Gamma_W)] \end{aligned} \quad (\text{H.30})$$

Using the following identity for the complex logarithm with cut

$$\lim_{\epsilon \rightarrow 0} \ln(-R \pm i\epsilon) = \ln(R) \pm i\pi, \quad (\text{H.31})$$

we find

$$\lim_{\Gamma_W \rightarrow 0} \int ds \rho(s) = \frac{2\pi i}{2\pi i} = 1, \quad (\text{H.32})$$

yielding indeed the above normalization

$$\lim_{\Gamma_W \rightarrow 0} \rho(s_i) = \delta(s_i - M_W^2). \quad (\text{H.33})$$

H.6 Results

We globally extract the Breit-Wigner factors in the term

$$\mathcal{A} = \frac{e^4}{s_w^4} \frac{\rho(s_1)\rho(s_2)}{256s_1s_2}, \quad (\text{H.34})$$

and rewrite the cross section as

$$\frac{d\sigma_{\text{cc3}}}{d\cos\theta} = \left(\frac{\sqrt{\lambda}}{s^2\pi} \right) \mathcal{A} [\mathcal{C}^{tt} \mathcal{G}^{tt} + \mathcal{C}^{st} \mathcal{G}^{st} + \mathcal{C}^{ss} \mathcal{G}^{ss}]. \quad (\text{H.35})$$

The new coupling functions take the final form

$$\begin{aligned} \mathcal{C}^{tt} &= 1 \\ \mathcal{C}^{ss} &= \frac{8M_Z^4 s_w^4 + 4(2\Gamma_Z^2(s)s_w^4 - M_Z^2 s_w^2)s + s^2}{s^2((s - M_Z^2)^2 + s\Gamma_Z^2(s))} \\ \mathcal{C}^{st} &= \frac{2(-2M_Z^4 s_w^2 - (2\Gamma_Z^2(s)s_w^2 - 2M_Z^2 s_w^2 - M_Z^2)s - s^2)}{s((s - M_Z^2)^2 + s\Gamma_Z^2(s))}. \end{aligned} \quad (\text{H.36})$$

After evaluating the γ -traces, the \mathcal{G} functions read

$$\begin{aligned}\mathcal{G}^{tt}(\cos\theta) &= C_1 + \frac{4s_1s_2C_2}{t^2} \\ \mathcal{G}^{ss}(\cos\theta) &= \lambda C_1 + 12s_1s_2C_2 \\ \mathcal{G}^{st}(\cos\theta) &= (s - s_1 - s_2)C_1 + \frac{4s_1s_2[s(s_1 + s_2) - C_2]}{t},\end{aligned}\tag{H.37}$$

with

$$\begin{aligned}C_1 &= 2s(s_1 + s_2) + C_2, \\ C_2 &= -t(s - s_1 - s_2 + t) - s_1s_2.\end{aligned}\tag{H.38}$$

The WW production angle $\cos\theta$ is contained in the invariant t :

$$t = (s_1 + s_2 - s + \sqrt{\lambda} \cos\theta).\tag{H.39}$$

One can further integrate out the production angle to obtain the double resonating cross section. For this, the following integrals are used

$$\begin{aligned}\int_{-1}^1 d\cos\theta \cos^n \theta &= 1, 0, 1/3 \quad \text{for } n = 0, 1, 2 \\ \int_{-1}^1 d\cos\theta t^{-1} &= 2\mathcal{L}(s, s_1, s_2) \\ \int_{-1}^1 d\cos\theta t^{-2} &= \frac{2}{s_1s_2},\end{aligned}\tag{H.40}$$

with

$$\mathcal{L}(s, s_1, s_2) \equiv \frac{1}{\sqrt{\lambda}} \ln \left[\frac{s_1 + s_2 - s + \sqrt{\lambda}}{s_1 + s_2 - s - \sqrt{\lambda}} \right].\tag{H.41}$$

The dynamic functions now take the form

$$\begin{aligned}\mathcal{G}^{tt} &= \frac{1}{6}[\lambda + 12s(s_1 + s_2) - 48s_1s_2 - 24(s - s_1 - s_2)s_1s_2\mathcal{L}(s, s_1, s_2)] \\ \mathcal{G}^{ss} &= \frac{\lambda}{6}[\lambda + 12(s_1s + s_1s_2 + s_2s)] \\ \mathcal{G}^{st} &= \frac{1}{6}[(s - s_1 - s_2)[\lambda + 12(s_1s + s_1s_2 + s_2s)] \\ &\quad + 24(s_1s + s_1s_2 + s_2s)s_1s_2\mathcal{L}(s, s_1, s_2)].\end{aligned}\tag{H.42}$$

H.7 The CC3 cross section

The above result needs to be integrated over s_1 and s_2 in order to obtain the total cross section. This is done numerically using **MATHEMATICA**. In the massless case the kinematic range for the integration variables are:

$$\begin{aligned}0 &\leq s_1 \leq s \\ 0 &\leq s_2 \leq (\sqrt{s} - \sqrt{s_1})^2.\end{aligned}\tag{H.43}$$

In figure 14 we plotted σ_{CC3} as a function of the CM-Energy \sqrt{s} . We observe the increase after the threshold and a decrease $\sim 1/s \cdot \ln(s/M_{\text{W}}^2)$ afterwards. Even though the individual s- and t-channel

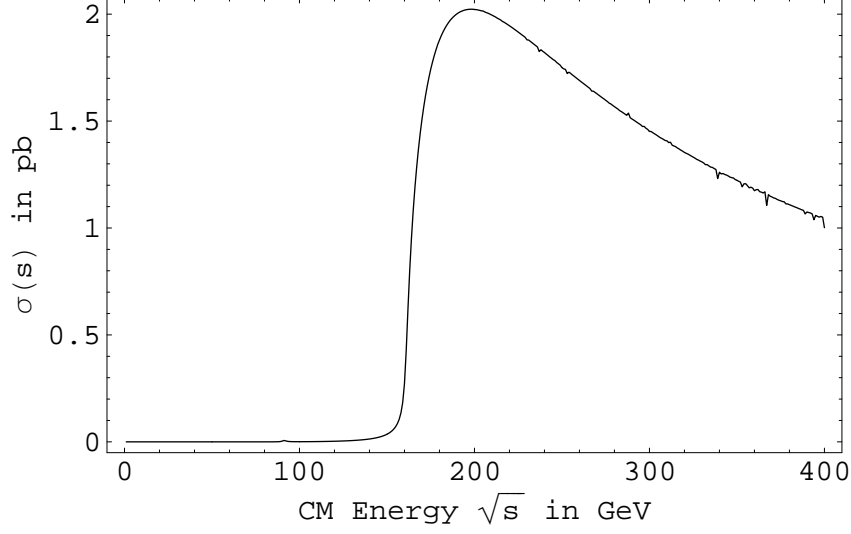


Figure 14: total decay rate $\sigma_{cc3}(s)$

contributions do not decrease, their interference term leads to gauge cancellations which further lead to the overall decrease that assures unitarity preservation.

The numerical results were obtained with the input quantities:

$$\begin{aligned}
\Gamma_V(s) &= (\sqrt{s}/M_V)\Gamma_V \\
\Gamma_Z &= 2.4952 \text{ GeV} \\
\Gamma_W &= 2.141 \text{ GeV} \\
M_Z &= 91.1876 \text{ GeV} \\
M_W &= 80.403 \text{ GeV} \\
\alpha(2M_W) &= (128.07)^{-1} \\
e(2M_W) &= 0.31324 \\
s_w(2M_W) &= 0.23004.
\end{aligned} \tag{H.44}$$

Using the narrow width approximation

$$\lim_{\Gamma_W \rightarrow 0} \rho(s_i) = \delta(s_i - M_W^2), \tag{H.45}$$

discussed in chapter 6, we can use the off-shell result to reproduce the on-shell one, first calculated in [90]:

$$\begin{aligned}
\sigma_{cc3,on} &= \frac{\beta e^4}{32\pi s_w^4 s} \left[\left(1 + \frac{2M_W^2}{s} + \frac{2M_W^4}{s^2} \right) \frac{L}{\beta} - \frac{5}{4} \right. \\
&\quad + \frac{M_Z^2(1-2s_w^2)}{(s-M_Z^2)} \left(\frac{2M_W^4}{s^2} \left(1 + \frac{2s}{M_W^2} \right) \frac{L}{\beta} - \frac{s}{12M_w^2} - \frac{5}{3} - \frac{M_W^2}{s} \right) \\
&\quad \left. + \frac{M_Z^4(8s_w^4 - 4s_w^2 + 1)\beta^2}{48(s-M_Z^2)^2} \left(\frac{s^2}{M_W^4} + \frac{20s}{M_W^2} + 12 \right) \right],
\end{aligned} \tag{H.46}$$

with the definitions

$$\beta = \sqrt{1 - 4M_W^2/s} \quad \text{and} \quad L = \ln \left(\frac{1+\beta}{1-\beta} \right). \tag{H.47}$$

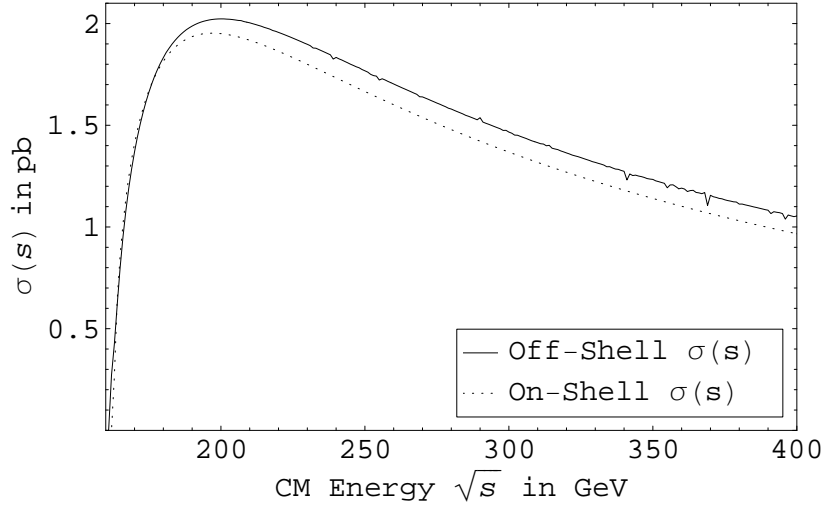


Figure 15: total On-Shell and Off-Shell decay rates $\sigma_{cc3}(s)$

In figure 15 we plotted both the On-Shell and the Off-Shell cross sections. We observe a flattening of the On-Shell case compared to the Off-Shell one.

H.8 Four body kinematics

We are interested in a parametrization of the four final momenta. In the corresponding phase space

$$\begin{aligned} d\Gamma_4 &\equiv \prod_{i=1}^4 \frac{d^3 p_i}{2p_i^0} \times \delta^4(k_1 + k_2 - \sum_{i=1}^4 p_i) \\ &= ds_1 ds_2 d\Gamma(12, 34) d\Gamma(1, 2) d\Gamma(3, 4) \end{aligned} \quad (\text{H.48})$$

we have eight independent integration variables, with the kinematic regions:

$$\begin{aligned} (m_1 + m_2)^2 &\leq s_1 \leq (\sqrt{s} - m_3 - m_4)^2, \\ (m_3 + m_4)^2 &\leq s_2 \leq (\sqrt{s} - \sqrt{s_1})^2, \\ -1 &\leq \cos\theta, \cos\theta_1, \cos\theta_2 \leq 1, \\ 0 &\leq \phi, \phi_1, \phi_2 \leq 2\pi. \end{aligned} \quad (\text{H.49})$$

The integration over ϕ just gives a factor 2π . We write down the momenta of the $2 \rightarrow 2$ process $e^+e^- \rightarrow W^{+*}W^{-*}$ in their center of mass system:

$$\begin{aligned} k_1 &= (p_0, -p\sin\theta, 0, p\cos\theta) \\ k_2 &= (p_0, p\sin\theta, 0, -p\cos\theta) \\ W_1 &= \frac{1}{2\sqrt{s}} (s + s_1 - s_2, 0, 0, \sqrt{\lambda}) \\ W_2 &= \frac{1}{2\sqrt{s}} (s - s_1 + s_2, 0, 0, -\sqrt{\lambda}), \end{aligned} \quad (\text{H.50})$$

with

$$p \equiv |\vec{p}| = \frac{\sqrt{\lambda(s, m_1^2, m_2^2)}}{2\sqrt{s}} \stackrel{m_i \rightarrow 0}{=} \frac{\sqrt{s}}{2} = p_0, \quad (\text{H.51})$$

and

$$\lambda \equiv \lambda(s, s_1, s_2), \quad k_1^2 = s_1, \quad k_2^2 = s_2. \quad (\text{H.52})$$

Note, that the W^- -boson is moving in the positive z-direction. Now we give the final momenta \tilde{p}_1 and \tilde{p}_2 in the W^- rest frame:

$$\begin{aligned} \tilde{p}_1 &= \frac{1}{2\sqrt{s_1}} \left(s_1 + m_1^2 - m_2^2, \sqrt{\lambda_{34}} \sin\theta_1 \cos\phi_1, \sqrt{\lambda_{34}} \sin\theta_1 \sin\phi_1, \sqrt{\lambda_{34}} \cos\theta_1 \right) \\ \tilde{p}_2 &= \frac{1}{2\sqrt{s_1}} \left(s_1 - m_1^2 + m_2^2, -\sqrt{\lambda_{34}} \sin\theta_1 \cos\phi_1, -\sqrt{\lambda_{34}} \sin\theta_1 \sin\phi_1, -\sqrt{\lambda_{34}} \cos\theta_1 \right), \end{aligned} \quad (\text{H.53})$$

with $\lambda_{12} \equiv \lambda(s_1, m_1^2, m_2^2)$. The key idea is now to boost \tilde{p}_1 and \tilde{p}_2 along the positive z-axes to bring them into the center of mass system of the incoming particles. \tilde{p}_3 and \tilde{p}_4 , which are defined analogous to (H.53) in the rest system of W^+ and will have to be boosted along the negative z-axes. For the Lorentz boost we need the velocity β of the W^- -boson, which we extract out of the momentum

$$W_{1,z} = \frac{\sqrt{\lambda}}{2\sqrt{s}} = \frac{M_W}{\sqrt{1-\beta^2}} \beta \quad (\text{H.54})$$

to give

$$\beta = +\sqrt{\frac{1}{1 + M_W^2/W_{1,z}^2}} = +\frac{\sqrt{\lambda}}{s + s_1 - s_2}. \quad (\text{H.55})$$

With $\gamma = (1 - \beta^2)^{-1/2}$ we get

$$\beta\gamma = \frac{\sqrt{\lambda}}{2\sqrt{s_1 s}} \quad \text{and} \quad \gamma = \frac{s + s_1 - s_2}{2\sqrt{s_1 s}}. \quad (\text{H.56})$$

The boosted momenta read:

$$\begin{aligned} p_1 &= \frac{1}{2\sqrt{s_1}} \left(\gamma(s_1 + m_1^2 - m_2^2) - \beta\gamma(\sqrt{\lambda_{34}} \cos\theta_1), \sqrt{\lambda_{34}} \sin\theta_1 \cos\phi_1, \sqrt{\lambda_{34}} \sin\theta_1 \sin\phi_1, \right. \\ &\quad \left. -\beta\gamma(s_1 + m_1^2 - m_2^2) + \gamma(\sqrt{\lambda_{34}} \cos\theta_1) \right) \\ p_2 &= \frac{1}{2\sqrt{s_1}} \left(\gamma(s_1 - m_1^2 + m_2^2) + \beta\gamma(\sqrt{\lambda_{34}} \cos\theta_1), -\sqrt{\lambda_{34}} \sin\theta_1 \cos\phi_1, -\sqrt{\lambda_{34}} \sin\theta_1 \sin\phi_1, \right. \\ &\quad \left. -\beta\gamma(s_1 - m_1^2 + m_2^2) - \gamma(\sqrt{\lambda_{34}} \cos\theta_1) \right). \end{aligned} \quad (\text{H.57})$$

In the massless case all final momenta are:

$$\begin{aligned} p_1 &= \frac{\sqrt{s_1}}{2} (1, \sin\theta_1 \cos\phi_1, \sin\theta_1 \sin\phi_1, \cos\theta_1) \\ p_2 &= \frac{\sqrt{s_1}}{2} (1, -\sin\theta_1 \cos\phi_1, -\sin\theta_1 \sin\phi_1, -\cos\theta_1) \\ p_3 &= \frac{\sqrt{s_2}}{2} (1, \sin\theta_2 \cos\phi_2, \sin\theta_2 \sin\phi_2, \cos\theta_2) \\ p_4 &= \frac{\sqrt{s_2}}{2} (1, -\sin\theta_2 \cos\phi_2, -\sin\theta_2 \sin\phi_2, -\cos\theta_2). \end{aligned} \quad (\text{H.58})$$

The general massive expression is given in equation (B.21) of [88].

References

- [1] M. Bohm, A. Denner and H. Joos, "Gauge theories of the strong and electroweak interaction," B.G.Teubner Stuttgart, 2001, third edition.
- [2] M.E. Peskin and D. V. Schroeder, "An Introduction To Quantum Field Theory," Harper-Collins Publishers, June 1995.
- [3] P. Ramond, "Field theory: a modern primer," Westview Press; 2 edition, December 21, 2001.
- [4] S. Weinberg, "The Quantum theory of fields. Vol. 1: Foundations," Cambridge, UK: Univ. Pr. (1995) 609 p.
- [5] V.A. Smirnov, "Feynman integral calculus," Berlin, Germany: Springer (2006) 283 p.
- [6] A. Smilga, "Lectures on quantum chromodynamics," Singapore, Singapore: World Scientific (2001) 322 p.
- [7] M. Planck , "Über das Gesetz der Energieverteilung im Normalspectrum," Annalen der Physik 43 (1901), pp. 553-563.
- [8] A. Einstein, "Über einen die Erzeugung und Verwandlung des Lichtes betreffenden heuristischen Gesichtspunkt," Annalen der Physik 17, 132-148, 1905.
- [9] N. Bohr, "On the Constitution of Atoms and Molecules," Philosophical Magazine, Series 6, Vol. 26. pg. 1-25, 1913.
- [10] L. de Broglie, "Recherches sur la théorie des quanta," Thèse de doctorat soutenue à Paris le 25 novembre 1924, Annales de Physique (10e série) III (1925) 22. Reproduced in: L. de Broglie, Recherches sur la théorie des quanta (Fondation Louis de Broglie, Paris, 1992).
- [11] W. Heisenberg, "Über quantentheoretische Umdeutung kinematischer und mechanischer Beziehungen," Z. Phys. 33 (1925) 879.
- [12] E. Schrödinger, "Quantisierung als Eigenwertprobleme," Annalen der Physik, 1926, 81, 109.
- [13] W. Heisenberg, "Über den anschaulichen Inhalt der quantentheoretischen Kinematik und Mechanik," Z. für Phys. 43, 172-198, 1927.
- [14] P.A.M. Dirac, "A Theory of Electrons and Protons," Proc. Roy. Soc. Lond. A **126** (1930) 360.
- [15] J. von Neumann "Mathematische Grundlagen der Quantenmechanik," Springer; 2. Aufl. edition (November 14, 1995)
- [16] C.N. Yang and R.L. Mills, "Conservation of isotopic spin and isotopic gauge invariance," Phys. Rev. **96** (1954) 191.
- [17] S.L. Glashow, "Partial Symmetries Of Weak Interactions," Nucl. Phys. **22** (1961) 579.
- [18] A. Salam and J.C. Ward, "Electromagnetic and weak interactions," Phys. Lett. **13** (1964) 168.
- [19] S. Weinberg, "A Model Of Leptons," Phys. Rev. Lett. **19** (1967) 1264.
- [20] F. Englert and R. Brout, "Broken symmetry and the mass of gauge vector fields," Phys. Rev. Lett. **13** (1964) 321.

- [21] P. W. Higgs, “Broken symmetries, massless particles and gauge fields,” *Phys. Lett.* **12** (1964) 132.
- [22] T. W. B. Kibble, “Symmetry breaking in non-Abelian gauge theories,” *Phys. Rev.* **155** (1967) 1554.
- [23] G. ’t Hooft and M.J.G. Veltman, “Regularization And Renormalization Of Gauge Fields,” *Nucl. Phys. B* **44** (1972) 189.
- [24] S. L. Glashow, J. Iliopoulos and L. Maiani, “Weak Interactions with Lepton-Hadron Symmetry,” *Phys. Rev. D* **2** (1970) 1285.
- [25] N. Cabibbo, “Unitary Symmetry and Leptonic Decays,” *Phys. Rev. Lett.* **10** (1963) 531.
- [26] M. Kobayashi and T. Maskawa, “CP Violation In The Renormalizable Theory Of Weak Interaction,” *Prog. Theor. Phys.* **49** (1973) 652.
- [27] H. Fritzsch, M. Gell-Mann and H. Leutwyler, “Advantages Of The Color Octet Gluon Picture,” *Phys. Lett. B* **47** (1973) 365.
- [28] D.J. Gross and F. Wilczek, “Ultraviolet behavior of non-abelian gauge theories,” *Phys. Rev. Lett.* **30** (1973) 1343.
- [29] H.D. Politzer, “Reliable perturbative results for strong interactions?,” *Phys. Rev. Lett.* **30** (1973) 1346.
- [30] I. Montvay and G. Munster, “Quantum fields on a lattice,” Cambridge, UK: Univ. Pr. (1994) 491 p., Cambridge monographs on mathematical physics.
- [31] J.C. Baez, “The True Internal Symmetry Group of the Standard Model,” <http://math.ucr.edu/home/baez/qg-spring2003/true>
- [32] H.J. Bhabha, “The scattering of positrons by electrons with exchange on Dirac’s theory of the positron,” *Proc. Roy. Soc. Lond. A* **154** (1936) 195.
- [33] M. Consoli, “One Loop Corrections To $e^+e^- \rightarrow e^+e^-$ In The Weinberg Model,” *Nucl. Phys. B* **160** (1979) 208.
- [34] Z. Bern, L.J. Dixon and A. Ghinculov, “Two-loop correction to Bhabha scattering,” *Phys. Rev. D* **63**, 053007 (2001) [arXiv:hep-ph/0010075].
- [35] E. W. N. Glover, J. B. Tausk and J. J. Van der Bij, “Second order contributions to elastic large-angle Bhabha scattering,” *Phys. Lett. B* **516** (2001) 33 [arXiv:hep-ph/0106052].
- [36] A. Penin, “Two-loop corrections to Bhabha scattering,” *Phys. Rev. Lett.* **95** (2005) 010408 [arXiv:hep-ph/0501120].
- [37] A. Penin, “Two-loop photonic corrections to massive Bhabha scattering,” *Nucl. Phys. B* **734** (2006) 185 [arXiv:hep-ph/0508127].
- [38] R. Bonciani, P. Mastrolia and E. Remiddi, “Vertex diagrams for the QED form factors at the 2-loop level,” *Nucl. Phys. B* **661** (2003) 289 [Erratum-ibid. B **702** (2004) 359] [arXiv:hep-ph/0301170].
- [39] R. Bonciani, P. Mastrolia and E. Remiddi, “QED vertex form factors at two loops,” *Nucl. Phys. B* **676** (2004) 399 [arXiv:hep-ph/0307295].

- [40] R. Bonciani, A. Ferroglia, P. Mastrolia, E. Remiddi and J. J. van der Bij, “Planar box diagram for the $n_f = 1$ 2-loop QED virtual corrections to Bhabha scattering,” Nucl. Phys. B **681** (2004) 261 [Erratum-ibid. B **702** (2004) 364] [arXiv:hep-ph/0310333].
- [41] M. Czakon, J. Gluza and T. Riemann, “Master integrals for massive two-loop Bhabha scattering in QED,” Phys. Rev. D **71**, 073009 (2005).
- [42] R. Bonciani, A. Ferroglia, P. Mastrolia, E. Remiddi and J.J. van der Bij, “Two-loop $n_f = 1$ QED Bhabha scattering differential cross section,” Nucl. Phys. B **701** (2004) 121 [arXiv:hep-ph/0405275].
- [43] R. Bonciani, A. Ferroglia, P. Mastrolia, E. Remiddi and J.J. van der Bij, “Two-loop $n_f = 1$ QED Bhabha scattering: Soft emission and numerical evaluation of the differential cross-section,” Nucl. Phys. B **716** (2005) 280 [arXiv:hep-ph/0411321].
- [44] R. Bonciani and A. Ferroglia, “Two-loop Bhabha scattering in QED,” Phys. Rev. D **72** (2005) 056004 [arXiv:hep-ph/0507047].
- [45] M. Bohm, A. Denner and W. Hollik, “Radiative Corrections to Bhabha Scattering at High-Energies. 1. Virtual and Soft Photon Corrections,” Nucl. Phys. B **304** (1988) 687.
- [46] F. A. Berends, R. Kleiss and W. Hollik, “Radiative Corrections to Bhabha Scattering at High-Energies. 2. Hard Photon Corrections and Monte Carlo Treatment,” Nucl. Phys. B **304** (1988) 712.
- [47] D. Y. Bardin, W. Hollik and T. Riemann, “Bhabha Scattering With Higher Order Weak Loop Corrections,” Z. Phys. C **49** (1991) 485.
- [48] M. Melles, “Exact results on $O(\alpha^2)$ single bremsstrahlung corrections to low angle Bhabha scattering at LEP/SLC energies,” Acta Phys. Polon. B **28** (1997) 1159 [arXiv:hep-ph/9612348].
- [49] G. Montagna, O. Nicrosini and F. Piccinini, “Precision physics at LEP,” Riv. Nuovo Cim. **21N9** (1998) 1 [arXiv:hep-ph/9802302].
- [50] A.B. Arbuzov, E.A. Kuraev and B.G. Shaikhatdenov, “Violation of the factorization theorem in large-angle radiative Bhabha scattering,” J. Exp. Theor. Phys. **88** (1999) 213 [Zh. Eksp. Teor. Fiz. **115** (1999) 392] [arXiv:hep-ph/9805308].
- [51] W. Placzek, S. Jadach, M. Melles, B.F.L. Ward and S.A. Yost, “Precision calculation of Bhabha scattering at LEP,” arXiv:hep-ph/9903381.
- [52] S. Actis, M. Czakon, J. Gluza and T. Riemann, “Two-Loop Fermionic Corrections to Massive Bhabha Scattering,” arXiv:0704.2400 [hep-ph].
- [53] T. Becher and K. Melnikov, “Two-loop QED corrections to Bhabha scattering,” JHEP **0706** (2007) 084 [arXiv:0704.3582 [hep-ph]].
- [54] S. Wolfram, “The Mathematica Book, Fifth Edition,” Wolfram Media; Fifth edition, August 22, 2003.
- [55] J. Gluza, K. Kajda and T. Riemann, “AMBRE - a Mathematica package for the construction of Mellin-Barnes representations for Feynman integrals,” arXiv:0704.2423 [hep-ph].
- [56] M. Czakon, “Automatized analytic continuation of Mellin-Barnes integrals,” Comput. Phys. Commun. **175** (2006) 559 [arXiv:hep-ph/0511200].

- [57] H. Lehmann, K. Symanzik and W. Zimmermann, “On the formulation of quantized field theories,” *Nuovo Cim.* **1** (1955) 205.
- [58] C. Becchi, A. Rouet and R. Stora, “Renormalization Of Gauge Theories,” *Annals Phys.* **98** (1976) 287.
- [59] L.D. Faddeev and V.N. Popov, “Feynman diagrams for the Yang-Mills field,” *Phys. Lett. B* **25** (1967) 29.
- [60] V.N. Gribov, “Quantization of non-Abelian gauge theories,” *Nucl. Phys. B* **139** (1978) 1.
- [61] T. Thiemann “Modern Canonical Quantum General Relativity,” Cambridge University Press; 2007.
- [62] F. Bloch, A. Nordsieck, *Phys. Rev.* **52**, 54 (1937)
- [63] T. Kinoshita, ”Mass singularities of Feynman amplitudes,” *J. Math. Phys.* **3** (1962) 650.
- [64] T.D. Lee and M. Nauenberg, Degenerate systems and mass singularities,” *Phys. Rev.* **133** (1964) B1549.
- [65] D.R. Yennie, S.C. Frautschi, H. Suura, ”The infrared divergence phenomena and high-energy processes,” *Ann. Pys.* **13** (1961) 379
- [66] S. Weinberg, ”Infrared Photons and Gravitons,” *Phys. Rev.* **140**, B516 - B524 (1965)
- [67] K. G. Chetyrkin and F. V. Tkachov, “Integration By Parts: The Algorithm To Calculate Beta Functions In 4 Loops,” *Nucl. Phys. B* **192** (1981) 159.
- [68] E.T. Whittaker & G.N. Watson, “A Course of Modern Analysis,” Cambridge University Press, (1927).
- [69] N.I. Usyukina, “On A Representation For Three Point Function,” *Teor. Mat. Fiz.* **22** (1975) 300.
- [70] E.E. Boos and A.I. Davydychev, “A Method of evaluating massive Feynman integrals,” *Theor. Math. Phys.* **89**, 1052 (1991) [*Teor. Mat. Fiz.* **89**, 56 (1991)].
- [71] V.A. Smirnov, “Analytical result for dimensionally regularized massless on-shell double box,” *Phys. Lett. B* **460** (1999) 397 [arXiv:hep-ph/9905323].
- [72] J.B. Tausk, “Non-planar massless two-loop Feynman diagrams with four on-shell legs,” *Phys. Lett. B* **469** (1999) 225 [arXiv:hep-ph/9909506].
- [73] T. Riemann, “Introduction to Mellin-Barnes Representations,” Talk given at CALC 2006, Dubna, Russia, <http://www-zeuthen.desy.de/~riemann/Talks/riemann-calc-2006.pdf>
- [74] S. Weinzierl, “The art of computing loop integrals,” arXiv:hep-ph/0604068.
- [75] [ALEPH Collaboration], “Precision electroweak measurements on the Z resonance,” *Phys. Rept.* **427** (2006) 257 [arXiv:hep-ex/0509008].
- [76] D. Y. Bardin *et al.*, “Zfitter: An Analytical Program For Fermion Pair Production In e^+e^- Annihilation,” arXiv:hep-ph/9412201.
- [77] D. Y. Bardin, P. Christova, M. Jack, L. Kalinovskaya, A. Olchevski, S. Riemann and T. Riemann, “ZFITTER v.6.21: A semi-analytical program for fermion pair production in e^+e^- annihilation,” *Comput. Phys. Commun.* **133** (2001) 229 [arXiv:hep-ph/9908433].

- [78] J.A.M. Vermaseren, “New features of FORM,” arXiv:math-ph/0010025.
- [79] J. Gluza, F. Haas, K. Kajda, T. Riemann, “Automatizing the application of Mellin-Barnes representations for Feynman integrals,” ACAT 2007 Proceedings, Amsterdam, The Netherlands, arXiv:0707.3567 [hep-ph]
- [80] S. Klein, ”Heavy Flavor Coefficient Functions in DIS at $O(a_s^2)$ and Large Virtualities,” Diplomarbeit, Universität Potsdam, 2006
- [81] J. Blümlein and S. Kurth, “Harmonic sums and Mellin transforms up to two-loop order,” Phys. Rev. D **60** (1999) 014018 [arXiv:hep-ph/9810241].
- [82] <http://mathworld.wolfram.com>
- [83] A.I. Davydychev and M.Y. Kalmykov, “Massive Feynman diagrams and inverse binomial sums,” Nucl. Phys. B **699** (2004) 3 [arXiv:hep-th/0303162].
- [84] E. Remiddi and J.A.M. Vermaseren, “Harmonic polylogarithms,” Int. J. Mod. Phys. A **15** (2000) 725 [arXiv:hep-ph/9905237].
- [85] J.A.M. Vermaseren, “Harmonic sums, Mellin transforms and integrals,” Int. J. Mod. Phys. A **14**, 2037 (1999)
- [86] M.A. Jack, “Semi-analytical calculation of QED radiative corrections to $e^+e^- \rightarrow f\bar{f}$ with special emphasis on kinematical cuts to the final state,” arXiv:hep-ph/0009068.
- [87] D. Lehner, “Initial State Radiative Corrections to Z^0 Pair Production in e^+e^- Annihilation – The Semi-Analytical Approach,” arXiv:hep-ph/9512301.
- [88] D.Y. Bardin and T. Riemann, “Off-shell W pair production in e^+e^- annihilation: The CC11 process,” Nucl. Phys. B **462** (1996) 3 [arXiv:hep-ph/9509341].
- [89] D.Y. Bardin, A. Leike and T. Riemann, “The Process $e^+e^- \rightarrow$ Lepton Anti-Lepton q Anti- q At Lep And Nlc,” Phys. Lett. B **344** (1995) 383 [arXiv:hep-ph/9410361].
- [90] W. Alles, C. Boyer and A.J. Buras, “W Boson Production In e^+e^- Collisions In The Weinberg-Salam Model,” Nucl. Phys. B **119** (1977) 125.
- [91] J. Biebel, “Predictions for the search for anomalous couplings of gauge bosons and leptons in e^+e^- scattering,” DESY-THESIS-2001-030
- [92] Particle Data Group, “Particle Physics Booklet,” Institute of Physics Publishing, July 2006.
- [93] E. Byckling and K.Kajantie , “Particle Kinematics,” John Wiley & Sons, 1973.

Zusammenfassung

Der Schwerpunkt dieser Diplomarbeit ist die Bhabha-Streuung $e^+e^- \rightarrow e^+e^-$. Bhabha-Streuung ist unter anderem an e^+e^- -Beschleunigern (wie z.B. LEP) von großer Bedeutung, wo man mit ihrer Hilfe die Beschleunigerluminosität bestimmt, welche direkten Einfluss auf die Genauigkeit aller weiteren Wirkungsquerschnittsmessungen hat.

In dieser Diplomarbeit wird der divergente Teil des Wirkungsquerschnittes von Bremsstrahlungskorrekturen zur Bhabha-Streuung berechnet. Es wird die Interferenz von allen Einschleifen-QED Fünf-Punkt Topologien (Kapitel 7 Abbildungen 6 und 7) mit den acht QED-Bremsstrahlungs Topologien untersucht.

Bei der Berechnung der Fünf-Punkt Funktionen treten zwei verschiedene Sorten von Infrarotdivergenzen auf. Durch die Schleifenintegration ergeben sich virtuelle IR-Divergenzen, sowohl der Skalar-, als auch der Tensorintegrale. Weiter tritt auf Grund der weichen Photonenemission eine reelle IR-Divergenz bei der Phasenraumintegration auf.

Die generelle Struktur der IR-Divergenzen im Standardmodell wird in Kapitel 4 diskutiert. Es wird gezeigt, dass reelle und virtuelle IR-Divergenzen sich Ordnung für Ordnung in der QED (Bloch-Nordsieck) gegenseitig wegheben. Da jedoch die Divergenzen der Fünf-Punkt Funktionen unter anderem auch mit Zweischleifen-Diagrammen korrespondieren (siehe Ende Kapitel 8), kann die Bloch-Nordsieck-Cancellation [62] nicht gezeigt werden.

Die Diplomarbeit beginnt mit einer kurzen Einführung in die theoretischen Grundlagen der Perturbationstheorie und die Struktur der elektroschwachen Teil des Standardmodells. Nach der oben erwähnten allgemeinen Diskussion der IR-Divergenzen berechnen wir sowohl den Born-Wirkungsquerschnitt der QED-Bhabha Streuung, als auch den Born-Beitrag zur QED-Bhabha-Bremsstrahlung.

Nach dem Einführen in Mellin-Barnes (MB) Darstellungen werden die `Mathematica` Pakete `AMBRE.m` [55] und `MB.m` [56] diskutiert, mit deren Hilfe die regularisierten MB-Integrale für die Skalar-, Vektor- und Tensorintegrale hergeleitet werden. Die Divergenzstruktur wird diskutiert und die divergenten Anteile der MB-Integrale werden explizit unter Verwendung des Residuen Theorems gelöst. Hierbei werden Lösungen in Form von inversen Binomialsommen gefunden, welche auf eine Unterklasse der in [83] diskutierten Funktionen zurückgeführt werden können.

Mittels der crossing symmetry, welche anhand eines Beispiels gezeigt wird, kann die Berechnung der Zählerstruktur von nur zwei der acht Fünf-Punkt Topologien reduziert werden. Der differentielle Wirkungsquerschnitt wird in Kapitel 8 in Abhängigkeit von den Photonen-Phasenraumintegralen P_1 und P_2 hergeleitet, welche in Kapitel 9 vollständig gelöst werden.

Der konstante Term der Phasenraumintegrale wird bis auf die Feynmanparameterintegrale reduziert. Für Emission von gleichen Beinen ergeben sich triviale Integrale, für initial-final Interferenz deutlich komplexere Integrale die nicht berechnet werden. Ein Großteil der Parameterintegrale der initial-initial bzw. final-final Interferenz sind in der `Mathematica` Datei `P1_ALPHA_Integrals.nb` gelöst.

Zusätzlich zu der Berechnung der Bhabha Wirkungsquerschnittes wird in Appendix G und H der elektroschwache Muonzerfall zu niedrigster Ordnung auf zwei verschiedenen Wegen, so wie der elektroschwache σ_{CC3} Wirkungsquerschnitt von W^+W^- -Produktion mit Hilfe von Breit-Wigner Faktoren hergeleitet.

Acknowledgement

First and Farmost, I would like to thank T.Riemann for supervising this thesis and all the time and effort that it has cost him.

I would like to thank my whole family, especially my parents Edgar and Gabriele, for supporting me during the last six years, for their finacial, and much more importantly, their personal support and help.

Furthermore I want to thank my colleagues and comrades in battle here at DESY Zeuthen: S.Actis, I.Bierenbaum, B.Blossier, N.Garron, I.Hailperin, K.Jansen, A.Shindler, J.B.Tausk and V.Weinberg for helpful disussions and encouragement.

Special thanks goes to my colleagues J.Gonzales Lopez, S.Klein and J.Schiefele for their friendship, support and dedication.

Last but not least, thanks to R.Oeckl for greatly supporting me.

Diese Diplomarbeit beinhaltet Beiträge zu folgender Publikation:

Automatizing the application of Mellin-Barnes representations for Feynman integrals,
J. Gluza, F. Haas, K. Kajda, T. Riemann
Proceedings of 11th International Workshop on Advanced Computing and Analysis Techniques in Physics Research (ACAT 2007), Amsterdam, The Netherlands
arXiv:0707.3567 [hep-ph]

Selbständigkeitserklärung

Hiermit erkläre ich, dass ich diese Arbeit im Rahmen der Betreuung am Deutschen Elektronen-Synchrotron in Zeuthen ohne unzulässige Hilfe Dritter verfasst und alle Quellen als solche gekennzeichnet habe.

Felix Haas, Potsdam den 15. Januar 2008.